INVESTIGATION OF PARAMETERS IN SINGLE- AND DOUBLE-NOZZLE ELECTROSPINNING FOR NANOFIBRE PRODUCTION

[1]HANNA SOFIA SALEHHUDIN, [2]EDZROL NIZA MOHAMAD, [3]WAN NUR LIZA MAHADI, [4]AMALINA MUHAMMAD AFIFI

[1,2,4]Department of Mechanical Engineering, University of Malaya, 50603 Kuala Lumpur, Malaysia
[3]Department of Electrical Engineering, University of Malaya, 50603 Kuala Lumpur, Malaysia
E-mail: [1]hanna.sofia@siswa.um.edu.my, [2]edzrol@um.edu.my, [3]wnliza@um.edu.my, [4]amalina@um.edu.my

Abstract - Electro spinning is a simple and versatile method of producing nanofibres, used in many applications. The process is governed by a number of parameters, and the effects of these parameters vary depending on the material used. Although the setup is simple, the process is complex and time-consuming, yielding very small amount of materials through hours of production. Multiple-nozzle electrospinning is a straightforward approach in increasing the production rate of nanofibres. However, the addition of nozzlesusually causes processing problems and lower fibre quality due to electric field interference between nozzles and non-uniformity of the process, limiting the possibility of mass production. The aim of this study is to investigate the effects of parameters in single- and multiple-nozzle electrospinning for future improvement of the method. In single-nozzle electrospinning, the effects and interaction between parameters were studied using response surface methodology (RSM). An empirical model was developed to predict the average diameter of polyethylene oxide (PEO) nanofibres in response to concentration, voltage, and nozzle-collector distance. Statistical analysis shows that for the current setup, the only significant parameter affecting fibre diameter is voltage. For the double-nozzle setup, the effects of voltage for internozzle distances of 1 and 2 cm were studied. Results show that jet deflection and fibre diameter can be reduced by increasing internozzle distance and reducing voltage.

Keywords-Electro spinning, multi-jet, nanofibres, nanotechnology, polymer

I. INTRODUCTION

Electro spinning is a method of drawing nanofibres from a solution by means of electric force. Compared to other fibre production methods, electrospinning by far has been the most preferred method due to its relatively simple setup, versatility, ease of production, and cost-effectiveness. Electrospinning has the ability to produce nanofibres with distinctive characteristics such as large surface-to-volume ratio, high porosity, controllable structure, and good tensile strength. Various types of nanofibres including multicomponent, core-sheath, hollow, and porous fibres can be electrospun from a wide range of materials. Polymers such as polyethylene oxide (PEO) and polyvinyl alcohol (PVA) are common materials used in electrospinning. Electrospun nanofibres prove to be useful in many applications including biomedicine and tissue engineering, filtration and separation, protective clothing, sensors, and energy devices[1]. The basic electrospinning setup typically consists of three major components; a high voltage power supply, a spinneret to feed the solution and a collector to deposit the electrospun fibres. The process has been described and explained in the literature[2,3].In a conventional single-needle setup, the solution is pumped through a syringe to form a liquid droplet at the tip of the needle. When a high voltage is supplied, the charged solution droplet at the tip deforms into a conical-shaped droplet known as the Taylor cone [4]. Above the critical voltage, the electrostatic force overcomes the surface tension of the fluid droplet, and a liquid jet is formed. The jet travels in an initially straight path, and slight perturbations eventually lead to bending instabilities in which the jet starts to form loops. The jet stretches, thins, and solidifies as it travels further downstream, before depositing onto the collector as thin nanofibres. The production rate of the conventional single-nozzle electrospinning setup is rather low, with flow rates of less than 1 ml/h, depending on the experimental conditions. For large-scale applications, multiple-jet electrospinning systems are designed to increase the productivity of the process. The study of multiple-nozzle electrospinning is currently an active area of research, although the number of research is significantly lower than that of single-nozzle electrospinning. In multiple-nozzle electrospinning, although the setup is simple and straightforward (only adding more nozzles), the process becomes more complex and less efficient as the number of jets increases. Difficulties arise due to electrical interference and mutual jet interaction, leading to processing problems and deterioration of fibre quality.Multiple-nozzle electrospinning also requires careful design and precision to ensure uniformity of the fibres throughout the process.

In this study, the effects of different parameters in single- and double-nozzle electrospinning are discussed. The relationship between the diameter of PEO fibres and electrospinning parameters from the single-nozzle setup was modelled using response surface methodology (RSM). RSM is a statistical approach used by many in the optimisation and prediction of the electrospinning process. The effects of varying parameters on the fibre diameter and jet deflection angle in double-nozzle electrospinning are also studied.

II. METHODOLOGY

Material preparation

Polyethylene oxide (PEO, molecular weight = 6×10^5 g/mol) was purchased from Sigma-Aldrich. PEO solution of different concentrations (6.5, 7.0, 7.5 wt%) were prepared by dissolving PEO powder in distilled water with the aid of magnetic stirring.

Electro spinning

The basic electrospinning setup is shown inFigure 1. A syringe pump was used to pump the PEO solution from a syringe with a 22G blunt stainless steel needle (0.7 mm OD, 0.4 mm ID, 10 mm length).The flow rate was set at 0.5 ml/h per nozzle. A high voltage DC power supply (up to 25 kV) was used to supply voltages between 10 to 20 kV. The electrospun PEO fibres were collected on an aluminium foil placed on a flat metal collector (40×40 cm), at a distance between 15 to 25 cm from the nozzle tip. The nozzle tip was positively charged, while the collector was negatively charged. Electrospinning was performed under ambient conditions, and each test was run for 30 minutes.

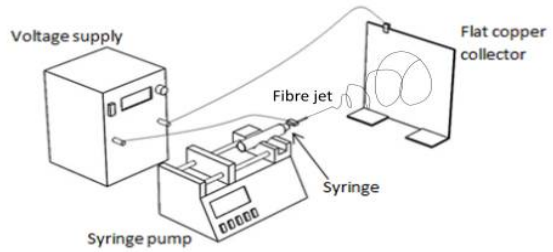

Figure 1: Schematic diagram of the basic electrospinning setup

Response surface methodology (RSM) was applied to model the effects of parameters in single-nozzle electrospinning. JMP software was used for the design of experiments and statistical analysis. The parameters varied were; (i) concentration of PEO solution, (ii) voltage, and (iii) nozzle-collector distance. For multiple-nozzle electrospinning, two nozzles are connected to a single syringe via tubes. The effects of varying voltage were investigated for internozzle distances of 1 and 2 cm. Other parameters were kept constant at base/middle values (concentration: 7 wt%, nozzle-collector distance: 20 cm). The jet deflection and diameter of fibres were observed and recorded.

Characterisation of nanofibres

The morphology of the electrospun fibres was observed using a Scanning Electron Microscope (SEM, Phenom ProX). Samples were sputter-coated with gold (Polaron SC7640, Thermo VG Scientific) prior to observation under SEM. For each sample, the average diameter of 20 fibres were measured.

Electric field simulation

Simulation of the electric field was carried out using a commercial software (ElecNet). Simulations were run for the single- and double-nozzle setup at internozzle distances of 1and 2 cm. Voltage and nozzle-collector distance were set at 10 kV and 10 cm respectively.

III. RESULTS AND DISCUSSION

Single-nozzle electrospinning (RSM)

The design of experiments consists of 15 runs, varying three factors; concentration (A), voltage (B), and nozzle-collector distance (C), and the average fibre diameter (Y) as the response parameter, as shown in Table 1. Y_p is the predicted fibre diameter based on the fitted quadratic model. Fibre diameters ranging from 114.28 to 203.08 nm were obtained, and minimal beading defects were observed for all samples. SEM photographs of the smallest and largest fibre diameter are shown inFigure 2.

No	*A* (wt%)	*B* (kV)	*C* (cm)	*Y* (nm)	Y_p (nm)
1	6.5	10	15	179.33	172.38
2	6.5	10	25	157.25	156.59
3	6.5	15	20	161.00	164.83
4	6.5	20	15	140.12	144.74
5	6.5	20	25	114.28	113.44
6	7.0	10	20	169.14	177.26
7	7.0	15	15	164.14	161.71
8	7.0	15	20	151.15	164.20
9	7.0	15	25	156.28	152.19
10	7.0	20	20	144.19	129.55
11	7.5	10	15	185.37	187.84
12	7.5	10	25	203.08	200.10
13	7.5	15	20	192.36	182.00
14	7.5	20	15	133.28	135.57
15	7.5	20	25	123.75	132.32

Table 1: Experimental parameters and results for the single-nozzle setup

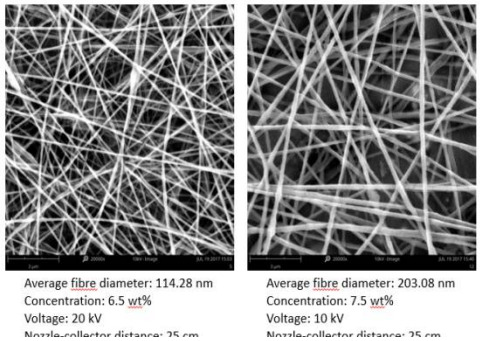

Figure 2: SEM photographs of the electrospun PEO fibres

The analysis of variance (ANOVA) indicated that only voltage (***B***) is a significant term ($P<0.05$) with a P-value of 0.0017, while other terms were not significant ($P>0.05$). Concentration (***A***) has a P-value of 0.0788, while other terms have P-values greater than 0.1. The R^2 value for the model is 0.914, indicating a good fit of the data. The generalised empirical model for the average fibre diameter of PEO is given as:

$$Y_p = 1816.4 - 518.36A + 28.52B - 6.66C - 2.46AB + 2.81AC - 0.16BC + 36.88A^2 - 0.43B^2 - 0.29C^2 \quad (1)$$

Since all terms other than B have no significant effects on average fibre diameter, the model can be simplified as:

Figure 3 shows the interaction profiles of the response model.Increasing the voltage from 10 to 20 kV leads to smaller fibre diameters. This is due to increased electric field strength and repulsive forces on the jet, which in turn facilitates jet stretching and thinning. From the fibre diameters measured, the reduction in fibre diameter with increasing voltage was in the range of 14 – 39%.

Increasing the solution concentration was found to slightly increase the fibre diameter. The change in diameter with concentration was in the range of 3 – 19% for most cases. In many studies using different materials, concentration is usually the most significant parameter affecting fibre diameter [5,6]. The increase in diameter with increasing concentration is attributed to the higher viscosity which tends to resist the stretching of the jet. In this study, the effect of PEO concentration was not significant because of the narrow range of concentration values (6.5-7.5 wt%) tested. However, a considerable increase of diameter from 157.25 to 203.08 nm (29%) was observed at low voltage (10 kV) and large nozzle-collector distance (25 cm). This observation contributes to the P-valuefor concentration which is quite close to the significant value of P<0.05.

Increasing the nozzle-collector distance tends to form thinner fibres as a larger distance allows more time for the jet to stretch. However, increasing the distance also reduces the electric field strength, which can lead to larger fibres. In this study, the average fibre diameter was not significantly affected by nozzle-collector distance, with changes between 4 – 14%. This observation is likely due to the balancing of the two opposite effects of varying nozzle-collector distance.

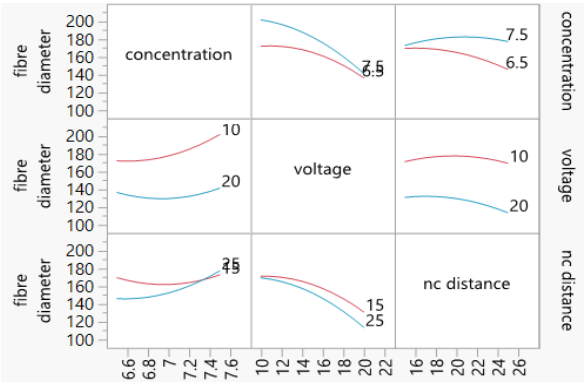

Figure 3: Interaction plots showing the effects of parameters on average fibre diameter

Double-nozzle electrospinning

The effects of varying internozzle distance and voltage for the double-nozzle setup were observed in terms of jet deflection angle and fibre diameter. The deflection angles were measured as shown in Figure, taking the average of the two angles.

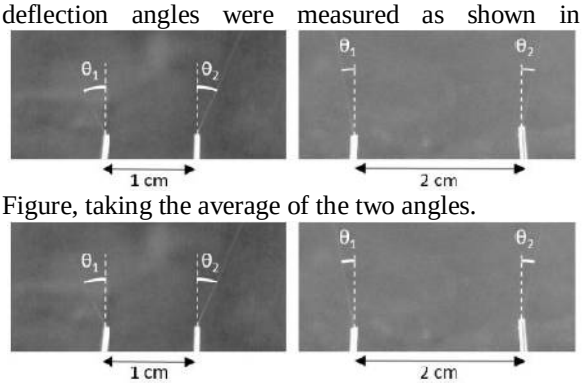

Figure 4. Photographs of jets in double-nozzle electrospinning

The results for the double-nozzle setup are shown in Table . For a single jet from a single nozzle, the initial straight path of jet is dictated by forces in the direction of the electric field, i.e. towards the collector. In a multiple-nozzle setup, the jets are also influenced by mutual Coulomb forces exerted by neighbouring jets, in addition to the electric field forces. The deviation of jets is caused by the resultant of these forces. Increasing the distance between nozzles reduces the effects of the Coulomb forces and hence reduces jet deviation.

Internozzle distance (cm)	Voltage (kV)	Deflection angle (°)	Average fibre diameter (nm)
1	10	15.7	144.53
	15	19.2	198.11
	20	24.1	197.17
2	10	6.3	120.01
	15	8.6	184.52
	20	9.9	188.49

Internozzle distance (cm)	Voltage (kV)	Deflection angle (°)	Average fibre diameter (nm)
1	10	15.7	144.53
	15	19.2	198.11
	20	24.1	197.17
2	10	6.3	120.01
	15	8.6	184.52
	20	9.9	188.49

Table 2. Results for the double-nozzle setup

The average jet deflection angle increased with increasing voltage for both internozzle distances of 1 and 2 cm, as shown in Figure. The increase in deflection angle with voltage is caused by the increase in jet charge density, which causes greater repulsion between the two jets.

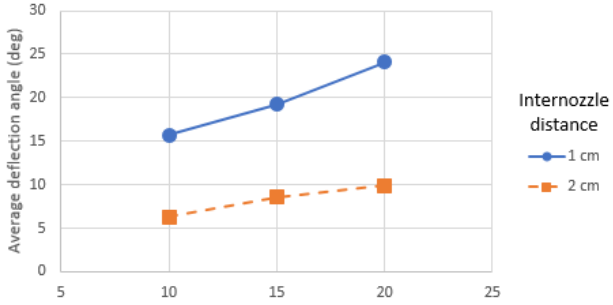

Figure5: Average jet deflection angle with voltage for double-nozzle setup

Figure 6 shows the distribution of fibre diameter with voltage. In the single-nozzle setup, fibre diameter tends to decrease with increasing voltage. However, the trend is different for the double-nozzle setup. For both internozzle distances of 1 and 2 cm, the average fibre diameter increased when voltage was increased from 10 kV to 15 kV. Further increasing the voltage to 20 kV, the changes in diameter became insignificant. In electrospinning, voltage is known to have two opposite effects on fibre diameter; (i) reduction in diameter due increased electric field strength and (ii) increase in diameter due to increased jet velocity. In the double-nozzle setup, the effects of increased velocity seems to outweigh the effects of electric field strength, likely due to electric field interference which weakens the electric field strength near the nozzles. Additionally, the initiation voltage is also higher for the double-nozzle setup (around 10 kV), while a lower voltage of around 5 kV is sufficient for the single-nozzle setup.

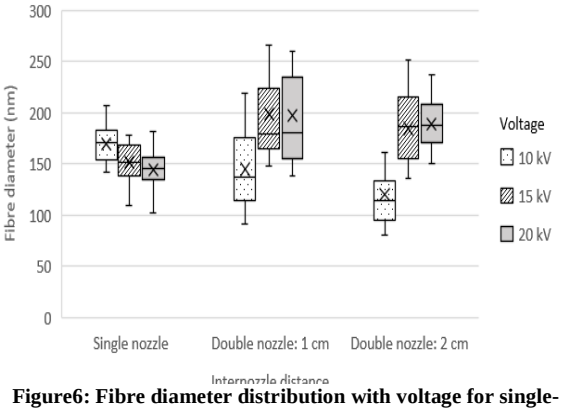

Figure6: Fibre diameter distribution with voltage for single- and double-nozzle setup

Figure 7. shows the distribution of electric field near the nozzles for different internozzle distances from the simulation. The electric field simulation only took into account the effects of the apparatus (nozzles and collector). The influence of the charged fluid jets were not included. The graph in **Error! Reference source not found.** shows that the electric field close to the nozzle is the highest for the single nozzle. The peak values for all setups are located at the tip of the nozzles. The electric field is reduced when two nozzles were employed, and the smaller internozzle distance (1 cm) shows the lowest peak value. Increasing the internozzle distance from 1 to 2 cm increases the electric field near the nozzles, thus forming slightly thinner fibres.

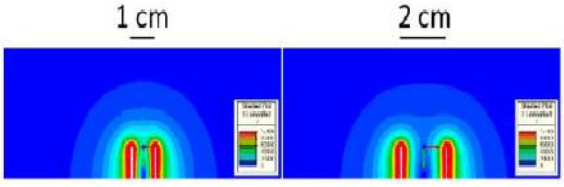

Figure7. Distribution of electric field strength around nozzles at different internozzle distances

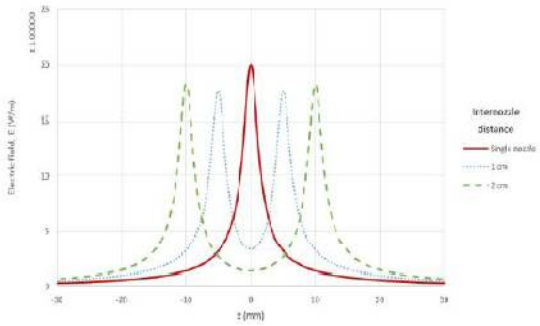

Figure 7 Graph of electric field strength along distance perpendicular to nozzle axis

In general, the average fibre diameter obtained from the single-nozzle setup is smaller than that of the double-nozzle setup due to greater electric field strength, except for when the voltage was set at 10 kV. The distribution of fibre diameter was also broader with two nozzles. Although the fibres were thinner for the double-nozzle setup at 10 kV, solution dripping was observed, causing wastage of materials and lower fibre deposition density. At 10 kV, the voltage supplied was insufficient to keep up with the rate of solution being drawn out. The flow rate thus needs to be reduced to overcome this issue, which will result in lower fibre production rate.

CONCLUSIONS

PEO nanofibres with diameters between 114.28 to 203.08 nm were successfully electrospun using single- and double-nozzle configurations. The effects of parameters on the electrospun PEO fibre diameter were modelled using RSM. From the model, voltage was found to be the most significant factor. The optimum (smallest) fibre diameter was obtained by setting the following parameters: concentration 6.5 wt%, voltage 10 kV, and nozzle-collector distance 25 cm. The production rate of nanofibres was doubled from 0.5 to 1.0 ml/h by using the double-nozzle setup.The electric field interference between nozzles generally results in larger fibre diameters and greater jet deflection, which can be reduced by using larger internozzle distance and lower voltage. A low voltage of 10 kV however caused processing problems including solution dripping and lower productivity.Results obtained for the double-nozzle setup serves as the starting point for future work in the design and optimisation of the multiple-nozzle setup, with the aim of increasing the production rate while maintaining the quality of nanofibres.

FUNDING/ACKNOWLEDGEMENTS

This work was supported by the Ministry of Higher Education, Malaysia under the Fundamental Research Grant Scheme (grant number FP058-2015A).

REFERENCES

[1] A. Haider, S. Haider, and I.-K. Kang, "A comprehensive review summarizing the effect of electrospinning parameters and potential applications of nanofibers in biomedical and biotechnology," Arabian Journal of Chemistry, 2015.

[2] K. Garg and G. L. Bowlin, "Electrospinning jets and nanofibrous structures," Biomicrofluidics, vol. 5, p. 13403, 2011.

[3] D. H. Reneker and A. L. Yarin, "Electrospinning jets and polymer nanofibers," Polymer, vol. 49, no. 10, pp. 2387–2425, 2008.

[4] [4] G. Taylor, "Electrically driven jets," Proceedings of the Royal Society A: Mathematical, Physical and Engineering Sciences, vol. 313, no. 1515, pp. 453–475, 1969.

[5] S. Y. Gu, J. Ren, and G. J. Vancso, "Process optimization and empirical modeling for electrospun polyacrylonitrile (PAN) nanofiber precursor of carbon nanofibers," European Polymer Journal, vol. 41, no. 11, pp. 2559–2568, 2005.

[6] K. Nasouri, A. M. Shoushtari, and M. Khamforoush, "Comparison between artificial neural network and response surface methodology in the prediction of the production rate of polyacrylonitrile electrospun nanofibers," Fibers and Polymers, vol. 14, no. 11, pp. 1849–1856, 2013.

★★★

BIOENGINEERING WITH YELLOW BAMBOO CULTURE (BAMBUSA VULGARIS) AS LAND SURFACE IN CONTROL OF IMPROVEMENT EROSION

[1]MENY SRIWATI, [2]SALEH PALLU, [3]MARY SELINTUNG, [4]RITA LOPA

[1]Doctoral Student Hasanuddin University,
[2,3,4] Civil Engineering Department Hasanuddin University
Email: [1]menysriwati@yahoo.com, [2]salehpallu@hotmail.com, [3]selintung_mary@yahoo.com, [4]ritalopa04@yahoo.com

Abstract - Erosion is the event of moving or transporting soil or parts of the soil from one place to another by the natural media.This study aims to analyze the of bioengineering with yellow bamboo as a surface layer of soil in erosion control with using slope 10%, 20%, and 30%.This research is conducted with 3 variations of rain intensity(I), namely 103 mm / hour, 107 mm / hour, 130 mm / hourby using rainfall simulator tool. The results demonstrate average of reduction of erosion rate on Yelolow Bamboo, from 3 various rainfalls, namely 87,011%, 91,816 %, 80,695%. This results indicate that intensity rainfall and erosion rate increase while treatment against Bioengineering with Yellow Bamboo decrase.

Keywords - Bioengineering, yellow bamboo, rain intensity, erosion control

I. INTRODUCTION

Erosion is the event of moving or transporting soil orparts of the soil from one place to another by natural media. In the event of erosion, soil or parts of the soil from a place is eroded and transported by natural media, such as water and wind, then it will be deposited to another place (Rahardiani, A.A.Sg.Dewi, 2014). Cliff erosion is the erosion of the soil on river cliffs and the grinding of the river bottom by flowing the river water. The process that takes place on cliff erosion is the process of erosion by streams and landslides on cliffs.The scour process occurs because the flow velocity of the river is great. (Rita Lopa and YukihroShimatani, 2013). Environmental Assessment Method For Small-River Restoration Plan of research stated that the restoration of the river influenced by the area condition. In addition, the purpose of restoration that is restoring the flood plains, increases flow velocity, and increases vegetation for breeding fish.Soil structure is one of the soil properties that strongly influence the outer forces, including erosion, therefore, the stability / structure of the soil structure is one of the necessary conditions to prevent the occurrence of erosion (Bunga Elifas.et.al,2011).

II. DETAILS EXPERIMENT

2.1. The time and Place of Research

Preliminary soil sampling, erosion soil sampling and yellow bamboo planting (bambusa vulgaris), physical soil and mechanical soil testing, soil organic content test, physical object modeling, rainfall data collection and analysis, and data validation. Location of Soil Sampling Rain simulation and analysis and data validation. The place of research carried out on:

1. Hydraulic Laboratory of Hasanuddin University Department of Civil Engineering.
2. Soil Mechanics Laboratory of Civil Engineering Department of Hasanuddin University.
3. Laboratory of soil chemistry and soil fertility, Faculty of agriculture, Hasanuddin University.

Fig1. Location of observation

2.2 Implementation of Research

2.2.1Standard Testing

Testing of physical and mechanical proprtiees of the soil is carried out in the soil mechanics laboratory, Civil Engineering Departemen, University Hasanuddin based on test standards. For the preparation of soil, this soil material.

2.2.2 Testing of Physical and Mechanical Properties of Soil

Dried until it reaches dry air conditions then the grains of soil are destroyed by using a hammer to pass the filter no.4 (four). The soil is then mixed with water evenly and then put into a sample box of 1.0 mx 0.7 mx 0.3 m in accordance with the required volume and then flattened and compacted with a standard compact system with a height falling 60 cm with 3 layers each Collision layer. Reaching a

thickness of 6.667 cm per layer of soil samples. And for testing with yellowbamboo vegetation do the planting with sample box size 1.0m x 0.7m x 0.3 m with respect to the distance between the plants and then measured growth for 2 months.

2.2.3 Measurement of Intensity Rainfall

Conducted rainfall simulator testing tool to ensure the amount of intensity that will be used. The amount of rain intensity based on the determination of the size of the disc opening, the rotation of the disk, and the magnitude of the pump pressure and the diameter of rain granules. A tilt adjusting device is placed in the rainfall simulator. Put the five containers with a diameter of 7.5 cm above the tool, 2 on the right, 2 on the left and 1 in the middle. The rainfall simulator is turned on and the intensity is set. Close the container first with the triplex cover so it will not fill the water, when the rainfall simulator is turned on, open the container cover and turn the stopwatch to time. After 15 minutes the container closes immediately, the rainfall simulator is turned off and the water contained in the container is measured by inserting into the measuring cup and recording. Thus the volumeand time are known so that the rain intensity can be determined. To get the desired rain intensity it is necessary to do repetitive experiments. The desired rain intensity based on Equation 3, obtained 103mm / hour, 107 mm / h and 130 mm / hour.For this study, the intensity of rainfall is used to the intensity of rainfall obtained from the rainfall simulator as shown in Table 1. below;

Category Rainfall	Intensity of Rainfall (mm/hour)	
	1 hour	24 hours
Trace	< 1	< 5
Light Rain	1 - 5	5 - 20
Moderate Rain	5 10	20 50
Heavy rain	10 - 20	50 - 100
Very heavy Rain	> 20	> 100

Source :Tristmodjo, Bambang (2008)

Table 1. Category Rainfall and intensity of rainfall

The equation which used to calculate rainfall intensity in artificial rain from rain simulation devices is following;

$$I = \frac{V}{A.t} \times 600 \qquad (1)$$

where

I = intensity of rainfall (mm/hour),
V = volume of water in the cups (ml),
A = The total area of the cups (cm2),
t = time (minute).

2.2.4 Implementation Running

After obtaining the desired rain intensity, ie103mm / hour, 107mm / hour and 130mm / hour, then the measurement is conducted for 1 hour. Every 15 minutes a measurement of the volume of water runoff is collected by using a container in the form of a bucket, then the water reservoir is stored for sediments. After 15 minutes, the water reservoir is replaced with a new water reservoir to accommodate runoff in the next 15 minutes.The samples are deposited at a site for ± 24 hours. The soil sample is then placed on a cup, then dried by oven for ± 24 hours. After dry then weighed to get the total weight.

2.3. Predicton of the rate of erosion by the model USLE

USLE (universal Soil loss Equation) is an equation for estimating the rate of soil erosionwhich developed By Wiecshmeier, W.H and D.D. Smith (1978). If comparing with another ground loss equation, USLE has a advantage that the variables have affected the amount of land loss. It can be calculated in detail and separated. Recently, USLE model is still considered to be the closest formula to reality, so it is more using than any other formula.

The ground loss equation can be seen as follows (Hardjoamidjojo S and Sukartaatmadja S, 2008);

$$E = R.K.LS.C.P \qquad (2)$$

Where :

E = Rate of Soil (EI),
R = Rainfall Erosivity parameter
K = Soil ErodibilityParameter, LS = a topographic factor, accounting for slope length and steepness
C = A Crop Cover Factor,
P = A ManagamentFactor.

The explanation of the five USLE model parameters, described as follows;

2.3.1 Rainfall Erosivityfactor (R)

Rainfall Erosivity Parameter (R) defines The number of units of rainfall erosion in a year. The value of erosivity (R) which is the destructive force of rain, can be determined by Equations 2 and 3, as follows (Suripin, 2001);R =

$$\sum_{i=1}^{n} EI_{30} \qquad (3)$$

$$EI_{30} = (E \times I_{30}) / 100 \qquad (4)$$

Where R is the rain erosivity index (MJ / ha / year); n is the number of rain events in a year, EI30 is an energy interaction with a maximum intensity of 30 minutes, where multiplication between rain energy (E = KJ / hh-mm) and maximum intensity 30min (I30 mm / h).To calculate the EI30 in Equation 4 it is necessary to obtain continuous rain data obtained from Automatic Rainfall Record. The circumstances and intensity of rainfall in various region depend on the circumstances, such as duration of rain, geographical location of a region, frequency of occurrence and etc.

While the rainfall intensity which used to predict erosion rate with USLE model is the daily rainfall intensity based onMononobe equation, as follows (Suripin, 2004);

$$I = \frac{R_{24}}{24}\left(\frac{24}{t}\right)^{\frac{2}{3}} \quad (5)$$

where

I = intensity of rainfall (mm/hour),

t = time (hour) from 2 to 3 hours, R24 = Maximum daily rainfall (for 24 hours) (mm). The annual kinetic energy of surface flow is estimated using a model by Kirkby (1976 in Hood, S.M et al., 2002). In this model, runoff is assumed to occur every time the daily rain exceed the critical value in accordance with the storage capacity of the surface layer. Measurement of magnitude of kinetic energy (Ek) in joule / m^2 / mm rain is used, as shown in the following equation;

$$Ek = 11{,}87 + 8{,}73 \log I \quad (6)$$

Where

I = intensity of rainfall (mm/hour).
Ek = kinetic energy (joule)

According to Hudson, 1971 For the tropics, advocate using Equation 7, as follows;

$$Ek = 29{,}8 - \frac{127.5}{1} \quad (7)$$

Where

I = intensity of rainfall (mm/hour).
Ek = kinetic energy (joule)

2.3.2Soil Erodibility Factor (K)

Hardiyatmo HC (2006), stated that the tendency of soil particles to erode is due to, (1) low on gravel, fine gradation, (2) height on silt and uniformly fine sand, (3) decreased with increasing clay content and organic matter, (4) increased with increasing sodium absorption ratio and increased with decreasing of ionic strength of water. Soil Erodibility (K), based on soil erodibility table (Hardiyatmo H.C (2006) that classified land based on USCS classification system is classified into SP (Sand Poor Graded) type group or bad graded sand with K value of 0.6-0.7. In this research, the value of K is 0.65.

2.3.3Length-Slope and Stepness Factor (LS)

The Slope factor is determined by lenght-slope (L) and Slope (S). Hardiyatmo H.C (2006), stated that this factor is combined between the influence of the length and slope with the symbol (LS). Where the S factor is the ratio of ground loss per unit area in the field to the ground loss on the 22.1 m (72.6 ft) experimental slope with a slope of 9%. To calculate LS, it used Equation 8, as follows;

$$LS = \frac{65s^2L'}{s^2+10.000} + \frac{4{,}6sL'}{(s^2+10.000)^{0{,}5}} + 0{,}065L' \quad (8)$$

Where

LS = Lenght-slope,
S = slope(%)and
L' = lenght-slope factor.

such asaddressingon9 equation,as following.

$$L = \left(\frac{L}{22.1}\right)^m \quad (9)$$

W here

L =Length-slope (m) which showing in Tablel 2, as follows;

Slope	m
< 1 %	0,2
1 % ≤ s < 3 %	0,3
3 % ≤ s < 5 %	0,4
s ≥ 5 %	0,5

Source : Hardiyatmo H.C (2006)

Table 2. m value

2.3.4. Cover ManagamentFactor (c)

The cover plant and land management (C) shows the overall of vegetation, litter, soil surface conditions, and land management on the size of the lost soil (eroded). Therefore, the magnitude of the C number is not always the same in the period of a year.Although the position of index C in the USLE equation is determined as an independent factor, the C value for Bioengineering with Yellow Bamboo.

2.5. Support Practice Factor (P)

The effectiveness of conservation measures in controlling erosion depends on the length and slope. Morgan (1988), stated that embankmenting and contour plowing can reduce soil erosion onslope by up to 50% compared to upward-down cultivation. Then, the ground loss on the contour strips decreased from 25% to 40% compared to the top-down cultivated land, depending on the slope

III. RESULT AND DISCUSSION

3.1 Result of measurement of growth of yellow bamboo bioengineering for 8 weeks

Sample	Time of measurement (Week)								Unit (cm)
	1	2	3	4	5	6	7	8	
1	23	136	153	182	207	226	245	276	cm
2	16	92	116	142	158	167	180	210	cm
3	14	34	164	175	183	216	239	263	cm

Table 3.The growth of yellow bamboo

Table 3 shows differeces of Yellow bamboo growth for 8 weeks. There are 3 yellow bamboos as the sample on this research where every sample was growing every week. From the first to the secomd week, Yellow bamboos increased rapidly. 3 samples reached respectively at 276, 210, and 263 in 8 weeks.

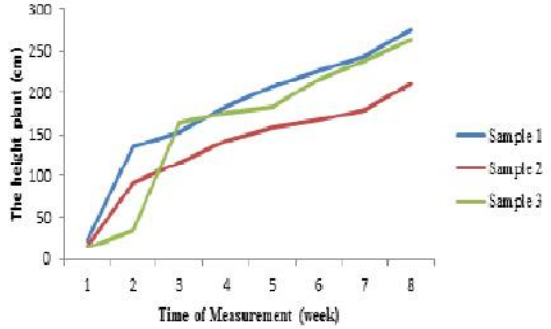

Fig.2. The growth of Yellow Bamboo

3.2 Rainfall Intensity Measurement Results

The measurement of rainfall intensity obtained by using rainfall measuring 2m x 1m is 103 mm / hour, 107 mm / hour, 130 mm / hour.

3.2.1 Erosion Rate Result of USLE model and Research Result.

The results of the erosion rate of USLE model and the results of the research can be known through laboratory testing using rainfall simulator tool on the original soil without bioenginering or the bioengineering bamboo yellow. The results obtained can be seen in the table 4 and 5.

Intesity of Rainfall	Slope	Erosion rate	
(mm/hour)	(degree)	Experiment (gr/m2/hour)	USLE (gr/m2/hour)
103	10	124,3	2995,431
	20	408,57	3375,925
	30	465,714	3829,580
107	10	199,786	2995,431
	20	621,429	3375,925
	30	1322,857	3829,580
130	10	235,714	2995,431
	20	1087,143	3375,925
	30	1395,714	3829,580

Table 4. Erosion Rate of The Study Results with Erosion Rate According to USLE On Without Bioengineering.

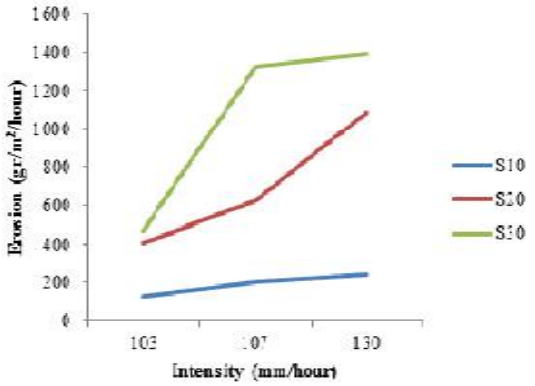

Fig.3. The effect of slope and intensity on resulting erosion without Bioengineering.

Intensity of rainfall	Slope	Erosion rate	
(mm/hour)	(degree)	Experiment (gr/m2/hour)	USLE (gr/m2/hour)
103	10	7,371	685,796
	20	60,471	772,909
	30	84,929	876,772
107	10	9,929	685,796
	20	77,9	772,909
	30	93,229	876,772
130	10	40,629	822,955
	20	144,386	927,491
	30	382,386	1052,127

Table 5.Erosion Rate of Research Results with Erosion Rate According To USLE By Using Yellow Bamboo Bioengineering

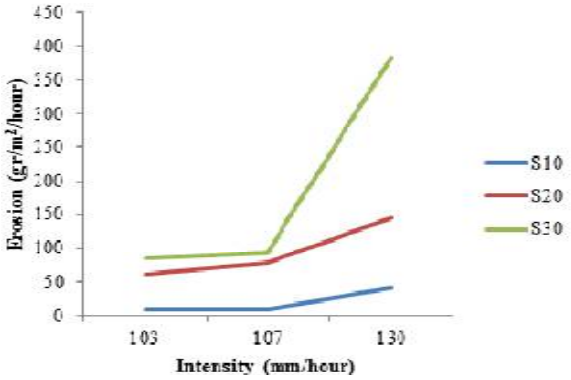

Fig.4. The effect of slope and intensity on resulting erosion by using Yellow Bamboo Bioengineering.

Table 4 and 5 compares the results of erosion rates by using 3 diffences of rainfall intensity on USLE model between using bioengineering and non using bioengineering. Based on result, both experiments show significant result where using bioengineering generated less erosion rates while non using engineering generated significant erosion rates.

Intensity of rainfall	Slope	Erosion rate (gr/m2/hour)		Eo %	Reduction %	Average %
(mm/hour)	(degree)	Non using Yellow bamboo	using Yellow bamboo			
103	10	124,3	7,371	5,930	94,070	87,011
	20	408,57	60,471	14,801	85,199	
	30	465,714	84,929	18,236	81,764	
107	10	199,786	9,929	4,970	95,030	91,816
	20	621,429	77,9	12,536	87,464	
	30	1322,857	93,229	7,048	92,952	
130	10	235,714	40,629	17,237	82,763	80,695
	20	1087,143	144,386	13,281	86,719	
	30	1395,714	382,386	27,397	72,603	

Table 6.Erosion Rate of Research Results with Erosion Rate According To USLE without non using Bioengineering and Using Yellow Bamboo Bioengineering

Tabel 6 Shows comparison of erosion rate which used by yellow bamboo and non-using Yellow Bamboo, from 3 various rainfall intensities, namely 103 mm/hour, 107 mm/hour, and 130 mm/hour. The value of the erosion rate occurs at rainfall intensity of 103 mm / hour, and average is 38.968% against the rate of erosion on the soil without using yellow bamboo. In addition, the rate of erosion on the ground without using yellow bamboo will be reduced at 87.011% if using yellow bamboo with intensity of rainfall 103 mm/hour. The rateof soil erosion uses yellow bamboo with using intensity of rainfall 107 mm / hour experiencedsignificant increasewhencompared to the rate of erosion occurring on the ground without using yellow bamboo. The erosion rate occurs at rainfall intensity of 107 mm / hour, and average is 24.554% against the rate of erosion on the ground without yellow bamboo. In other words, the erosion rate on the ground without yellow bamboo will be reduced at 91.816% if using yellow bamboo with intensity of rainfall 107 mm/hour. Similarly, if the soil uses yellow with rainfall intensity of 130 mm / hour shows a decrease if compared to the rate of erosion that occurs on the ground without using yellow bamboo The value of the erosion rate occurs at rainfall intensity of 130 mm / hour, and average is 19,305% against the rate of erosion on the soil without using yellow bamboo. In addition, the rate of erosion on the ground without using yellow bamboo will be reduced at 80.695% if using yellow bamboo with intensity of rainfall 130 mm/hour.

CONCLUSIONS

From the results of research, comparing to erosion rate between using yellow bamboo and Non-use Yellow Bamboo with using 3 various rainfall intensities, can be written conclusions as follows;

1. Without using yellow bamboo, erosion rate increases. In contrast, with using yellow bamboo, erosion rate decreases.
2. The results demonstrate average of reduction of erosion rate on Yelolow Bamboo, from 3 various rainfalls, namely 87,011%, 91,816 %, 80,695%. Rainfall intensity and erosion rate increase while treatment against Bioengineering with using Yellow Bamboo decrase

ACKNOWLEDMENTS

We would like to thank all whom involved directly and indirectly in completing this paper. Special thanks to research group of hydrolika labolatory.

REFERENCES

[1] Bunga Elifas, Saleh pallu,Mary Selintung,Arsyad Thaha, 2011." Studi laju erosi tanah pasir kelempungan yang distabilisasi dengan aspal emulsi". PIT HATHI XXVII, Ambon
[2] Hardjoamidjojo, S., danSukartaatmadja, S. 2008. TeknikPengawetan Tanah dan Air. Yogyakarta :GrahaIlmu Offset.
[3] Hardiyatmo, H.C. 2006. Penanganan Tanah LongsordanErosi.Yogyakarta : Gajah Mada University.
[4] Rahardiana, A.A.Sg.Dewi. 2014. Konsep Ekohidraulik Sebagai Upaya Penanggulangan Erosi. PADURAKSA, Volume 3 Nomor 1, Juni 2014 ISSN : 2303 – 2693.
[5] Rita Lopa & Yukihiro Shimatani. 2013. Environmental Assessment Method For a Small – River Restoration Plan. Int.J.Sus.Dev.Plann.Vol 8, No.4.
[6] Suripin. 2001. Pelestarian Sumber Daya Tanah dan Air, Yogyakarta : Andi Offset.
[7] Suripin. 2004. Sistem Drainase Perkotaan Yang Berkelanjutan. Yogyakarta : Andi Offset.
[8] Sutiyono. Budidaya Bambu. Peneliti Pusat Pengembangan Peningkatan Produktifitas Hutan. Bogor.
[9] Triatmodjo, Bambang. 2008. HidrologiTerapan. Yogyakarta : Beta Offset.

★★★

SEDIMENTATION ANALYSIS OFBILI-BILI DAMAS AN EFFORT FOR THE DAM CONTINUITY

[1]ISKANDAR RAHIM, [2]M.S.PALLU, [3]M.A.THAHA, [4]FAROUK MARICAR

[1]Doctoral Student in Civil Engineering, Hasanuddin University, Makassar
[2,3,4]Lecturer in Civil Engineering, Hasanuddin University, Makassar
[1]iskandarrahim@outlook.com ,[2]salehpallu@gmail.com,[3]athaha_99@yahoo.com, [4]fkmaricar@yahoo.com

Abstract - Bili-Bili damin Jeneberang River has operated since 1999 and it is planned to continue until 2049. In 2004, landslide on the upstream side of Bawakaraeng Mountain caused the increase of sedimentation in the dam. The aim of this study is to define the percentage of the sediment increase in the dam storage, the remaining useful life of the dam, and efforts for the dam continued.In this study, the calculation of sediment distribution based on actual measurement together with area increment and area reduction method is done. It is found that storage in 2011 is 79,17 %of the effective storage, 18,11 % in the dead storage, and 2,69% in the flood control area, so the dam can operate until 2023.

Keywords - Bili-Bili dam, sedimentation, storage

I. INTRODUCTION

Bili-bili dam is a multipurpose dam established in 1999 for flood control, irrigation, raw water supply, and hydroelectric power plant. This dam was collecting water fromJeneberang River and located in Bili-bili Village, Parangloe District, Gowa Regency. Bili-bili started operating in 1999. (Figure 1)

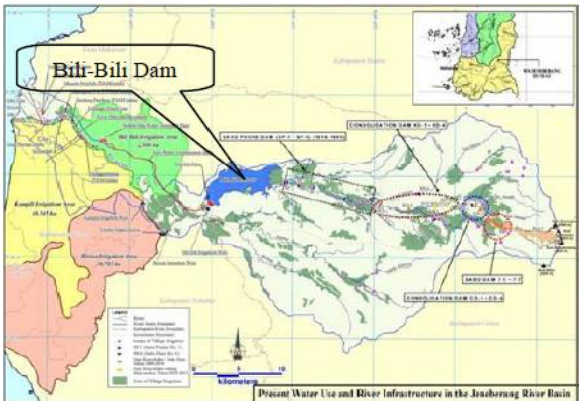

Figure 1. Location Map of Bili-bili dam

A catchment area of the Bili-bili dam is 384,40 km^2, which is planned to operate until 50 years(JRBDP,2004). Until now, potential sediment resulted by the caldera of the Bawakaraeng Mountain in 2004 is big enough and will flow to the downstream when the intensity of rainfall is high and settles along the river channel to the Bili-bili dam whichit caused the increase of sedimentation in Bili-bili dam. Furthermore, it will reduce the lifetime of the dam and threaten the continuity of the dam's function.

According to the study in 2009, (Yachiyo Engineering CO.,LTD, 2009) the amount of sediment in Bili-bili dam is 62.744.000 m^{3}for 11 years and exceeded the dead storage of the damwhich planned for 50 years is29.000.000 m^3, but until 2017 Bili-bili dam is still operating. Therefore, a particular study is needed to estimate the sediment in the dam.

The specific issues reviewed in this study are:

1. How is the distribution of the sediment in storage area and dam's capacity reductionbecause of the sedimentin 2012, 2018, 2028, 2038,and 2048.
2. How long is the remaining lifetime of the damover17years.

II. METODOLOGY

Suspended load is calculated by using equation(Suwarno, 1991) :

$Qs = 0.0864\ C.\ Qw$

Qs = Sediment discharge (ton/day)
C = Sediment concentration (mg/liter)
Qw = water disharge (m^3/second)
0,0864 is unit factor

The curve of sediment flow, which the regression line between sediment transport and water discharge is made with equation $Qs = a.Qw^{b.}$. Bed loadis estimated using the table of Borland and Maddok.The relationship between suspended sediment concentration, material type and percentage of bed load and suspended load is created.

Data used in this study are:

1. Dam's discharge inflow 1999-2011
2. Suspended Load for 3 years
3. Results of Laboratory testing results of Bili-bili dam's sediment
4. Data of storage and the area of initial inundation
5. Echosounding data 2007-2011
6. Technical data of Bili-bili dam

Area increment and reduction empirical methodis a method to estimate the distribution of sedimentationin the dam which contains approximation of the change in the real surface of a dam's base, reflected by the decrease of surface area as a result of sedimentation in the dam(Ilyas et al,2002). Area increment and reduction empirical method is based on observation

in dams where accumulation and distribution of sedimentation have a specific correlation with the dam's shape.

Determination of the dam's shape is obtained from the mvalue defined as a slope line obtained from the description data of initial depth and capacity of the dam.

The basic equation of empirical method is(USBR,782):

$$S = \int_0^{Yo} A\,dy + \int_{Yo}^{H} K\,a\,dy$$

S = The total of sedimentation at the dam
0 = Initial zero elevation in the dam
Yo = Zero elevation of the new capacity in the dam after sedimentation periods
A = Surface area of inundation
dy = Increase of depth
H = Total depth of the dam in normal water surface
K = Constant value based on the balance of the change of relative sedimentation surface
a = Relative sedimentation surface

Equation to determine the relative sediment surface (Priyantoro, 1987) is:

$$a_p = Cp^{\ m}(1-p)^n$$

The approaches used in calculating the useful life of Bili-bili dam is:

1. Elevation increase approach
2. Volume approach

III. RESULT AND DISCUSSION

1. Sediment Distribution in the Dam

The volume and rate of sedimentation in 1997-2011 according to echosoundingcalculation is shown in table 1.

YEAR	YEAR OF OPERATION	ANNUAL SEDIMENT 10^6 m3	KOMULATIF EDIMENT 10^6 m3	RATE OF SEDIMENTATION 10^6 m3
1997	-	0.000	0.000	0.000
2001	3	8.376	8.376	2.094
2004	6	14.558	22.934	4.853
2005	7	21.743	44.678	21.743
2006	8	6.571	51.249	6.571
2007	9	1.211	52.460	1.211
2008	10	9.509	61.968	9.509
2009	11	13.258	75.226	13.258
2010	12	6.788	82.015	6.788
2011	13	2.794	84.808	2.794

Table 1. The volume and rate of sedimentation

Estimation of the volume and rate of sedimentation in the future will be done by determining the curve shape which suitable with the distribution of the sedimentation volume started after landslide in 2004 is shown in Figure 2.

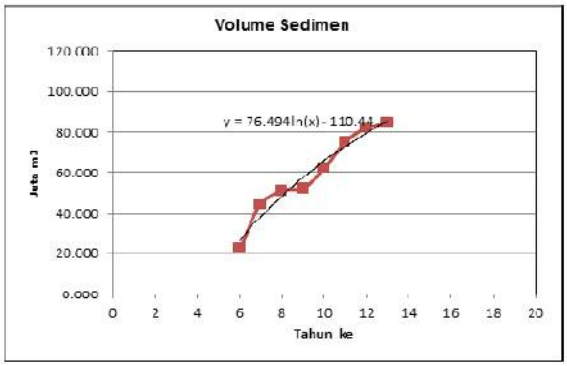

Figure2. Graphics of the sedimentation volume regression

Based on graphics in figure 2 an equation of the regression line is obtained:

y = 76,494 ln(x) – 110,44

Table 2 predicted the future volume of sedimentation of Bili-bili dam using this equation. One of the factors that affect the distribution of sedimentation is the dam's shape. The dam's shape is determined based on the correlation between the initial depth and dam's capacity.Bili-bili dam is type II.

YEAR	YEAR OF OPERATION	VOLUME OF SEDIMENTS 10^6 m3	RATE OF SEDIMENTATION 10^6 m3 / Year
1997	-	0.000	0.000
2001	3	8.376	2.094
2004	6	22.934	4.853
2005	7	44.678	21.743
2006	8	51.249	6.571
2007	9	52.460	1.211
2008	10	61.968	9.509
2009	11	75.226	13.258
2010	12	82.015	6.788
2011	13	84.808	2.794
2012	14	91.432	6.6239
2018	20	118.716	3.9236
2028	30	149.731	2.5933
2038	40	171.737	1.9367
2048	50	188.806	1.5454

Table 2. Prediction of the volume and rate of sedimentation in Bili-bili dam

According to the result of area increment and reduction empirical method, the new zero elevation of the sedimentation shown in table 3. Table 3. Proportion of the new zero elevation From the table 3, it seems like the new zero elevation of the sediment using area increment method is close to the actual circumstances in echosounding calculation.

There is a change of the damsstorage capacity depicted in the curved graphic of capacity and area of the new inundation as a result of the accumulation of sediment in the dam (Figure 3).

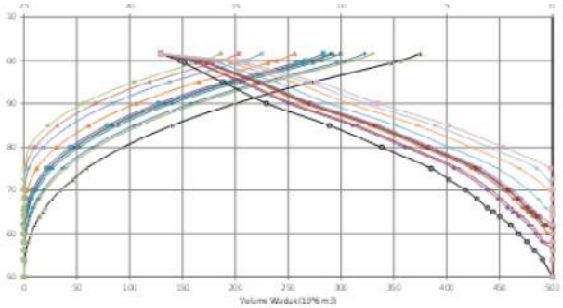

Figure 3. The capacity curvature and the dam's area

The prediction of the distribution of sedimentation volume in each storage elevation in 2012, 2018, 2028, 2038, until 2048 can be seen in Figure 4.

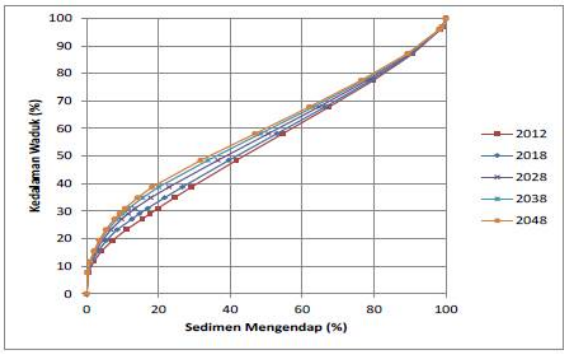

Figure 4. Distribution of sedimentation in Bili-bili dam

Table 4 showedthe distribution of dead storage capacity. There was a reduction from 2005 by28,58% of the total sedimentation 44,68 millionm^3 to 18,14% of 84,81 million m^3 in 2011, while in the effective storage area, the percentage of the sediment was increased from 70,05% of the total sedimentation 44,68 million m^{3}in79,17% of 84,81 million m^{3}sediment. It indicated that the sedimentation tends to be in the effective storagearea of the dam. The movement of sedimentation is shown in Figure 5.

Table 4. Distribution of the sedimentation in the dam's storage capacity

Number	Year	Spooler Dead				Spooler Effective				Catchment Flood			
		Initial Capacity	Actual Capacity	Sediment	Percent	Initial Capacity	Actual Capacity	Sediment	Percent	Initial Capacity	Actual Capacity	Sediment	Percent
		Million m3	Million m3	Million m3	%	Million m3	Million m3	Million m3	%	Million m3	Million m3	Million m3	%
1	2001	29.00	27.11	1.89	22.54	305.00	298.50	6.50	77.55	41.00	41.01	-0.01	-0.09
2	2004	29.00	23.20	5.80	29.90	305.00	287.62	17.38	75.77	41.00	41.25	-0.25	-1.07
3	2005	29.00	16.23	12.77	28.58	305.00	273.70	31.30	70.05	41.00	40.39	0.61	1.37
4	2006	29.00	15.75	13.25	25.86	305.00	269.00	36.30	70.25	41.00	39.01	1.99	3.89
5	2007	29.00	15.29	13.71	26.14	305.00	268.07	36.93	70.45	41.00	39.19	1.81	3.46
6	2008	28.00	14.91	14.09	22.74	305.00	258.62	46.38	74.36	41.00	39.20	1.80	2.95
7	2009	29.00	13.69	15.31	20.36	305.00	247.55	57.45	76.36	41.00	38.53	2.47	3.28
8	2010	29.00	13.58	15.42	18.81	305.00	240.95	64.35	78.09	41.00	38.46	2.54	3.10
9	2011	29.00	13.62	15.38	18.14	305.00	237.86	67.14	79.17	41.00	38.72	2.28	2.69

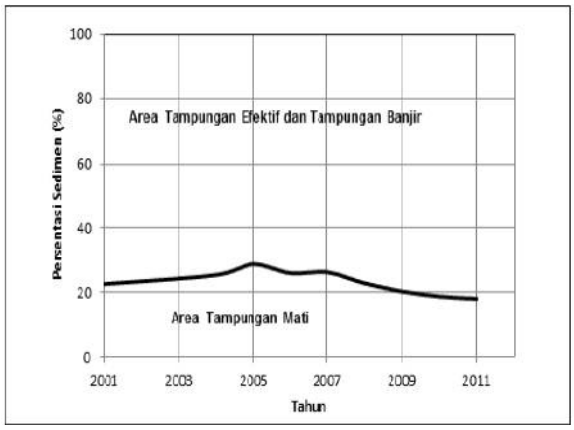

Figure 5. The movement of sedimentation in the storage area

Prediction of the reduction of the storage capacity trend compared to the dam's initial storage capacity:
2012: 283,63 million m3 = 75,62% of the initial storage.
2018: 236,35 million m3 = 68.35% of the initial storage.
2028: 225,33 million m3 = 60,08% of the initial storage.
2048:186,260 million m3 = 49,66% of the initial storage.

2. Lifetime

The lifetime of the dam is commonly calculated based on sediment elevation in the base intake. If the elevation of the sediment has reached the base intake, the normal service was disrupted so the lifetime was considered to be over. Table 5showed the remained lifetime of Bili-bili dam. The sediment was predicted to fulfill the dead storage in 2023.

Year	Volume on elevation ≤ +65,00 m	Catchment Sediment	Sediment Filled the Spool	T Operation	Rate of Sediment	Remaining Age of Reservoirs
	m3	m3	m3	Year	m3/Year	Year
2001	27,111,982.00	29,000,000.00	1,888,018.00	3.00	629,339.33	43.08
2004	23,197,556.00	29,000,000.00	5,802,444.00	6.00	967,074.00	23.99
2005	16,232,094.00	29,000,000.00	12,767,906.00	7.00	1,823,986.57	8.90
2006	15,745,962.00	29,000,000.00	13,254,038.00	8.00	1,656,754.75	9.50
2007	15,287,459.00	29,000,000.00	13,712,541.00	9.00	1,523,615.67	10.03
2008	14,907,273.00	29,000,000.00	14,092,727.00	10.00	1,409,272.70	10.58
2009	13,686,593.00	29,000,000.00	15,313,407.00	11.00	1,392,127.91	9.83
2010	13,575,646.00	29,000,000.00	15,424,354.00	12.00	1,285,362.83	10.56

Table5. The calculation of lifetime based on the dead storage volume

3. Effort in handling the sedimentation

Consider the critical condition of Bili-bili dam, the effort that must be taken to adding the lifetime of the dam is dredging.

CONCLUSION

1. Sediment which was entered to the dam until 2011 (84,81 million m^3) is distributed in the flood control: 2,69%, effective storage:79,1%, and dead storage:18,1%.
2. Based on the elevation of Minimum Operation Level (MOL) +65,00 the remained lifetime of

Bili-bili dam is 11,64years, while based on the dead storage volume in +65,00 elevation with the capacity of 29 million m3 the remained lifetime of the dam is until 2023.

3. The effort that must be taken to maintain the function of the Bili-bili dam is dredging by taking up the sediment around the dam's intake.

BIBLIOGRAPHY

[1] Chang,Shou-Young, and Yen,Chin-Lien, 2002, "Simulation of Bed Load Dispersion Process", Journal of Hydralics Engineering Vol 123, Mar, p. 331-342.

[2] Di Stefano, C.; Ferro, V; and Porto, P., 2000, "Slope Curvature Influence on Soil Erotion and deposition", water Resources Research, Vol 136, Feb, p. 607-612.

[3] Ilyas, M.Arief. Budiarto,T. 2002. Tinjauan Pengaruh Erosi-Sedimentasi dan upaya Konservasi Beberapa Waduk di Pulau Jawa. Prosiding Simposium Nasional Pencegahan Bencana Alam. ISBN : 979-8763-04-1 hal. 227-236

[4] Morris, G.L, Fan J. 1997. Reservoir Sedimentation Handbook. McGraw – Hill. Co. New York. USA.

[5] Priyantoro, D. 1987. Teknik Pengangkutan Sedimen. Penerbit Fakultas Teknik Universitas Brawijaya. Malang.

[6] Soewarno, 1991. Hidrologi, Pengukuran dan pengolahan Data Aliran Sungai (Hidrometri). Penerbit Nova. Bandung.

[7] USBR. 1974. Design Of Small Dams. Oxford & IBH Publishing CO, New Delhi India.

[8] Walker, J., 2001, "The Use of sediment modeling techniques to address the differing needs of management on the river Eden", Cumbria, UK, Water & Enviromental Management Journal, Vol 15, Nov, p. 252-257.

[9] Yachiyo Enggineering Co.,LTD. 2009. Additional Consulting Services of Countermeasures For Sediment Problems on Bili-Bili Dam Under Urgent Disaster Reduction Project For MT. Bawakaraeng Annex No.1. Hydrological Study. Kementerian Pekerjaan Umum.

★★★

DETERMINATION OF VITAMIN C RED GUAVA (PSIDIUM GUAJAVA LINN) FRUIT JUICE, WITH VARIATION OF BEVERAGE PACKAGING

[1]NOVRIYANTI LUBIS., [2]RISKA PRASETIAWATI., [3]WULAN SEPTIANI

[1]Garut University, [2]Garut University, [3]Garut University
E-mail: novri_sung@yahoo.co.id, riskasantosa@gmail.com, wulanseptiani1994@gmail.com

Abstract- The quantitative analysis of vitamin C content from variations beverage packaging containing red guava (Psidium Guajava Linn) fruit juice had been done. In this study, 4 samples were obtained from the shopping center in Garut and Bandung City. Samples were tested quantitatively by 2,6-dichlorophenol indophenol titration method. The results showed different concentration of 4 samples consist of tetra pack packaging, tin, glass, and plastic bottles, such as; 17.99 mg/100 gr, 31.46 mg/100 gr, 13.00 mg/100 gr, and 12.01 mg/100 gr, respectively. These result indicated that the packaging variations affected to the level of vitamin C content which was characterized by decreased levels of vitamin C. It means the levels of vitamin C from this research were not in accordance to nutritional value information on the packaging. Tetra pack packaging was the most stable compared to other packaging even though it had a shorter expired date than with other.

Index Terms— Vitamin C, variations beverage packaging, red guava, titration 2,6- dichlorophenol indophenol.

I. INTRODUCTION

Vitamin C is one of the nutrients and having function as antioxidants, effectively to protect free radicals that can damage cells. Low intake of fiber can be affect the intake of vitamin, because fiber vegetables, and fruits are also a good source of vitamin C [3].

One of the food products that are processed in the form of packaging, which is currently circulating in the market is fruit-flavored soft drinks in containers. Fruit drinks packaging is very easy to find in department stores (supermarket) [3].

Absolute human needs vitamin C from outside the body. In fact, people prefer to drink fruit beverage packaging compared to the vitamin C in fresh fruits, which are easily found anytime and their use is relatively more practical.

This research can give the information to public and consumer, about they daily intake of vitamin C and the most vitamin C stable in several variations of guava fruit beverage packaging.

Based on the above researchers wanted to determine levels of vitamin C in some beverage packaging red guava fruit (Psidium guajava L) determined by titration methods 2,6-diklorofenol indofenol, which one of the most stable beverage packaging levels of vitamin C in some variations of the packaging used. The benefits of doing this study to determine the levels of vitamin C and source of information on the levels of vitamin C in some guava fruit beverage packaging .

II. LITERATURE REVIEW

A. Morphology of Plants

Guava (Psidium guajava) is a well known cultivated tree because of the paste and jelly made from its fruits. The fruit (which is technically a type of berry) has a thin, yellow, slightly sour edible outer layer; within, there are numerous yellow seeds more than 3 to 5 mm long in a juicy pinkish or yellow pulp. The fruits are unusually rich in vitamin C. The outer layer of the fruit is preserved and canned commercially, as is the juice.

B. Nutrient Ingredients

Guava fruit have nutrient levels, in 100 grams of fresh guava fruit content complete content 0.9 g protein, 0.3 g fat, 12.2 g carbohydrate, 14 g calcium, phosphorus 28 mg, iron 1.1 mg, vitamin A 25 SI, 0.02 mg vitamin B1, vitamin C 87 mg and 86 grams of water with total calories by 49 calories. Seeds dried guava containing [2] 14% protein and 13% starch.

C. Benefits Consumption Guava

Guava fruit can be eaten fresh. Fruits are raw or undercooked widely used for rujakan. In addition, the fruit was processed into syrup, fruit juice, nectar, jelly, jam, confectionery, and dodol. In the medical world guava into drugs that can treat various diseases, among others : swollen gums, mouth sores, etc. [2].

D. Vitamin C

Vitamin C is a white crystalline water-soluble. In the dry state of vitamin C is quite stable, but under no circumstances soluble, vitamin C is easily destroyed by exposure to air (oxidation), especially when exposed to heat. Oxidation is accelerated by the presence of copper and iron. Vitamin C is unstable in alkaline solutions, but fairly stable in acidic solutions. Vitamin C is the most unstable vitamin [4].

The primary role of vitamin C to keep the structure of collagen is a protein that connector to all net fibers, skin, tendons, cartilage, and other tissues of human body. Collagen can heal broken bones, bruises, minor bleeding, and minor injuries. Vitamin C also plays an important role in helping the absorption of iron and

sharpen awareness. As an antioxidant, vitamin C can neutralize free radicals throughout the body. Through the influence of laxatives, vitamin C can also improve the disposal of feces [1].

The function of Vitamin C

The function of Vitamin C is to help the liver neutralize toxins or drugs, prevent cancer, antioxidants, and to the growth of bones and teeth [9]. The daily requirement of vitamin C for adults is about 60 mg, for pregnant women 95 mg, children 45 mg, and infants 35 mg, due to the pollution in the environment, among others by the fumes of motor vehicles and smoke, the use of vitamin C needs to be increased up to twice as much (10) of 120 mg.

Sources of Vitamin C

Fruits and vegetables fresh is Sources of the richest natural vitamin C. Vitamin C is often called Fresh Food Vitamins, raw fruit contains more vitamin C than ripe fruit. Vitamin C is water soluble and can be easily damaged by oxidation, heat and alkali. Because it's so not a lot of vitamin C is lost, and the incision should be avoided excessive destruction. Cooking with little water and sealed until tender much destroys vitamin C [1].

E. Titration Method 2,6-diklorofenol indofenol (DCPIP)

Reagents 2.6 diklorofenol has the chemical formula 2,6- (Cl) 2C 6H 3OH have physical and chemical properties include essentially solid form, molar mass of 163 g / mol, 211ºC boiling point, melting point of 56-58ºC, and the solubility in water 2000 mg / L. These compounds can cause skin irritation, eye irritation, toxic and flammable. 2,6-diklorofenol indofenol solution serves as a dye or indicator that gives a color change during the titration. 2,6-DCPIP solution in neutral or alkaline atmosphere will be blue were under acidic conditions will be pink. When 2,6-DCPIP reduced by ascorbic acid it would be colorless, and when all the ascorbic acid has been reducing 2,6-DCPIP then the excess solution of 2,6-DCPIP little already be seen by the staining [4].

The principle of the vitamin C content analysis of 2,6-DCPIP titration method is to set the levels of vitamin C in food by titration with 2,6-DCPIP where there is a reduction reaction of 2,6- DCPIP the presence of vitamin C in an acid solution. Ascorbic acid to reduce the 2,6- DCPIP in a solution that is colorless. End point marked with a color change to pink in acidic conditions [7].

In this titration, when all the ascorbic acid in the solution has been used up, there will not be any electrons available to reduce the DCPIPH and the solution remains pink due to the DCPIPH. The end point is a pink color that persists for 10 seconds or more, if there is not enough ascorbic acid to reduce all of the DCPIPH.

F. Packaging

Tetrapack

Packaging is commonly used as a milk beverage, tea, juice, and more. The following are the layers that exist in aseptic packaging paper and tetrapack are sorted from the outermost layer to the innermost layer are: Polyethylene (LDPE), paper cartons, polyethylene (LDPE), aluminum foil, Adhesive polymer, and M-polyethylene. The packaging is made with aseptic and UHT packaging.

Glass

Packaging glass used for baby food, fruit juices, pasta sauces, fish and meat depends on the acid product, whether sterilized or pasteurized. Advantages of glass packaging impermeable to water, gases, odors and microorganisms, do not react with packed product, and can be recycled.

Tin Can

A tin can, tin steel can, steel packaging or a can, is a container for the distribution or storage of goods, composed of thin metal. Many cans require opening by cutting the "end" open; others have removable covers. Cans hold diverse contents: foods, beverages, oil, chemicals, etc. Steel cans are made of tinplate (tin-coated steel) or of tin-free steel. In some locations, even aluminium cans are called "tin cans". However, it is now widely used tin-free steel is steel coated with chromium to prevent corrosion [8].

Plastic Bottle

A plastic bottle is a bottle constructed from plastic. The size ranges from very small sample bottles to large. Although plastic has many advantages, there are also weaknesses plastic when used as food packaging, which is a certain type (eg PET) does not stand the heat, releasing potentially harmful compounds that are derived from the residual monomers from polymers and plastics are materials that are difficult biodegradable so it can pollute the environment [9].

III. METHODS

Vitamin C was measured using 2,6-DFIF titration method. The samples studied are some beverage packaging guava (Psidium guajava L.) with different packaging are : tetrapack, glass, cans, and plastic bottles.

In this study, the first phase to validate methods of analysis that 2,6-DPCIP titration method first determines the accuracy, precision and detection limits. The second stage examination vitamin C content in guava fruit beverage packaging using a method that has been validated. Preparing a sample by measuring the sample volume packaging fruit drinks. From the above experimental results can be calculated amount of vitamin C in every 100 grams of beverage packaging Guava fruits studied.

According to AOAC 2002, the levels of vitamin C can be calculated using the formula:

Levels of vitamin C (mg / g) = $\frac{(Vt-Vb) \times \text{equality} \times Vi}{Vp \times Bs}$

III. EQUIPMENT AND MATERIALS

Equipment

The tools used for titration and analysis of 2,6-DCPIP vitamin C by using 2.6 –DCPIP are an analytical balance, 100 mL flask, desiccator, brown glass bottle, 100 mL flask, stir bar, funnel, blender, filter paper, measuring flask of 50 mL, 250 mL flask, 250 ml glas beaker, micro pipette, pipette, and tissue.

Materials

Materials used are guava, guava fruit beverage packaging with a variety of containers with an expiration date (expiration date) in particular, 2,6-DCPIP (Merck), ascorbic acid (Merck), glacial acetic acid (Merck), distilled water, metaphosphate acetic acid (Merck), concentrated sodium bicarbonate (APS Ajax Finecham).

IV. RESEARCH

A. Sample Collection and Determination

Samples used for validation of the titration method 2,6-DCPIP red guava fruit (Psidium guajava. L) obtained from the area Tarogong Garut district. While the sample studied for quantitative analysis of vitamin C are a couple of drinks packaging guava (Psidium guajava L.) containing vitamin C to be studied with different packaging are tetrapack, glass, cans, and plastic bottles.

B. Preparation of Samples

Samples are cleaned, weighed about 100 grams and then cut into small pieces put into a blender and then added about 20 mL of metaphosphate-acetic put in a blender, then blended, then weighed 10g then added 100 mL volumetric flask and add sour metaphosphate-acetate until the line mark. Homogenized, and then filtered.

C. Preparation of Reagent solution

A solution of 2,6-diklorofenol indofenol (DCPIP)

Dissolve 50 mg of sodium 2,6-DFIF that has been stored in a desiccator, then added 50 mL of water containing 40 mg of Na bicarbonate concentrated when it is dissolved to 200 mL of water added. Then filtered into a brown glass bottle. 2,6-DCPIP standard solution used within 3 days and standardized before use.

Quantitative Test on Samples

A total of 4 samples were taken each 5 mL in 100 mL Erlenmeyer each added 2 mL of strong acid and shaken metaphosphate then a solution of 2,6-DCPIP titration and titration is stopped until the pink solution.

V. RESULTS AND DISCUSSION

The human body does not naturally provide Vitamin C, and it is classified as "water-soluble". Vitamin C weighs 176.1 grams and has a molar mass of 68 grams per mole. Its density measures around 1.694 grams per cubic centimeter with a melting point of 190 degrees Celsius. Vitamin C boils at 553 degrees Celsius. Vitamin C is a white crystalline water-soluble. In the dry state of vitamin C is quite stable, but under no circumstances soluble, vitamin C is easily destroyed by exposure to air (oxidation), especially when exposed to heat [4].

In this study, the determination of vitamin C levels in samples of beverage packaging such as plastic bottles, tetrapack, cans and glass bottles. This is done to determine the most stable vitamin C levels between the packaging variations. In this study, the first phase of the analytical method validation 2,6-DCPIP titration method to determine in advance the accuracy, precision and limit of detection . Determination of vitamin C content of guava juice is done to validate 2,6-DCPIP titration method. The accuracy of test results is done by adding a standard solution of vitamin C. A good analytical method has an accuracy range of average recovery test for analyte concentration of 0.001% -0.01% in the samples tested was 90% -107% [10]. Percent recovery obtained by 91.96%. These results indicate a closeness between the results of the analysis with the real values of 2,6-DCPIP titration method used in this study fit for use and provide valid.

Precision test done to prove the accuracy of the practitioner or a work based on the level of accuracy of the results of the analysis indicated standard deviation (SD) and the relative standard deviation [15]. Levels of vitamin C in the juice plus the standard 25 mg vitamin C obtained from measurements taken as 6 replication is entered into the equation precision test. Value percent this research RSD 1.7394%. Accuracy of the tool can be good if the value of RSD less than 11% [10]. 1.7394 % RSD value is less than 11%, which means that the 2.6-DCPIP titration method used has good accuracy prices so that the instrument fit for use in the analysis of vitamin C. The limit of detection was defined as the lowest analyte concentration that was detected by the method specified confidence level [10]. Detection limits obtained by the concentration of 2 ppm. The next stage is the determination of the levels of vitamin C in the sample. The principle of the vitamin C content analysis of 2,6-DCPIP titration method is to set the levels of vitamin C in food by titration with 2,6-DCPIP where there is a reduction reaction of 2,6-DCPIP the presence of vitamin C in an acid solution. Ascorbic acid to reduce the 2,6-DCPIP in a solution that is colorless. Function of reagent as an indicator of electron-accepting color and vitamin C which will change the dye from blue to red. End point marked with a color change to pink in acidic conditions]. Samples metaphosphate-acetic acid is added to prevent oxidation of vitamin C in the sample as long as the vitamin C will be a lot of exposure to oxygen, heat, and others. Therefore, to prevent excessive oxidation then added metaphosphate-acetic acid. In addition, metaphosphate-acetic acid solution also

serves to separate the vitamin C that is bound to protein.

The reactions occurring 2,6-DCPIP and vitamin C can be seen in Figure 1

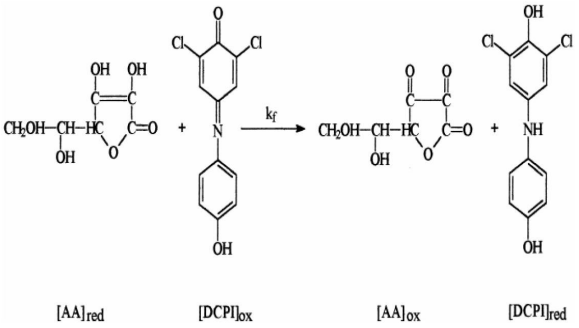

Fig. 1 Oxidation Vitamin C with 2,6-DCPIP

Assay of vitamin C in this study using the titration method in triplo. This method uses a dye solution as pentiter and sample solution as titrant. The sample used in this study beverage packaging, namely red guava fruit drink plastic bottles, tetrapack, cans and glass bottles. Then compare it with nutritional value information contained on the packaging label. Levels of vitamin C which is indicated on the packaging label expressed in percent RDA. Here, the information content of vitamin C contained on the packaging label per serving the drink plastic bottles (120%) in 150 mL, tetrapak (115%) in 250 ml cans (260%) in 238 mL glass bottles (20%) in 33 mL. To obtain the sequence of levels of vitamin C based label do the calculation in the same volume that is 100 grams for all products, for example in tetrapak contained 100 grams of vitamin C as much as 115% RDA.

The calculations are as follows:

$$\text{Mass vitamin C} = \frac{\text{mass of vitamin C}}{100} \times \text{RDA Vit C}$$

$$= \frac{115}{100} \times 60 \text{ mg}$$

$$= 69 \text{ mg}$$

$$\text{Mass Vitamin C in 100 mg} = \frac{100 \text{ mg}}{250 \text{ mg}} \times 69 \text{ mg}$$

$$= 27.6 \text{ mg}$$

When compared with information from the packaging label, all products have vitamin C levels decline. The order of the vitamin C content in percent of RDA per 100 grams by the label are as follows:

1. Beverage cans (65.54 mg / 100 g)
2. Beverage Packaging tetrapack (27.6 mg / 100 g)
3. Drink bottles plastic (48 mg / 100 g)
4. Drink a glass bottle packaging (36.36 mg / 100 g)

in the research that has decreased very high to a low run private consecutively on beverage packaging plastic bottles, glass bottles, cans, and tetrapack. Sample 1 juice in plastic bottles which have advantages and disadvantages as follows; advantages: the nature of gas and water vapor permeability of plastic packaging materials low, causing a longer shelf life of the product. While the drawbacks that the monomer substances and small molecule contained in plastic that can migrate into the packaged foodstuffs. Migration occurs as influenced by the temperature of food or storage and processing. The higher the temperature, the more monomers can migrate into. And based on the measurement results on Monday, June 13 th, 2016 on the drink plastic bottles has a vitamin C content of 12.01 mg / 100 g, which amount is measured 7 months ahead of expiration. While on the packaging label for 48 mg / 100 g . This shows that the levels of vitamin C in beverages plastic bottles experienced a drastic decline, it is because in addition to processing, the expiration date is also the transmission of light into the packaging, sometimes required in order to view the contents of the packaging.

Sample 2 juice in tetrapack packaging. The process of making the packaging consists of six layers arranged from the outermost layer to the innermost layer:

a. Polyethylene (LDPE) is the layer that provides protection from humidity environmental outside of the package.

b. Paperboard serves as the guardian of the stability of the form and give the strength of the various pressures.

c. Polyethylene (LDPE) in the third layer serves as an adhesive.

d. Aluminum foil is useful to keep the liquid from light, oxygen, and
off-flavorsas well as maintaining the stability of taste.

e. Adhesive polymer in the fifth layer serves as an adhesive.

f. M-polyethylene is the innermost layer that serves as a sealing.

This packaging has advantages and disadvantages. Those advantages are created by and UHT aseptic packaging. Aseptic packaging is packaging material in a container that meets the four conditions, in the sterile container products or place and environment in product filling and packing containers used must be sealed to prevent re-contamination during storage. While the UHT (Ultra High Temperature) that is heating to a high temperature (135ºC-150ºC) for 2-5 seconds. And based on the measurement results on Monday, June 13 th, 2016 at tetrapack packaging beverages have vitamin C content of 17.99 mg / 100 g which amount was measured 5 months before expiration. While on the packaging label of 27.6 mg / 100 g This shows that the levels of vitamin C in tetrapack packaging beverages has decreased, it is caused during processing and storage.

3 samples of juice in cans which have advantages and disadvantages as follows; advantages that can reduce the concentration of oxygen, so as to reduce the possibility of changes due to oxidation reactions such as oxidation of vitamins, fats, discoloration and corrosion processes. If the storage conditions

allowing the microbes to grow, then the microbes would multiply and spoil the food in the cans. And based on the measurement results on Monday, June 13 th, 2016 on beverage cans had higher levels of vitamin C that is 31.46 mg / 100 g, which amounts are measured 6 months before expiry. While on the packaging label of 65.54 mg / 100 g This shows that the levels of vitamin C in beverage cans experienced a drastic decline, it is because in addition to processing, expiration date cans also have a corrosive nature caused much residual oxygen in foodstuffs, especially in air spaces, temperature, and storage time.

Sample 4 juice in a bottle glass has advantages and disadvantages as follows; ie the excess glass packaging does not react with the product packed.. And based on the measurement results on Monday, June 13th, 2016 on the beverage packing glass bottles have the vitamin C content of 13.00 mg / 100 g, which amount is measured 7 months ahead of expiration. While on the packaging label of 36.36 mg / 100 g This shows that the levels of vitamin C in the packaged beverage glass bottles decreased. This is due in addition to the processing and storage glass bottle packaging also has the properties of invisibility is less favorable for vitamin C is sensitive to light.

Table I Result Quantitative Analysis Of Sample

Sample Packaging	Titration	Weight Sample (gram)	Volume 2.6-DCPIP as Volume Titration (mL)	Level (mg/100gr)	Average Level (mg/100gr)	Level Packaging (mg/100gr)	Expired Date
Plastic Bottle	1	10.015	0.6	13,12			
	2	10.032	0.5	9.82	12.01	48	January, 11, 2017
	3	10.026	0.6	13.10			
Tetrapack	1	10.362	0.6	19.02			
	2	10.445	0.5	18.87	17.99	27.6	November, 7, 2016
	3	10.217	0.6	16.08			
Tin Can	1	10.030	1.2	32.76			
	2	10.221	1.2	32.14	31.46	65.46	Desember, 23, 2016
	3	10.027	1.1	29.49			
Glasses Bottle	1	10.050	0.6	13,07			
	2	10.040	0.6	13.09	13.00	36.36	January, 21, 2017
	3	10.220	0.6	12			

CONCLUSIONS

The results of quantitative assay of vitamin C in some variation of beverage packaging using 2,6-DCPIP obtained vitamin C content of red guava fruit drinks packaging tetrapack measured at 5 months prior to the expiry of 17.99 mg / 100 g whereas on the packaging label of 27.6 mg / 100 g, cans were measured at 6 months before the expiry of 31.46 / 100 g while the label packaging by 65.54 mg / 100 g, the glass bottles was measured at 7 months before expired at 13.00 mg / 100 g while the label packaging by 36.36 mg / 100 g and plastic bottles were measured at 7 months before the expiry of 12.01 / 100 g while the label is 48 mg / 100 g. This indicates that the packaging variations affect levels of vitamin C were characterized by a decrease in the levels of vitamin C, so that the levels of vitamin C research results do not match the information on the packaging of nutritional value. Beverage packaging the most stable compared to other packaging is tetrapack beverage packaging due to decreased vitamin C is less even though the expiration date is closer than any other packaging that they have a longer time expired.

REFERENCES

[1] Winarno, FG 2004, "Food Chemistry and Nutrition", PT. Gramedia Pustaka Utama, Jakarta, Pg. 154.

[2] Parimin 2005, "Variety Guava Cultivation and Utilization", Sower Swadaya, Jakarta, Pg. 7-11.

[3] Wardani, LA, 2012, "Validation of Methods of Analysis and Determination of Content Vitamin C in Beverage Packaging by spectrophotometry UV Visible", MIPA UI, Depok, Pg. 25-33.

[4] Almatsier, Sunita, 2010, "Basic Principles of Nutrition", PT. Gramedia Pustaka Utama, Jakarta, Pg. 185-190.

[5] Sudarmadji, S., 2010, "Analysis of Food and Agriculture", Publisher Liberty, Yogyakarta, Pg. 165.

[6] Stars, M., 2010, "Biochemical Engineering Research", Erland, Jakarta56-59.

[7] Achmad Djaeni Sediaoetomo, 2000, "Science of Nutrition for Students and Professionals in Indonesia", Volume I, Dian Rakyat, Jakarta, Pg. 75-76.

[8] Syarief, R., S.Santauna, St.Ismayana B., 1989, "Food Packaging Technology", Laboratory of Food Process Engineering, PAU Food and Nutrition, IPB, Pg. 9.

[9] Nurminah, M., 2002, "The Nature of Various Materials Research and Paper and Plastics Packaging Materials Packaged Effect on" digital USU, Medan, Pg. 15-19

[10] Harmita 2004, "Implementation Guidelines for Methods and Method Validation Calculations", Science Magazine Kefarmasiaan, Department of Pharmacy FMIPAUI, Pg. 1-6.

★★★

IMPLEMENTING MPI COMMUNICATION INFRASTRUCTURE IN A BROWSER-BASED DISTRIBUTED COMPUTING ENVIRONMENT

[1]CHUNG YUNG, [2]LUCAS PAN

[1,2]Department of Computer Science and Information Engineering, National Dong Hwa University
E-mail: {yung@mail, 610421218@gms}.ndhu.edu.tw

Abstract—The goal of this paper is to utilize the web browsers as a distributed computing environment. We analyze the advantages and disadvantages to popular communication infrastructures for distributed systems when implementingthem in a browser-based distributed computing environment. Our analysis shows that MPI is one of the good candidates that may be implemented in a browser-based distributed computing environment for its simplicity and its compatibility with the popular web browsers, such Google Chrome and Mozilla Firefox. With our MPI infrastructure, we implement a distributed merge sort system that may be executed in three configurations of the distributed environment: one client with one server, one client with two servers, and one client with four servers. Since almost all the computers and mobile devices have web browsers installed, our infrastructure may be easily ported to the distributed systems with various hardware configurations.

Index Terms— Distributed communication models, web browsers as computing environments, distributed systems.

I. INTRODUCTION

As modern browsers have evolved into sophisticated computing environments [1], [2], the goal of our work is exploring the possibility to utilize the web browsers as a distributed computing environment.

The prosper development of high-speed computer networks nurtures the evolution of distributed systems [3]. By the definition given by Tanenbaum and Steen [4], a distributed system is a collection of independent computers that appears to its users as a single coherent system.

The mechanism of interprocess communication is at the heart of all distributed systems [4]. Among various communication models proposed for efficient communication, the standard message passing interface (MPI) [5]is one of the most popular infrastructures used in practical distributed systems [6-9]. Since the official MPI bindings are currently defined only for C, Fortran, and C++, there are a few efforts working on extending MPI to the other programming languages and platforms [10-14].
With a sandboxing technology, the modern browsers allow safely running native programs, and usually the browsers offer a standard interface in theJavascript language[1], [2]. This motivates our investigation on implementing the MPI communication infrastructure in a browser-based distributed computing environment with an interface in Javascript.
Our investigation includes three phases. First, we analyze the advantages and disadvantages to popular communication infrastructures for distributed systems when implementing them in a browser-based distributed computing environment. Our analysis shows that MPI is one of the good candidates that may be implemented in a browser-based distributed computing environment. Second, we slightly modify the standard MPI infrastructure and propose anapplication program interface for developing distributed software in a browser-based computing environment. We reference the official proposal of the message passing interface standard [5], and apply the required modifications for the use in a browser-based computing environment.

And last, we implement the proposed MPI infrastructure and apply it when developing a browser-based distributed merge sort system. The result shows the feasibility of our proposal.

The rest of this paper is organized as follows. In Section 2, we survey a few communication infrastructures for distributed systems, and we analyze their advantages and disadvantages when implementing in a browser-based distributed computing environment. The discussion motivates the proposal of a modified version of the MPI infrastructure specialized for a browser-based distributed environment, which we describe in Section 3. Section 4 presents our implementation and application to the browser-based distributed merger sort system. The case study shows the feasibility of our proposal in Section 3. At last is a brief conclusion.

II. BACKGROUND

In this section, we discuss a few communication infrastructures proposed for distributed systems in the literature. We analyze their advantages and disadvantages when implementing them in a browser-based computing environment.

According to the discussion in [4], we classify the communication infrastructures for distributed systems into four categories: remote procedure call (RPC) based infrastructures, message-oriented communication (MOC) based infrastructures, stream-oriented communication (SOC) based infrastructures, and multicast communication (MCC) based infrastructures.

A. RPC-based Infrastructures

The communication infrastructures that allow programs to call procedures located on the other machines are known as remote procedure call, or often just RPC. For example, when a process on machine A calls a procedure on machine B, the calling process on A is suspended, and the execution of the called procedure takes place on B. Information can be transported from the caller to the callee in the parameters and can come back in the procedure result [4].

For the consideration of implementing RPC-based infrastructures in a browser-based computing environment, we found that such infrastructures usually require the compilers to have the information about the remote procedures in order to generate efficient execution code, and it is a little bit complicated for a browser to make corresponding adjustment.

B. MOC-based Infrastructures

The message-oriented communication (MOC) infrastructures in distributed systems allow asynchronous implementations of the communication mechanism and thus are applied in many distributed systems with inherent asynchronous nature [4]. Among various models proposed for MOC-based infrastructures, the message passing interface (MPI) is designed for high-performance parallel applications and makes it easy to understand the diversity in different communication primitives.

Since the message-oriented primitives have a popularly recognized standard and allow the developers to easily write highly efficient applications, the MOC-based infrastructures, especially MPI, can be used together with web browsers when implementing the communication infrastructure.

C. SOC-based Infrastructures

The scream-oriented communication (SOC) infrastructures in distributed systems are designed for the use of exchanging time-dependent information such as audio and video streams [4]. It is not interested in the work described in this paper.

D. MCC-based Infrastructures

The multicast communication (MCC) infrastructures are designed for the support of sending data to multiple receivers [4]. With the advent of peer-to-peer technology and notably structured overlay solutions, it is now easy to set up communication paths for multicast. It is not interested in the work described in this paper, either.

III. PROPOSED MPI INFRASTRUCTURE

In this section, we present the proposed MPI infrastructure, which is slightly modified from the standard MPI [5] with an intension of implementation in a browser-based distributed computing environment.

```
1. MPI_Init (argc, argv);
2. MPI_Finalize ( );
3. MPI_Comm_size (MPI_COMM_WORLD, &nproc);
4. MPI_ Comm_ rank (MPI_COMM_WORLD, &myid);
5. MPI_ Send ((void *)&data, icount,
   DATA_TYPE, idest, itag, MPI_COMM_WORLD);
6. MPI_ Recv ((void *)&data, icount,
   DATA_TYPE, isrc, itag, MPI_COMM_WORLD,
   istat);
```

Figure 1: Proposed API for an MPI infrastructure

We propose that the MPI infrastructure for a browser-based distributed computing environment have the six methods whose application program interface (api) is listed in Figure 1.

- MPI_Init initializes MPI execution environment.
- MPI_Finalize terminates the MPI execution environment.
- MPI_Comm_sizedetermines the size of the group associated with a communicator.
- MPI_Comm_rankdetermines the rank of the calling process in the communicator.
- MPI_Sendperforms a blocking send.
- MPI_Recvperforms a blocking reception for a message.

Please note that our proposed MPI infrastructure is targeted for the client/server model shown in Figure 2. In such cases, the methods listed in the proposed MPI infrastructure facilitate the synchronous communication for reads and writes.

IV. A CASE STUDY ON DISTRIBUTED MERGE SORT

For verifying the feasibility of the proposed MPI infrastructure presented in the previous section, we implement a distributed merge sort system, which is executed in a browser-based computing environment. The implementation is in the Javascript language. The implemented distributed merger sort system has been tested on both Windows 8 and Ubuntu 14.04 operating systems withthe Google Chrome browsers [15] (version 60.0.3112.113) installed.

The block diagram for the distributed merge sort that we implement is show in Figure 3, which includes an html file for the web page, a json file for transmitting data objects, and five js files of Javascript programs.

Our implementation of the distributed merge sort system includes a flexible configuration module such that the system may be executed for three configurations of the distributed platforms: one client / one server, one client / two servers, and one client / 4 servers.

Figure 4 shows the message-passing behavior for the distributed merge sort system in the three configurations.

- In the one client / one server configuration, the

client main module calls to a random number module to generate a list of numbers for sorting. It calls to the server main module, passing the list of numbers. The server main module calls to the merge sort module for sorting, and then return the sorted list of numbers to the client.

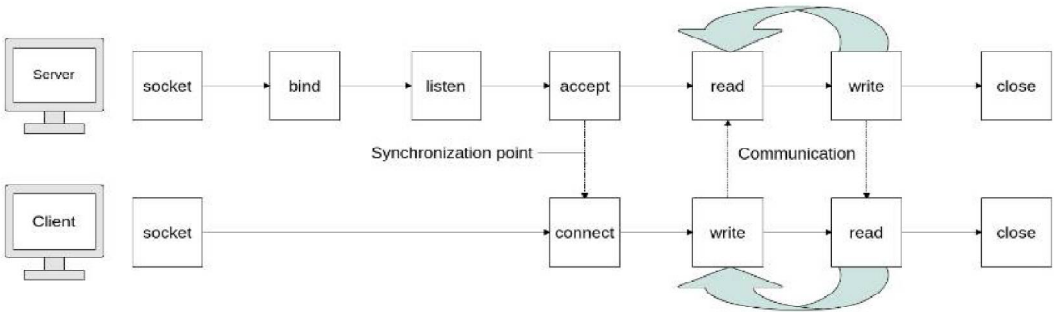

Figure 2: The targeted client/server model

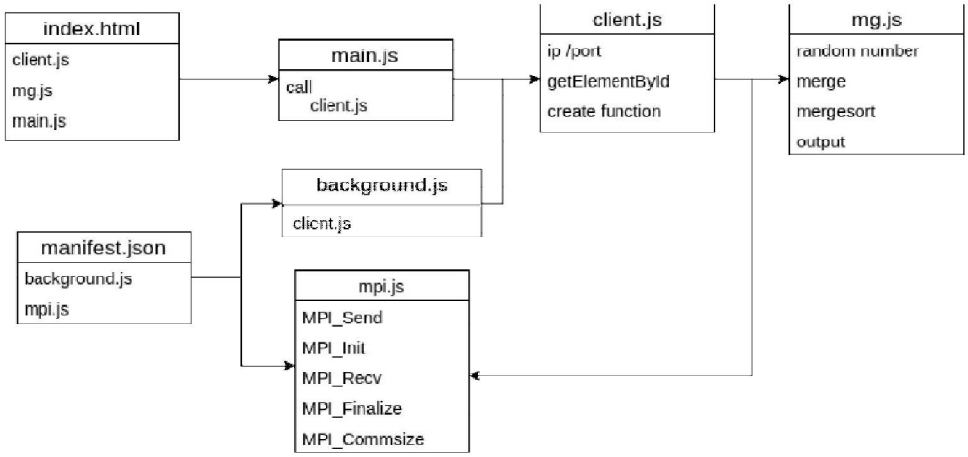

Figure 3: Block diagram of a distributed merge sort system

- In the one client / two servers configuration, the client main module calls to a random number module to generate a list of numbers for sorting. It calls to the two server main modules simultaneously, passing a half of the list to each. Each of the server main modules calls to the merge sort module on its site for sorting, and then returns the sorted list of numbers to the client. Finally, the client main module calls to the merge sort module on its site for sorting the two lists returned and then generates the overall sorted list.
- In the one client / four servers configuration, the client main module calls to a random number module to generate a list of numbers for sorting. It calls to the four server main modules simultaneously, passing a quarter of the list to each. Each of the server main modules calls to the merge sort module on its site for sorting, and then returns the sorted list of numbers to the client. Finally, the client main module calls to the merge sort module on its site for sorting the four lists returned and then generates the overall sorted list.

Figure 5 includes the screen snapshots of running the distributed merge sort system. Figure 5 (a) is the screen snapshot of running the distributed merge sort system in the one client / one server configuration, while Figures 5 (b) and (c) are those of one client / two servers and one client / four servers configurations, respectively.

CONCLUSION

In this paper we present our work in exploring the possibility of implementing the MPI communication infrastructure in a browser-based distributed computing environment.

We first analyze the advantages and disadvantages to popular communication infrastructures for distributed systems when implementing them in a browser-based distributed computing environment, and our analysis shows that MPI is one of the good candidates that may be implemented in a browser-based distributed computing environment.

Then, we slightly modify the standard MPI infrastructure and propose an application program interface for developing distributed software in a browser-based computing environment.

And last, we implement the proposed MPI infrastructure and apply it when developing a browser-based distributed merge sort system. The result shows the feasibility of our proposal.

A final note is that since almost all the computers and mobile devices have web browsers installed, our implemented MPI infrastructure may be easily ported to the distributed systems with various hardware configurations.

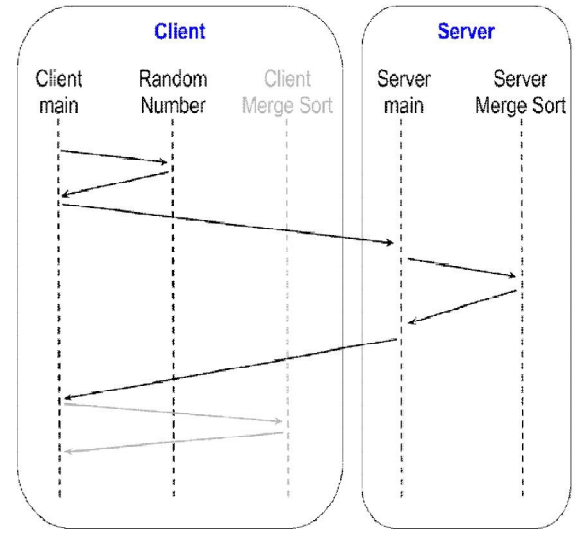

(a) In one client / one server configuration

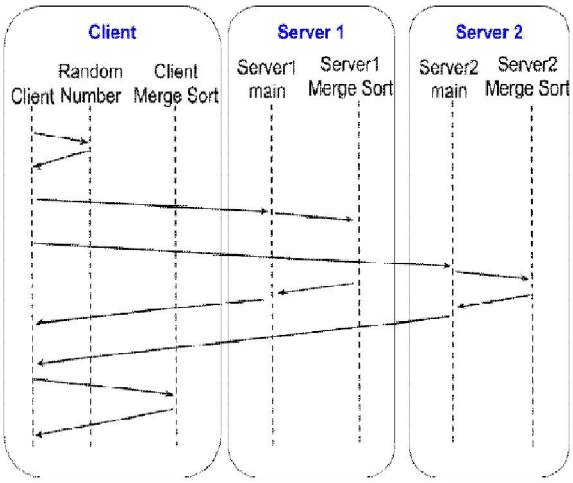

(b) In one client / two servers configuration

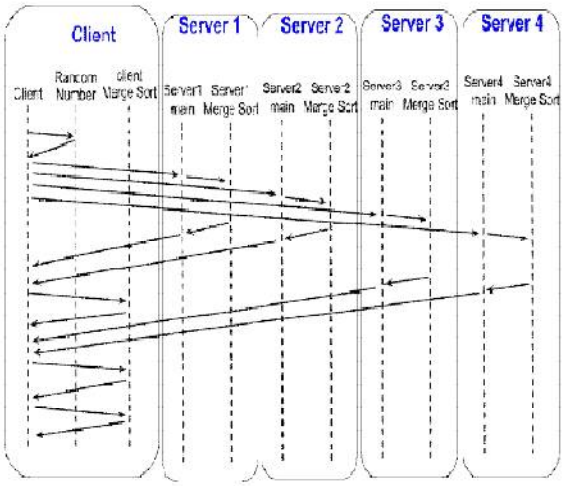

(c) In one client / four servers configuration

Figure 4: The message-passing behavior

REFERENCES

[1] A.Saini, M. S. Gaur, V.Laxmi, and P. Nanda,"sandFOX: Secure Sandboxed And Isolated Environment for Firefox Browser,"Proceedings of the 8th International Conference on Security of Information and Networks (SIN '15), pp. 20-27, September 2015.

[2] J.Mickens, and M.Dhawan,"Atlantis: Robust, Extensible Execution Environments for Web Applications,"Proceedings of the Twenty-Third ACM Symposium on Operating Systems Principles (SOSP '11), pp. 217-231, October 2011.

[3] C. Yung, W.-K. Tu, and C.-C. Hsu,"A Table-Driven Algorithm of Garbage Collection for Active Objects,"The Communication of the Institute of Information & Computing Machinery, vol. 11, no. 3, pp. 41-55, September 2008.

[4] A. S. Tanenbaum, and M. van Steen, Distributed Systems: Principles and Paradigms, 2nd Edition, Prentice-Hall, Inc., 2006.

[5] MPI Forum, "MPI: A Message-Passing Interface Standard," Technical Report, The Message Passing Interface Forum, November 1994.

[6] E.M. Ammann,"DIPC-a Monitor for Distributed Inter-process Communication," Proceedings of Euromicro Workshop on Parallel and Distributed Processing, pp. 272-279, January 1995.

[7] J. vanKatwijk, Y. Peng, and J. Zalewski, "Performance Comparison of Four Software Architectures for Distributed Computations,"Proceedings of the International Conference on Parallel Computing 1999 (Parco'99), pp. 582-589, August 1999.

[8] L. Chai, R. Noronha, and D. K. Panda, "MPI over uDAPL: Can High Performance and Portability Exist Across Architectures?"Proceedings of theSixth IEEE International Symposium onCluster Computing and the Grid (CCGRID 06), vol. 1, pp. 16-29, May 2006.

[9] K.Qureshi, and H. Rashid,"A Performance Evaluation of RPC, java RMI, MPI and PVM," Malaysian Journal of Computer Science, vol. 18, no. 2, pp. 38–44, December 2005.

[10] A.Nelisse, J.Maassen, T.Kielmann, and H. E. Bal, "CCJ: Object-based Message Passing And Collective Communication in Java,"Concurrency and Computation: Practice and Experience, vol. 15, no. 3-5, pp. 341-369, March 2003.

[11] B. Carpenter, V.Getov, G. Judd, A.Skjellum, and G. Fox, "MPJ: MPI-like Message Passing for Java,"Concurrency and Computation: Practice and Experience, vol. 12, no. 11, pp. 1019-1038,September 2000.

[12] M.Eggen, and R.Eggen,"Java versus MPI in a Distributed Environment,"Proceedings of the International Conference on Parallel and Distributed Processing Techniques and Applications, pp. 390-395, July 1999.

[13] M. Baker, B. Carpenter, G. Fox, S. H.Ko, and S. Lim, "mpiJava: An Object-Oriented Java Interface to MPI," Proceedings of the 11th IPPS/SPDP'99 Workshops Held in Conjunction with the 13th International Parallel Processing Symposium and 10th Symposium on Parallel and Distributed Processing, pp. 748-762, April 1999.

[14] S.Bansal, and N.Pandey,"An Overview of Portable Distributed Techniques,"International Journal of Computer Science Issues (IJCSI), vol. 7, issue 3, no. 1, pp. 27-32, May 2010.

[15] Google, Inc., "What are Chrome Apps?" https://developer.chrome.com/apps/about_apps, as viewed on May 2017.

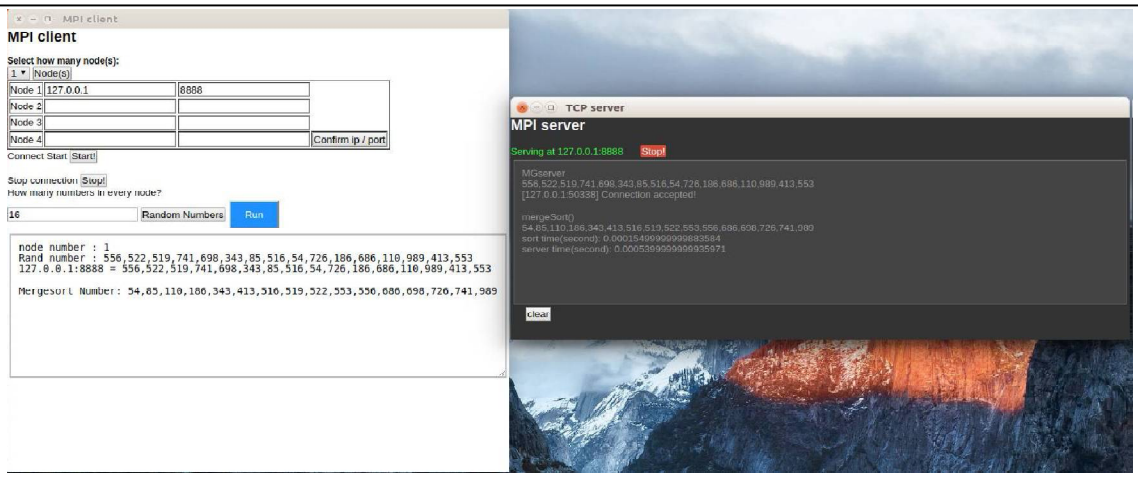

(a) In one client / one server configuration

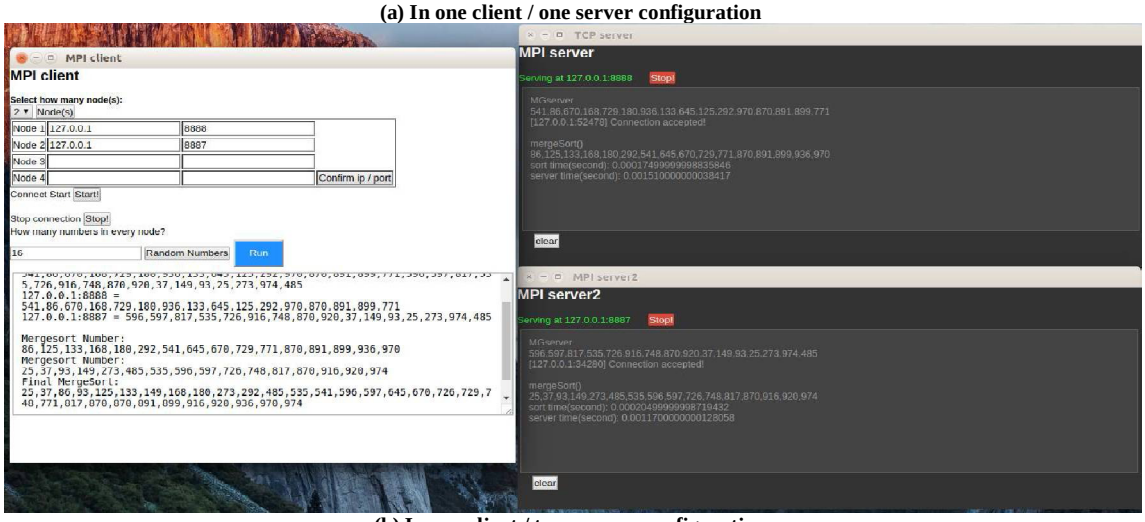

(b) In one client / two servers configuration

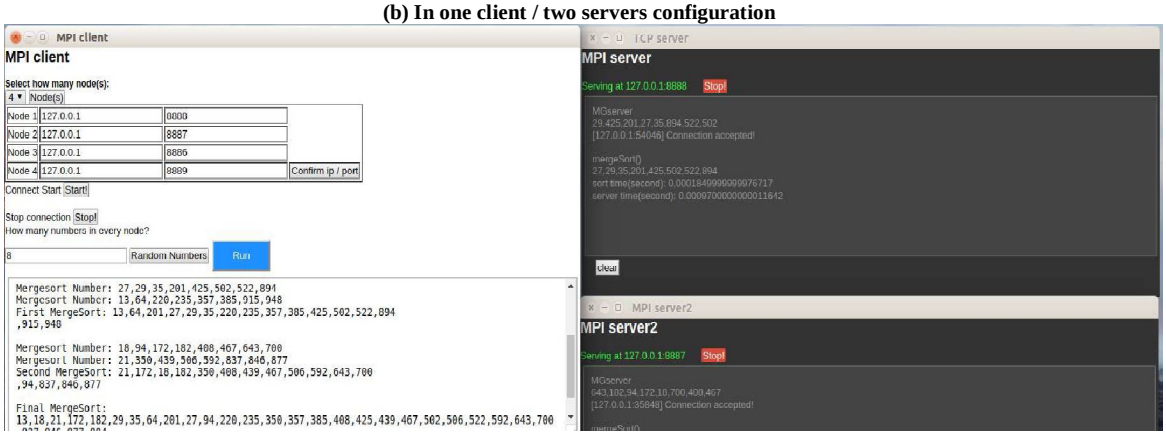

(c) In one client / four servers configuration

Figure 5: The snapshot of running our implementation

★★★

CONCRETE MIXTURE WITH PLASTIC AS FINE AGGREGATE REPLACEMENT

[1]CHIEN-CHUNG CHEN, [2]NATHAN JAFFE, [3]MATT KOPPITZ, [4]WESLEY WEIMER, [5]ALBERT POLOCOSER

[1,2,3,4,5]Purdue University Calumet, Missouri University of Science and Technology, Missouri University of Science and Technology, Missouri University of Science and Technology, Missouri University of Science and Technology
E-mail: [1]chien-chung.chen@purduecal.edu, [2]njjz72@mst.edu, [3]mjkd5d@mst.edu, [4]wawdm3@mst.edu, [5]apf29@mst.edu

Abstract- The objective of this research is to investigate the effectiveness of using waste plastic as fine aggregate replacement in concrete mixtures. The compressive and tensile strengths of various concrete specimens were tested to determine how the incorporation of recycled plastic as a replacement fine aggregate would affect the development of strength in the mixes. Six mixes were compared at replacement increments of 0%, 10%, 20%, 30%, 50% and 100%. All stages of plastic replacement showed a noticeable decrease in compressive strength. The 10% replacement level only showed a 15% loss of compressive strength at 28 days compared to the control. Despite being much weaker in compression, the tensile strength test showed that the 10%, 20% and 30% replacement increments were stronger in tension compared to the control. An additional test was conducted to determine whether the plastic aggregate would change the heat absorption and heat transfer of the concrete. This test showed noticeable difference between the test samples and the control. The 10%, 20% and 30% replacement mixes showed a significant decrease in heat absorption, and a minor decrease in heat transfer through the test slab.

Index Terms- Alternative recycling methods, green concrete, plastic, sustainable building materials.

I. INTRODUCTION

Concrete, one of the most common construction materials, requires a large amount of natural resources and energy. Natural resources used in concrete mixtures include lime stone, clay, sand, natural gravel, crushed stone, and water. With the rapid development in urban areas around the world in the recent years, our natural resources are depleting in an ever-increasing rate.Therefore, it is necessary to develop a new material that consumes less natural resources and energy in order to make our construction methods more sustainable. Many efforts have been made to study the use of waste/by product materials, such as fly ash, slag, silica fume, and natural pozzolan, to replace portland cement in a concrete mixture [1-6].

Others [7-12]
studied effects of plastic in concrete mixtures as aggregate replacement on material properties.While the previous studies showed potential advantages of using plastics in concrete (e.g., light weight and low energy consumption),they also reported some disadvantages, such as decreases in compressive strength and flexural strength of plastic concrete mixtures with the increase of the plastic ratio in the mixtures. Furthermore, material properties of plastic concrete mixtures may vary depending on the type of plastics that is used in the mixtures. For this reason, it was of interest of this research to study effects of one type of plastics, high-density polyethylene (HDPE), on concrete properties. This paper investigated the application of HDPE plastic on partial/full fine aggregate replacement for concrete mixtures.

II. EXPERIMENTAL PROGRAM

A. Material Preparation

Concrete materials used in this study included type I portland cement, river sand, ¾ inch crushed limestone,and water. Both sand and crushed limestone used in this study conformed to ASTM C33 [13]for concrete aggregates as fine and coarse aggregates. HDPE was selected as the plastic for fine aggregate replacement in this study. The purpose for the experiment was to determine how best to incorporate construction waste materials back into concrete saving both energy and reducing the need to discard plastic waste into landfills. The experiment began by finding the gradation of the fine aggregate owing to that the gradation of sand could provide a baseline for the desired incorporation of recycled HDPE plastic as a fine aggregate replacement option.Sieve analysis was performed on a river sand sample to determine its gradation. The gradation test was conducted in accordance with ASTM C 136 [14],and the results can be found below in Table 1. Initially, the goal was to mimic the sand gradation with the plastic gradation exactly; however, after a sieve analysis of the pulverized HDPE plastic was completed, this was deemed impracticable. As seen in Figure 1, the pulverized HDPE plastic has a much finer gradation than the sand. To accurately replace the gradation of the sand with the plastic, all of the plastic would have had to been sieved, weighted, and then remixed at the correct ratios. This process would have resulted in a lot of wasted plastic, which would have been counterproductive to the green initiative this project intended to propose.

Table 1: Sand gradation

Sieve Number	Diameter (mm)	Mass of plasticRetained (grams)	Percent Retained (%)	Percent Finer (%)
3/8"	9.53	0.0	0%	100.0%
4	4.75	13.6	0.9%	99.1%
8	2.36	89.1	5.9%	93.2%
16	1.18	183.5	12.2%	81.0%
30	0.60	419.1	27.8%	53.2%
50	0.30	641.6	42.6%	10.6%
100	0.15	155.6	10.3%	0.3%
Pan	-	3.9	0.3%	0.0%
	Sum =	1506.4		

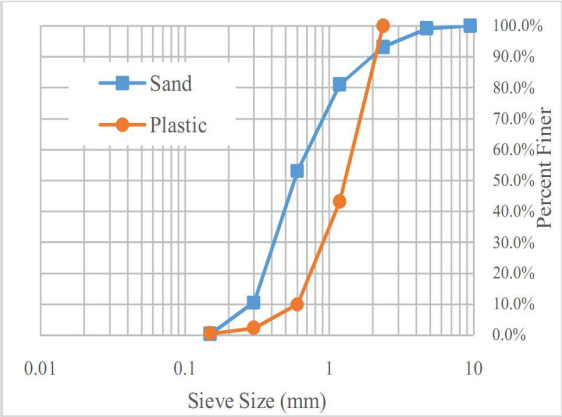

Figure 1 Gradation of sand and HDPE plastic

Further analysis of the pulverized plastic revealed that the plastic retained on the #8 sieve and larger was flat and elongated. Therefore, these sizes were disregarded, collected and re-pulverized. The increased surface area from the strips would have caused a destabilization of the concrete mixture. Also the elongated strips would have incorporated slick surfaces within the concrete, which could prevent the cement from properly adhering to the aggregate. After removing the flat and elongated pieces, another sieve analysis was performed, and the results can be found in Table 2.

Table 2: Plastic gradation from pulverization

Sieve Number	Diameter (mm)	Mass of plastic Retained (grams)	Percent Retained (%)	Percent Finer (%)
8	2.36	0.0	0.0%	100.0%
16	1.18	199.1	57.0%	43.0%
30	0.60	115.4	33.0%	10.0%
50	0.30	27.2	7.8%	2.2%
100	0.15	6.1	1.8%	0.5%
Pan	-	1.6	0.5%	0.0%
	Sum =	349.5		

In order to compensate for the removal of the #8 sieve size and above, and to model better the initial gradation of the sand, HDPE plastic pellets were added to the pulverized plastic. The quantity of pellets added was based on the original gradation of the river sand. The design gradation determined for the tests can be found in Table 3.The percent of pellets added to the plastic was based on the percent retained on the #4 and #8 sieve of the sand, i.e., the percent retained on the #4 and #8 sieve from the sand gradation (Table 1) equals the percent retained on the #8 sieve for the plastic (Table 3).

Table 3: Plastic gradation used in mix for design

Sieve Number	Diameter (mm)	Percent Retained (%)	Percent Finer (%)
4	4.75	0%	100%
8	2.36	6.8%	93.2%
16	1.18	53.1%	40.1%
30	0.60	30.8%	9.3%
50	0.30	7.3%	2.1%
100	0.15	1.6%	0.4%
Pan	-	0.4%	0%

B. Mix Design

Using the aforementioned materials, mix proportions for one control mix and five experimental mixes were created. The control mix was designed with a 0.5 water to cement ratio. The mix design was determined so that a reasonably concrete strength would be achieved to adequately determine the strength degradation induced by the increasing quantity of plastic. The experimental sample mixes utilized the same mix design with the exception of the fine aggregate. Mix designs for the control mix and the five experimental mixes with varying fine aggregate replacement levels are shown in Table 4.

The water content of the actual batch weight was adjusted to account for the absorption of the aggregates. For the HDPE plastic, due to the susceptibility of plastic to heat, an absorption testrequiring heating samples in an oven was difficult to perform. Based on the manufacturer specifications, the HDPE plastic had an absorption between 0% and 0.1%. Therefore, for the purpose of this experiment, it was assumed that the HDPE had no absorption. Recycled white HDPE plastic resin was used for the experiment to amplify the potential reflectivity of the concrete. The HDPE plastic replaced the sand by volume. As mentioned previously, both the HDPE plastic and the sand were in a state of 0% absorption. Therefore, as the volume of sand was reduced and plastic added, the water content in the sample mixes did not need to be adjusted.

Table 4: Mix proportions (kg/m^3)of the control and sample mixes

Material	Control	10%	20%	30%	50%	100%
CA (SSD)	1098	1098	1098	1098	1098	1098
FA (SSD)	829	746	663	580	414	0
Cement	307	307	307	307	307	307
Water	153	153	153	153	153	153
Plastic	0	14	27	41	68	137

C. Test Procedures

After the concrete mixtures were properly mixed, the temperature of the batch was recorded. Then the air content was determined using the pressure method in accordance with ASTM C231 [14]. Also, the slump of each concrete mix was measured according to ASTM C143 [15]. Seven 100 mm(diameter) x 200 mm (height) cylinders and one 305 mm (width) x 305 mm(length) x 25 mm(thickness) slab were produced for each mix. Cylinder specimens were made following ASTM C31 [16]. The cylinders were used for compression and tension tests, and the slab was used for testing the heat absorption of the control and experimental samples. The specimens were initially cured for twenty four hours and then placed in a water tank and cured for twenty seven days. Two cylinders were broken at seven days, fourteen days, and twenty eight days following ASTM C39 [17]. The splitting tensile strength was measured with the last cylinder. The cylinder was cut in half and the splitting tensile strength was performed on both specimens. The slabs were initially cured for twenty four hours and then removed from the molds and placed in a water tank for twenty seven days. For testing, the slabs were placed on a concrete floor. 250 watt heat lamps with reflectors were placed one foot above the slab. The lamps were run for seventy five minutes. The temperatures were measured on the front and back every fifteen minutes with an infrared heat gun.

D. Results and Discussions

Table 5provides the results of the fresh concrete tests. Due to its light weight property, the plastic aggregate caused a reduction in the unit weight of the concrete. The concrete showed a resistance to compaction, or more appropriately stated, the concrete would only remain compacted temporarily. Immediately after the concrete was rodded or vibrated the plastic acted like a spring. The plastic expanded in order to alleviate the internal stress induced by the compaction, and the expansion, in turn, created an increased air content within the concrete. Furthermore, the slump tests proved futile. Since the plastic caused expansion within the concrete, the slump test could not be considered an indicator of potential workabilityof the concrete with plastic as partial/full fine aggregate replacement. In the case of the 100% replacement sample, the slump cone grew in size, hence a negative slump valuewas recorded. Although the slump for the control and 10% replacement samples wasconsidered workable. The mixes with plastic replacement levels beyond 10% showed significant loss in workability. Especially, for the 50% and 100% replacement levels, the mixesshowed lost cohesion and exhibited unworkable conditions. The measured temperatures for all samples were comparable.

Table 5: Fresh concrete properties of test specimens

Percent Replacement (%)	Slump (mm)	Temperature (°C)	Air Content (%)	Unit Weight (kg/m^3)
0	0	18	2.1	2,387
10	5	16	2.3	2,323
20	0	17	2.3	2,243
30	0	19	4.4	2,179
50	5	17	5.6	2,034
100	-5	17	10.2	1,698

Table 6 and Table 7 show the compressive strength and strength loss of test specimens, respectively. Results showed a significant variation in the strengths of the concrete samples. As the percentage of plastic replacing the sand increased, the compressive strength of the concrete decreased.At 10% replacement of the fine aggregate with HDPE, the strength of the concrete decreased by approximately 15%. Likewise, at 20% replacement, over 30% of the compressive strength of the concrete was lost. The 50% and 100% replacement samples lost cohesion and suffered from extreme loss of compressive strength. Additionally, both samples were found to be pervious. This was likely due to the unusual shape of the HDPE aggregate and the excessively high air content. The 28 day compressive strengths for the 30% plastic replacement sample turned out to be unusually weak. The reason for this anomaly was uncertain and warranted further investigation. The most likely explanation was that the cylinders broken at 28 days were poorly compacted or otherwise flawed, and these internal flaws caused the cylinders to break prematurely. It would be highly unusual for a 28-day compressive strength to be below the 7-day and 14-day compressive strengths for the same batch of concrete.

Table 6: Compressive strength of test specimens

Percent Replacement (%)	Compressive Strength		
	7-day (MPa)	14-day (MPa)	28-day (MPa)
0	26.7	37.3	41.2
10	22.9	32.5	35.2
20	18.3	24.8	28.0
30	12.1	18.2	8.1
50	6.2	9.8	9.5
100	0.8	0.9	1.1

Table 7: Compressive strength loss

Percent Replacement (%)	% Strength Loss vs. Control		
	7-day (%)	14-day (%)	28-day (%)
0	0.0	0.0	0.0
10	14.2	12.9	14.6
20	31.5	33.5	32.0
30	54.7	51.2	80.3
50	76.8	73.7	76.9
100	97.0	97.6	97.3

The split-cylinder testsshowed a different result as compared to that of the compression tests, i.e., the compression tests showed a loss of strength with the increase of plastic while the split-cylinder tests showed the opposite. As can be seen in Table 8, the control batch was weaker in tension than the 10%, 20% and 30% replacement mixes. Even the 30% replacement mix which was over 50% weaker in compression vs the control mix, was 2% stronger in splitting tensile strength. It appeared that the addition of HDPE plastic caused fundamental changes the way that concrete behaved. It was likely that the inherent stringiness of the plastic (a byproduct of the shredding/pulverizing process) provided internal shear and tensile reinforcement. The plastic behaved in a similar fashion to the way steel and synthetic fiber reinforcement fortified the concrete inhibiting the spread of cracks and fractures. Determining the optimum level of plastic replacement of the fine aggregate to attain the greatest tensile strength would require additional research and testing. The optimum amount of plastic cannot be directly interpolated because the tensile strength is dependent on two distinct variables: the compressive strength of the concrete and the amount of plastic in the mix. Additional study will be necessary to determine how each of the variables affect the tensile strength.

Table 8: Splitting tensile strength of cylindrical test specimens

Percent Replacement (%)	Splitting Tensile Strength (MPa)
0	3.15
10	3.30
20	3.70
30	3.20
50	2.80
100	0.20

There was a significant difference in the amount of heat absorbed by the concrete samples that incorporated plastic to replace the sand in the concrete mixture. Table 9 tabulates the difference in temperatures between the front and back surfaces of the concrete slab. Detailed temperature data measured during the testsare reported in Appendix. Results showed that the 10%, 20% and 30% aggregate replacement mixes absorbed heat at a slower rate as compared with the control. Furthermore, all of the sample mixes had a higher temperature differential between the front and back of the slabs compared to the control mix. The 50% and 100% replacement levels showed a much higher temperature differential compared to the other mixes, but they also absorbed much more heat than the other mixes. It is likely that at these higher replacement levels, the higher air content in the concrete inhibited the transfer of heat through the slab. Additionally, at the 50% and 100% replacement levels, the plastic was visible on the surface of the slabs. It is possible that the plastic on the surface absorbed a large percentage of the heat, preventing its ability to pass through the concrete slab.

Table 9: Temperature differentials measured from thermal conductivity tests

Percent Replacement	Temperature Differential (°C)				
(%)	15 mins	30 mins	45 mins	60 mins	75 mins
0	0.6	1.1	2.2	4.4	1.4
10	4.2	-0.8	1.7	4.4	3.9
20	5.0	1.1	5.0	10.6	4.4
30	3.9	3.3	2.8	1.9	2.2
50	8.9	6.1	7.8	7.8	5.3
100	27.5	27.8	23.1	26.9	28.3

CONCLUSIONS

The following conclusions can be drawn from this research study:

1. The temperature of the fresh concrete containing the HDPE plastic was comparable to that of the ordinary concrete.
2. The air content of the test samples increased with an increase in the percent replacement. The increase in air content was more significant when the percent replacement is greater than 30%.
3. Owing to the expansion caused by the HDPE plastic within the concrete, the slump test results could not be used as an indicator for the workability of concrete containing the HDPE plastic used in this study. For the materials used in this study, the workability of concrete decreased significantly for specimens with the plastic replacement level greater than 10%.
4. As expected, the unit weight of concrete decreased with an increase in the percent replacement owing to the light weight property of the HDPE plastic and the increase of air content due to the plastic replacement.
5. As the percent replacement increased, the compressive strength of the concrete decreased.More than 50% strength loss was observed for specimens with the percent replacementbeyond 30%.
6. The 10%, 20%, and 30% replacement samples exhibited higher splitting tensile strength than that of

the control sample. However, such increase was not observed for the specimens with percent replacement greater than or equal to 50%. The results suggested that a properpercentage of fine aggregate replaced by the HDPE plastic may be beneficial to tensile strength development.

7. The increase in the percent replacement increases the air content of the HDPE concrete, inhibiting the transfer of heat through the slab.

ACKNOWLEDGEMENT

This research is funded by the Opportunities for Undergraduate Research Experiences (OURE) program at Missouri University of Science and Technology. The authors would like to thank Conco Co. for providing the aggregates and portland cement for this research project.

REFERENCES

[1] Helmuth, R., Fly ash in cement and concrete, AP040T, Portland Cement Association, 1987, 203 pages.
[2] Malhotra, V. M., Pozzolanic and cementitious materials, Gordon and Breach Publishers, Amsterdam, 1996, 208 pages.
[3] ACI Committee 234, Guide for the use of silica fume in concrete, ACI 234R-96, American Concrete Institute, Farmington Hills, Michigan, 1996, 51 pages.
[4] ACI Committee 233, Ground granulated blast-furnace slag as a cementitious constituent in concrete, ACI 233R-95, American Concrete Institute, Farmington Hills, Michigan, 1995, 18 pages.
[5] ACI Committee 232, Use of fly ash in concrete, ACI 232.2R-96, American Concrete Institute, Farmington Hills, Michigan, 1996, 34 pages.
[6] ACI Committee 232, Use of raw or processed natural pozzolans in concrete, ACI 232.1R-00, American Concrete Institute, Farmington Hills, Michigan, 2001, 24 pages.
[7] Al-Manaseer, A. A., Dalal, T. R., Concrete containing plastic aggregates, Concrete International, 1997, 19(8), pp.47-52.
[8] Soroushian, P., Plasencia, J., Ravanbakhsh, S., Assessment of reinforcing effects of recycled plastic and paper in concrete, ACI Materials Journal, 2003, 100(3), pp.203-207.
[9] Batayneh, M., Marie, I., Asi, I., Use of selected waste materials in concrete mixes, Waste Management, 2007, 27(12), pp.1870-1876.
[10] Marzouk, O. Y., Dheilly, R. M., Queneudec, M., Valorization of post-consumer waste plastic in cementitious concrete composites, Waste Management, 2007, 27, pp.310-318.
[11] Ismail, Z. Z., Al-Hashmi, E. A., Use of waste plastic in concrete mixture as aggregate replacement, Waste Management, 2008, 28, pp.2041-2047.
[12] ASTM C33 / C33M-13, Standard Specification for Concrete Aggregates, ASTM International, West Conshohocken, PA, 2013.
[13] ASTM C136 / C136M-14, Standard Test Method for Sieve Analysis of Fine and Coarse Aggregates, ASTM International, West Conshohocken, PA, 2014.
[14] ASTM C231 / C231M-14, Standard Test Method for Air Content of Freshly Mixed Concrete by the Pressure Method, ASTM International, West Conshohocken, PA, 2014.
[15] ASTM C143 / C143M-12, Standard Test Method for Slump of Hydraulic-Cement Concrete, ASTM International, West Conshohocken, PA, 2012.
[16] ASTM C31 / C31M-12, Standard Practice for Making and Curing Concrete Test Specimens in the Field, ASTM International, West Conshohocken, PA, 2012.
[17] ASTM C39 / C39M-14a, Standard Test Method for Compressive Strength of Cylindrical Concrete Specimens, ASTM International, West Conshohocken, PA, 2014.

★★★

IMPACT OF PLANT HEIGHT AND IRRIGATION ON THERMAL PERFORMANCE OF EXTENSIVE GREEN ROOFS IN RIYADH CITY

[1]ASHRAF MUHARAM, [2]ELSAYED AMER, [3]NASSER AL-HEMIDDI

[1,2,3]king Saud university, king Saud university, king Saud university
E-mail: [1]ashraf.muharam@yahoo.com, [2]s_amereg@yahoo.com, [3]dr_n_hemiddi@yahoo.ca

Abstract- Increasing worldwide environmental concerns (Global warming, depletion of natural resources, acidrains, air and water pollutions, and ozone depletions) have led to the development of environmentally friendly construction practices. Green roof is one of the sustainable practices for reducing the environmental impact of a building. The study aim was identifying the impact of plant height and irrigation on thermal performance of an extensive green roof system in Riyadh city influenced by tropical and harsh climate.The experimental validations were applied on residential building in Riyadh city during the summer season in 2014. The experimental validations results indicated that the tall grass with average height from 6 to 15cm can reduce the temperature of internal air from 0.5 to 1°C, in comparison to the short grass with average height from 3 to 6 cm in similar conditions. While, the temperature of internal air differences were of 0.0±0.5°C with regular irrigation or irregular irrigation. However, when irrigation stopped more than two days, the grass would wither. Finally, this study has demonstrated that the grass height was more effective for its impact on the thermal performance than regular or irregular irrigation.

Keywords- Internal Temperatures,Irrigation,ShortGrass, Tall Grass, Thermal Performance.

I. INTRODUCTION

Green canopy have an important role for roof cooling, which is depending on plant species in terms of shading, evapotranspiration, and irrigation which acts as an insulator. The experimental results of [3]confirm that the plant canopy reflects 13% of incident global solar radiation and absorbs 56%, so that the solar radiation entering the system can be then estimated as 31% of the incident global solar radiation. The thermal behavior of a green roof is a complex phenomenon (such as shading, evapotranspiration, conductivity and absorption) and involves combined heat and mass transfer exchanges. Various studies have analyzed the thermal performance of green roofs in different plant varieties. According to [5]–[2], different plants have different results at the levels of effectiveness. As the amount of the coverage increased, the magnitude of the temperature changed (decreased). Because of this, the parametric variations in leaf area index (LAI) and foliage height thickness are carried out to determine the modulation of canopy air temperature, the reduction in the temperature width, and to estimate the penetrating heat flux. Also, foliage acts as a shading device under which convection provokes heat thermal exchange, but foliage absorbs part of the thermal energy because of its vital process of photosynthesis.
Furthermore, the results being drawn from the study of [8]showed that the effects of temperature reduction decrease with plant height. The best reductions in temperature occurred in 35 cm plants, followed by 15 cm and then 10 cm plants. The results also indicate that plants with green colored leaves are more effective than purple/red leafed plants in rooftop heat insulation. The leaf surface temperatures in this study were measured with infrared thermal imagers. However, the study of [15] found out that the most important parameter, when considering vegetation, is the foliage density. The foliage height alone is not one of the crucial factors affecting the performance of this cooling technique, but only in combination with the density of the vegetation layer. Moreover, the study of [1]found out that a larger leaf area index(LAI) reduces the solar flux penetration, stabilizes the fluctuating values, and reduces the indoor air temperature. Also, the study showed notably that in terms of evapotranspiration (ET) and solar heat gains factor (SHF), the foliage density and hence the vegetable canopy type selection influence the thermal efficiency of the climatic insulation greatly. In addition, the study of [10]compared the thermal effectiveness among three kinds of plant (Sedum, Plectranthus, and Kalanchoe) on an extensive green roof in an Indian Ocean area under a tropical humid climate. The results showed that Sedum green roof led to a higher heat restitution rate with 63%, than for Plectranthus (54%), and Kalanchoe (51%). In general, the results drawn from the study of [11] showed that a green roof which has high vegetation density acts as a passive cooling system. The incoming thermal gain is about 60% lower than when the roof has no vegetation. Irrigation is required to sustain vegetation throughout the extended dry periods. The water requirements of the plant species is from 2.6 to 9.0 L/m2per day, depending on the plant kind and the surrounding conditions [14]. Moreover, the study of [7]compared the irrigation among four plant types (C. chinense, C. variegatum, S. trifasciata, and cv. Laurentii). The study indicated that if plant leaves have greater evapotranspiration rates, they would not adapt to arid and severe environments for longer periods, thereby increasing water consumption. In contrary, plants with low evapotranspiration rates are suitable for arid and severe environments, thereby saving water resources. In addition, the study of [13]provided experimental evidence for a positive effect of the water retention

layer on water status and drought survival of plants growing over green roofs. The water retention layer is better than the natural sand and soil for increasing the amount of water available in green roof systems. Therefore, some studies investigated the irrigation impact on the thermal performance of the extensive green roofs. According to [12]–[2]the presence and the quantity of water largely influence the thermal properties of green roofs. In fact, a wet roof provides additional evapotranspiration, which prevents the heat flux in buildings and acts as a passive cooler by removing heat from buildings. Also, the study of [4]found out that the difference between the soil surface temperature of a dry substrate and a saturated substrate is about 25 °C. In conclusion, the study of [9]found out that supplemental irrigation is required for maintaining plant diversity on an extensive green roof, but not necessarily plant cover or biomass which depends on the growing media type being used. Also, the results showed that planting extensive green roofs with a mix of plant species can ensure the survival of some species; maintaining cover and biomass when supplemental irrigation is turned off to conserve water, or during extreme drought.

II. METHODOLOGY

The method being adopted in this research depends on the mixed scanning approach which involves reviewing the research problem in the literature and compare the theoretical findings with the experimental validations in order to identify the impact of plant height and irrigation on the thermal performance of the extensive green roof in Riyadh city.

2.1 Application study

In order to obtain an experimental data regarding the thermal behavior of extensive green roofs and their interactions with the energy performance of buildings, an experimental platform with green roofs system was constructed in the Deraib region which is located in the north of Riyadh city. The experimental platform is a simple repetition of residential rooms being built by similar materials. The platform consists of two rooms which are used for the study of treatment of the energy efficiency of buildings by using a selective standard for extensive green roof properties, and conventional roofs (concrete roof with depth of 15cm), see Figure (1). Also, the facades of these rooms will be painted with the Paige color, see Figure (2). To reflect a real urban setting, the experiment was conducted on the residential building that could simulate both physical and geometrical similarities in reality. The application study consists of three stages: the stage of experiment preparation, the stage of data collection, and the stage of data analysis and discussion.

2.2 Heat measurement equipment

The normality of temperature and the relative humidity data was checked by using (The EL-USB-2-LCD+) which measured the air temperature and the relative humidity inside the rooms and outside the rooms every five minutes. Thermocouples sensors (ANRITSU Digital handheld thermometer - ANRITSU MTER CO.,LTD) were arranged in different levels within the model to include the components of the empirical model so as to measure the covariance of temperature. Heat flux sensors were placed on the surface of the plants, walls, and at the ceiling layer in order to assess the amount of the heat conduction of those components. The results of the experiment were analyzed by using the statistical analysis program of Microsoft Excel.

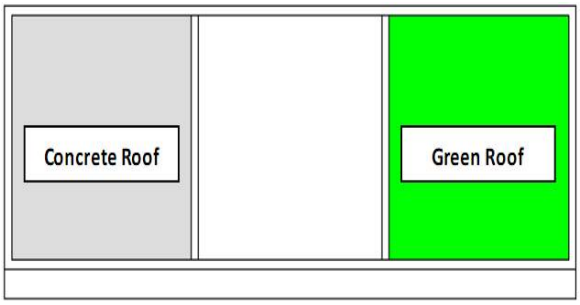

Figure: (1) The Plan's view of the experimental program.

Figure: (2) shows the exterior finishes in test rooms.

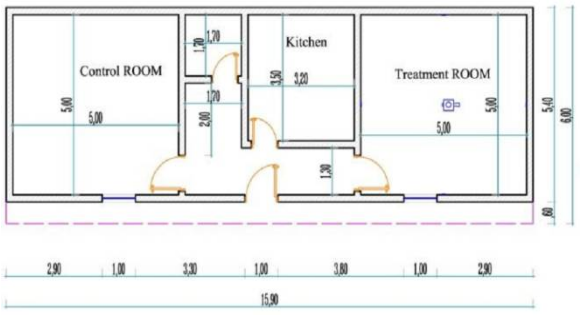

Figure: (3) A Plan's view of the rooms being tested.

A Pre-cultivated system (Vegetative Blanket - Tifway 419 Bermuda) was used in this experiment. This type typically comes in rolled that can be placed on any roof and be grown off-site. Also, this type has a good advantage ; namely, it is very thin (very lightweight option) compared to the other types.

An extensive green roof system consists of following matter Figure (4):

- A5 mm thick styrene butadiene rubber (SBR) waterproofing membrane (preventing water from

reaching the roof decking in an actual field installation).

- A 0.1 mm thick polyethylene slip sheet allowed any moisture in the waterproofing membrane to exit the system and saving water for irrigation.
- A 3 cm thick gravels which is as drainage layer and saving soil from erosion.
- A 2 cm thick sand that acts as a filter layer for drainage.
- A 4 cm thick soil which consists of mixed ratio (1:1:3) –(batamos: clay soil: soft sand) with organic materials.
- A 3 cm thick vegetative roll layer with Cynodondactylon (Bermuda- Tifway - 419) grass.

Drainage pipes of excess water from the growing medium were channeled and installed in the corners of the green roof substrate to allow water to drain freely from the system.

2.3 Installation of Measuring devices

There are 24 sensors that are used in this test. Eight sensors are in the green roof system, see Figure (5), two sensors are in the concrete roof system, six sensors are in the treatment room walls, six sensors control room and two sensor out test rooms.

III. DATA COLLECTION AND ANALYSIS

Thermal performance of extensive green roofs was during the warm period. The warm period chosen for the analysis was in June 2014 from (06-June to 23-June), which is a representative of a typical summer season in Riyadh city. The daytime is characterized by high loads of solar radiation with an average air temperature of 42◦C and an average relative humidity of 15.1%. Days presented winds with daily average and max value from 4.0 km/h to17.0 km/h.

3.1 Grass Height

A Tall Grass

Figure (6) shows the high of grass during the time period test. The height was from 8cm to 15cm. Figure (7) shows that the average values of the internal air temperature differences were of 5.5±2°C among the treatment and control rooms with tall grass, when the external air temperature reached to 44°C.

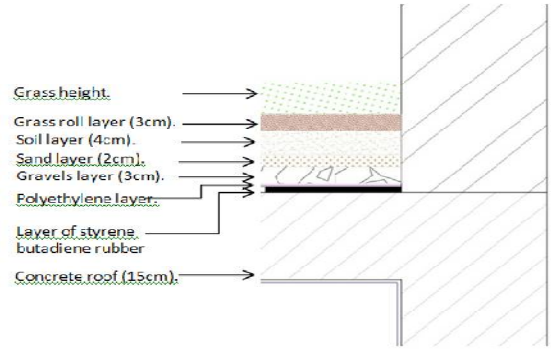

Figure: (4) The vertical section shows the various components of the extensive green roofing system

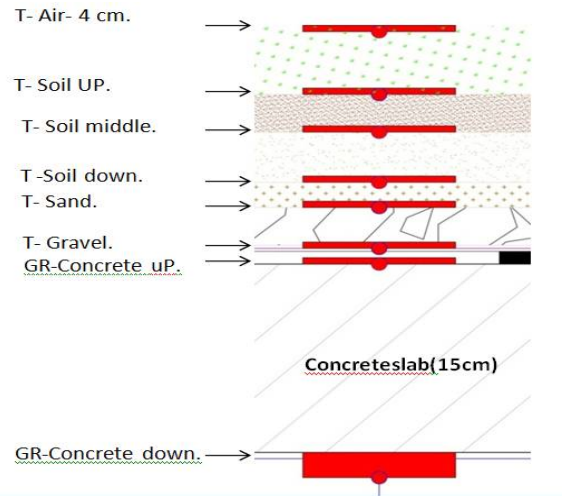

Figure: (5) The vertical section shows the sensors' places in the extensive green roof system.

Figure: (6) Shows the growth of the tall grass of (8-15) cm during the testing period.

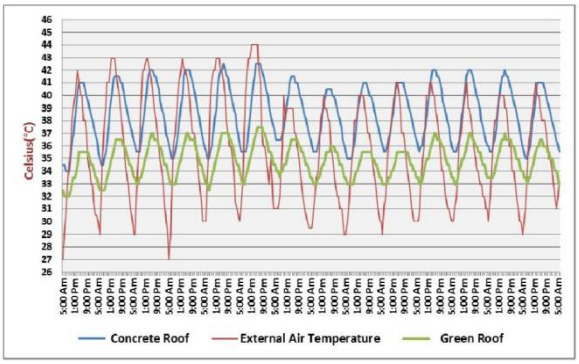

Figure: (7) Temperature variation of the internal air temperature in treatment room and control room with tall grass during the time period from 6-6-2014 at 5:Am to 20-6-2014 at 5:Am.

Figure (8) shows the temperature of thermocouples in substrate layer of extensive green roof system. The average values of substrate layers temperature differences were of 1±.01°C during the testing time period. The maximum temperature of substrate layers reached to 50°C when the external air temperature was 43°C and the minimum temperature of substrate layers reached to 34°C when the external air temperature was 28°C. However, the internal ceiling temperature was lower than the top layer of substrate (grass layer) up from 4°C to 14°C. While the air temperature at 4cm in

the grass layer reached 58°C because of the evapotranspiration phenomenon. Also, Figure (8) shows that the performance of substrate layers were different during the time period of day. During the night period, the lower layers of temperature were lower than the uppers layers of temperature. While during daylight period, the lower layers of temperature were higher than the uppers layers of temperature.

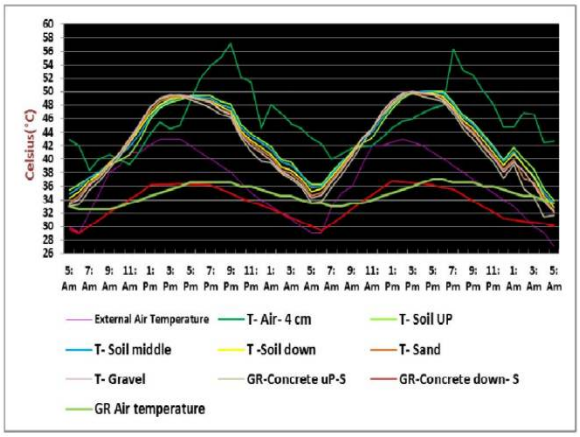

Figure: (8) Temperature variation of substrate layers with tall grass (regular irrigation) during the time period from 7-6-2014 at 5: Am to 9-6-2014 at 5:Am.

B Short Grass

Figures (9 and 10) show the method of cutting grass to test the impact of grass height on the thermal performance of the extensive green roof system. The grass height after cutting was from 3cm to 5cm.

Figure: (9) Shows the method of cutting grass.

Figure: (10) Shows short grass on 20-6-2014.

Figure (11) shows that the average values of the internal air temperature differences were of 5.5±2.5°C for the extensive green roof system (with short grass) being compared to the concrete roof system, when the maximum external air temperature reached 42°C and the minimum external air temperature reached 29°C. Also, Figure (12) shows the temperature of thermocouples in the substrate layer of the extensive green roof system after cutting grass with 5cm height. The average values layers temperature differences were of 2.5±.01°C during the daylight. The maximum temperature of substrate layers reached to 51°C when the temperature of external air was 41°C. However, the temperature of internal ceiling was lower than the top layer of the substrate (grass layer) from 7°C to 13°C during the daylight.

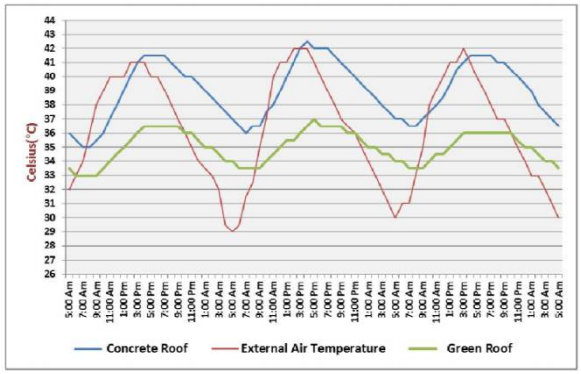

Figure: (11) Temperature variation of the internal air temperature in test rooms with short grassduring the time period from 20-6-2014 at 5:Am to 23-6-2014 at 5:Am.

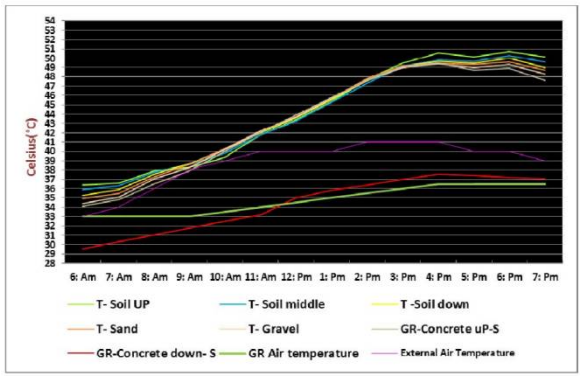

Figure: (12) Temperature variation of substrate layers with short grass (regular irrigation) during the time period from 20-6-2014 at 6:Am to 20-6-2014 at 7:Pm.

3.2 Irrigation

Irrigation was required to sustain vegetation throughout the extended dry periods. The water requirements of the plant species in this experiment were 6.0 L/m2 per day. The manual irrigation method was used at 6:30 pm every day for five to six minutes, see Figure (13).

Figure: (13) The method of manual irrigation during the testing period.

A The impact of irrigation on the temperature of internal air As shown in Figure (14), the temperature of internal air in the treatment room (with regular irrigation) was lower than the temperature of internal air in the same room (without irrigation for one day to two days). The differences were of 0.5°C during the

testing period. This means that the higher the water volumetric content, the lower the minimum of the daily temperature.

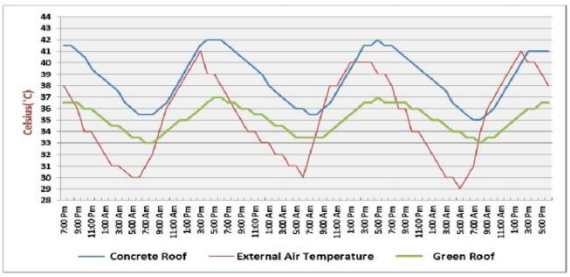

Figure: (14) Temperature variation of the internal air temperature in treatment room and control room with tall grass (first day irrigation, next day off and third day off too) during the time period from 160-6-2014 at 7:Pm to 19-6-2014 at 5:Pm.

B The impact of irrigation on the performance of substrate layers

Figure (15) shows the impact of regular and irregular irrigation on the temperature of substrate layers in the extensive green roof system with tall grass through the thermocouples sensors. When the temperature of external air was 40°C, the average values layers of the temperature differences were of 2.5±.5°C during the daytime. When regular irrigation, the maximum temperature of substrate layers reached 49°C, while with irregular irrigation (day off) the maximum temperature of substrate layers reached 51.4°C .

In addition, While the air temperature at 4cm in the grass layer reached 57.8°C on the day of regular irrigation. It reached 49.5°C on the day with irregular irrigation (day off) because of the evapotranspiration phenomenon. Before the irrigation, the soil temperature of the layer surface reached 49°C, while the water was cold. So, the water evaporated and the air temperature increased.

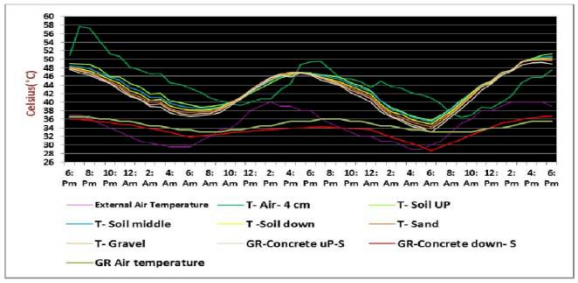

Figure: (15) Temperature variation of substrate layers temperature in extensive green roof system with tall grass (first day irrigation and the second day off) during the time period from 12-6-2014 at 6: Pm to 14-6-2014 at 6:Pm.

IV. DISCUSSIONS

The discussion focused on the impact of substrate components (grass height and water content) and the temperature of internal walls on the thermal performance of the extensive green roof system. The discussion includes the temperature variation of the internal air, Substrate layers, and internal (Globe) temperature.

4.1 Grass Height

The tall grass with average height from 6 to 15cm can reduce the temperature of internal air from 0.5 to 1°C, in comparison to the short grass with average height from 3 to 6 cm in similar conditions, as it is shown in Table (1). In the treatment room with tall grass, the temperature of internal airvaried from 35.5 to 33°C. But in the treatment room with short grass, the temperature of internal air varied from 36.5 to 33.5°C. This means that the leaf area and the foliage height thickness could reduce penetrating heat flux by shading and evapotranspiration phenomenon.

Moreover, the grass height has a significant impact on the temperature of the substrate layer. As shown in Table (2), the temperature of substrate layers varied from 50 to 32°C with tall grass, while the temperature of substrate layers varied from 51 to 33°C the maximum temperature of the external air were 43°C and 41°C respectively during the daylight. So, the tall grass temperature of substrate layers was lower than that of the short grass during similar conditions. However, the temperature of beneath layer in the substrate (Gravels layer) was lower than the top layer in the substrate (soil layer) during the first morning hours. But at noon, the gravel layer temperature was higher than the soil layer, due to the increasing of the thermal storage.

Celsius	Internal Air Temperature			
	Time period from 15-6-2014 at 5: Am to 16-6-2014 at 5:Am.		Time period from 20-6-2014 at 5: Am to 21-6-2014 at 5:Am.	
	External Air Temperature	Treatment Room (Green Roof) Tall Grass	ExternalAir Temperature	Treatment Room (Green Roof) Short Grass
Maximum	41°C	35.5°C	41°C	36.5 °C
Minimum	29°C	33°C	30°C	33.5°C
Difference	12°C	2.5°C	11°C	3°C

Table: (1) Temperature variation of the internal air temperature in treatment room with tall grass and with short grass.

Celsius	Substrate layers Temperature Variation			
	Time period from 7-6-2014 at 6: Am to 7-6-2014 at 7: Pm.		Time period from 20-6-2014 at 6: Am to 20-6-2014 at 7: Pm.	
	External Air Temperature	Treatment Room (Green Roof) Tall Grass	ExternalAir Temperature	Treatment Room (Green Roof) Short Grass
Maximum	43°C	50°C	41 °C	51 °C
Minimum	30°C	32°C	33°C	33°C
Difference	13°C	18°C	8°C	18°C

Table: (2) Temperature variation of substrate layers temperature with tall grass and with short grass.

4.2 Irrigation

As shown in Table (3), the regular irrigation or irregular irrigation in the extensive green roof system did not have a significant impact on the thermal behavior of the extensive green roof system. The temperature of internal air in the treatment room with regular irrigation varied from 36.5 to 33.5°C during the daylight, while it varied from 37 to 33.5°C in the treatment room with irregular irrigation when the external air temperature varied from 40 to 31°C and from 40 to 30°C, respectively. The temperature of internal air with regular irrigation was lower than that with irregular irrigation. The temperature differences were of 0.0±0.5°C. However, when irrigation stopped more than two days, the grass would wither. In addition, as shown in Table (4), the temperature of substrate layers varied from 49 to 33.6°C with regular irrigation, while the temperature of substrate layers with irregular irrigation varied from 51.4 to 33°C when the external air temperature varied from 40 to 30°C during the daylight. The substrate layers temperature differences were of 2.4±0.6°C with regular or irregular irrigation. From these results and through the comparison of the impact of grass height and irrigation on the thermal performance of extensive green roof, the grass height was more effective for its impact on the thermal performance than regular or irregular irrigation.

Celsius	Internal Air Temperature			
	Time period from 12-6-2014 at 5: Am to 12-6-2014 at 5: Pm.		Time period from 18-6-2014 at 5: Am to 18-6-2014 at 5: Pm.	
	External Air Temperature	Treatment Room (Green Roof) regular irrigation	ExternalAir Temperature	Treatment Room (Green Roof) Irregular irrigation
Maximum	40°C	36.5°C	40°C	37°C
Minimum	31°C	33.5°C	30°C	33.5°C
Difference	9°C	3°C	10°C	2.5°C

Table: (3) Temperature variation of substrate layers temperature with regular and irregular irrigation.

Celsius	Substrate layers Temperature Variation			
	Time period from 13-6-2014 at 5: Am to 13-6-2014 at 7: Pm.		Time period from 14-6-2014 at 5: Am to 14-6-2014 at 7: Pm.	
	External Air Temperature	Treatment Room (Green Roof) regular irrigation	ExternalAir Temperature	Treatment Room (Green Roof) Irregular irrigation
Maximum	40°C	49°C	40°C	51.4°C
Minimum	29°C	33.6°C	29°C	33°C
Difference	11°C	16°C	11°C	18°C

Table: (4) Temperature variation of the internal air temperature in treatment room with regular and irregular irrigation.

CONCLUSION

A number of conclusions can be drawn from the experimental study presented and
discussed in this study. The conclusions are the main results of this study.

The results of this study indicate that:

- Tall grass (6 to 15) cm was better than short grass (3 to 5) cm for reducing the temperature of internal air from 0.5 to 1°C.
- Tall grass (6 to 15) cm has a significant impact on the temperature of the substrate layer during the daylight in comparison with short grass (3 to 5). The temperature variation reached 3.8°C.
- The regular irrigation or irregular irrigation in the extensive green roof system did not have a significant impact on the thermal behavior of the extensive green roof system, especially for internal air temperature. The maximum temperature variation was up to 0.5°C. However, when irrigation stopped more than two days, the grass would wither.
- Water content with regular irrigation could cool the temperature of substrate layers more than irregular irrigation. The substrate layers temperature differences were of 2.4±0.6°C with regular or irregular irrigation.
- The temperature of internal walls in the treatment room (Green Roof) was higher than that in the control room (Concrete Room). However, the temperature of internal air in the treatment room was lower than that in the control room due to the use of the extensive green roof system. The temperature differences of internal air were of 5.5±2°C.
- Due to the increase of the thermal storage, the temperature of the beneath layer in the substrate (Gravels layer) was lower than the top layer in the substrate (soil layer) during the first morning hours, while at noon the gravel layer temperature was higher than the soil layer.

ACKNOWLEDGMENTS

This project was supported by the Research Center of Architecture and Planning College, King Saud university, Kingdom of Saudi Arabia.

REFERENCES

[1] Abalo, S., Banna, M. and Zeghmati, B. “Performance analysis of a planted roof as a passive cooling technique in hot-humid tropics,” Renewable Energy Journal, Vol. 39,pp.140–148, 2012.

[2] Berardi, U., Hoseini, A.M.G. and, Hoseini, A.G.“State-of-the-art analysis of the environmental benefits of green roofs,”Applied Energy Journal, Vol. 115,pp.411–428, 2014.

[3] D’Orazio, M., Di Perna, C. and Giuseppe, E.D. “Green roof yearly performance: A case study in a highly insulated building under temperate climate,”Energy and Buildings Journal, Vol. 55,pp.439–451, 2012.

[4] Djedjig, R., Ouldboukhitine, S., Belarbi, R. and Bozonnet, E.“Development and validation of a coupled heat and mass

transfer model for green roofs," International Communications in Heat and Mass Transfer, Vol. 39,pp.752–761, 2012.

[5] Kumar, R. and Kaushik, S. "Performance evaluation of green roof and shading for thermal protection of buildings," Building and Environment Journal, Vol. 40,pp.1505- 1511 , 2005.

[6] Lin, B., Yu, C., Su, A. and Lin, Y. "Impact of climatic conditions on the thermal effectiveness of an extensive green roof," Building and Environment Journal, Vol. 67,pp.26–33, 2013.

[7] Lin, Y. and Lin, H. "Thermal performance of different planting substrates and irrigation frequencies in extensive tropical rooftop greeneries," Building and Environment Journal, Vol. 46,pp.345–355, 2011.

[8] Liua, T.C., Shyu, G.S., Fang, W.T., Liu, S.Y. and Cheng, B.Y."Drought tolerance and thermal effect measurements for plants suitable for extensive green roof planting in humid subtropical climates,"Energy and Buildings Journal, Vol. 47,pp.180–188,2012.

[9] MacIvor, J.S., Margolis, L., Puncher, C.L. and Matthews, B.J.C. "Decoupling factors affecting plant diversity and cover on extensive green roofs,"Journal of Environmental Management, Vol. 130,pp.297–305, 2013.

[10] Morau, D., Libelle, T. and Garde, L. "Performance Evaluation of Green Roof for Thermal Protection of Buildings In Reunion Island," Energy Procedia Journal, Vol. 14,pp.1008–1016, 2012.

[11] Olivieri, F., Perna, C.D., D'Orazio, M., Olivieri, L. and Neila, J. " Experimental measurements and numerical model for the summer performance assessment of extensive green roofs in a Mediterranean coastal climate," Energy and Buildings Journal, Vol. 63,pp.1–14, 2013.

[12] Santamouris, M. "Cooling the cities – A review of reflective and green roof mitigation technologies to fight heat island and improve comfort in urban environments,"Solar Energy journal, 2012.

[13] Savi, T., Andri, S. and Nardini, A."Impact of different green roof layering on plant water status and drought survival,"Ecological Engineering Journal, Vol. 57,pp.188–196, 2013.

[14] Schweitzer, O. and Erell, E. "Evaluation of the energy performance and irrigation requirements of extensive green roofs in a water-scarce Mediterranean climate," Energy and Buildings Journal, Vol. 68,pp.25- 32, 2014.

[15] Theodosiou, T.G. "Summer period analysis of the performance of a planted roof as a passive cooling technique," Energy and Buildings Journal, Vol. 35,pp.909–917, 2003.

★★★

AN ANALYSIS OF MOBILE BANKING CUSTOMERS FOR A BANK STRATEGY AND POLICY PLANNING

BEHROOZ NOORI

[1]Department of Industrial Engineering West Tehran Branch, Islamic Azad University Tehran, Iran
E-mail: [1]b.noori@wtiau.ac.ir, [2]bnoori@gmail.com

Abstract-Online banking is increasingly common. Financial institutions deliver online services via various electronic channels, subsequently diminishing the importance of conventional branch networks. This study proposed an integrated data mining and customer behavior scoring model to manage existing mobile banking users in an Iranian bank. This segmentation model was developed to identify groups of customers based on transaction history, recency, frequency, monetary background. It classified mobile banking users into six groups. This study demonstrated that identifying customers by a behavioral scoring facilitates marketing strategy assignment. Then the bank can develop its marketing actions.Thus, the bank can attract more customers, maintain its customers, and keep high customers' satisfaction.

Keywords- Data mining;mobile data, mobile banking; customer segmentation

I. INTRODUCTION

The newly emerging channels of online banking and rapidly increasing penetration rates of mobile phones motivate this study(C. S. Chen, 2013).

The internet has had a significant impact on financial institutions, allowing consumers to access many bank facilities 24 hours a day, while allowing banks to significantly cut their costs. Research has shown that online banking is the cheapest delivery channel for many banking services (Koenig-Lewis, Palmer, & Moll, 2010; Robinson, 2000). A number of studies have identified advantages to bank customers, including cost and time savings as well as spatial independence benefits (Koenig-Lewis et al., 2010).

According to Gartner's prediction of leading trends of 2012 in mobile applications, mobile commerce (m-commerce) remains the most important one. Gartner further forecasts that mobile devices will replace PCs as the main device to access the internet. As for the third quarter of 2012, IPSOS indicated that "The era of Multi-Screen has come, and smartphones account for the purchasing behavior of 65% of mobile device users." According to that report, 66 percent of the smartphone holders in Taiwan access the internet via a smartphone at least once daily; approximately 57 percent of the customers perform mobile searches; and 40 percent of the customers shop via mobile phones(IPSOS, 2012). These statistics reflect vigorous growth in the scale of m-commerce. However, mobile banking remains in its infancy, and international adoption rates demonstrate the strong potential of m-commerce(FRB, 2012). Therefore, data mining for mobile banking is of priority concern for further developing mobile banking services (MBSs) (C. S. Chen, 2013).

Moreover, recent developments in Internet connectivity have led to a renewed interest in Internet banking among specific groups of working individuals. Moreover, with the rapid development of mobile and smart phones, Internet banking has become more conducive to many more individuals, since they can carry out their banking transactions anywhere and anytime (Govender & Sihlali, 2014; Lee & Chung, 2009). Mobilebanking, an extension of Internet banking, provides time independence, convenience, prompt response to customers and cost savings. These benefits serve as an opportunity for banks to increase consumer market through mobile services. Furthermore, mobile technologies, such as smart phones, PDAs, cell phones, and iPads have not only become ubiquitous, but also trendy among young adults(Govender & Sihlali, 2014).

Moreover, in recent years the market orientation has changed to customer centric view. After realizing the importance of simultaneous use of various channels, banking and financial companies are now paying attention to mobile banking especially when it comes to maintenance of customer relationships (Sangle & Awasthi, 2011). The ability to identify customer's most pressing need at a given moment of time is one of the promising propositions of mobile banking. Advanced mobile technologies help banks in offering new services like viewing account details, fund transfer, balance enquiry, loan details, bill payments, enquiry about credit card and demat account and add value to existing ones by disseminating the information at userdefined time and place(Sangle & Awasthi, 2011).

Besides, banking was at the forefront of the service sectors that migrate customers from face-to-face transactions to computer-mediated transactions. With the development of m-commerce, similar expectations have been held out that much banking activity that is currently carried out online through fixed line internet terminals will migrate to mobile devices. The range of services that can be undertaken while mobile is likely to increase, and mobile phones are likely to evolve as ubiquitous payment devices(Koenig-Lewis et al., 2010; Wilcox, 2009).

Market segmentation is one of the most important areas of knowledge-based marketing. In banks, it is

really a challenging task, as data bases are large and multidimensional(Zakrzewska & Murlewski, 2005).

Though a number of aspects have been studied for m-commerce, very little is reported regarding the customer segmentation of mobile banking from customer relationship management (CRM)perspective(Wong & Hsu, 2008). The knowledge of the key mobile user segments in financial sector is still lacking. This study attempts to add to the body ofliterature by data mining in mobile banking services(Sangle & Awasthi, 2011).

In relation to customer-centric business intelligence, banks are usually concerned with the following commonMarketing and sales concerns(D. Chen, Sain, & Guo, 2012):

- Who are the most / least valuable customers to the bank? What are the distinct characteristics of them?
- Who are the most / least loyal customers, and how are they characterized?
- What are customers' transaction behavior patterns? Which services have customers purchased together often?Which types of mobile banking users are more likely to respond to a certain promotion mailing?
- What are the sales patterns in terms of various perspectives such as services, regions and time (weekly, monthly, quarterly, yearly and seasonally), and so on? and
- What are the user segments in terms of various perspectives(D. Chen et al., 2012)?

  In order to address these marketing concerns, data mining techniques have been widely adopted,coupled with a set of well-known businessmetrics about customers' profitability andvalues, for instance, the recency, frequencyand monetary (RFM) model, and thecustomer life value model(D. Chen et al., 2012).

In this article a case study of using datamining techniques in customer-centricbusiness intelligence for a bankwas presented. The main purpose of this analysis is to helpthe bank better understand its mobile banking customersand therefore conduct customer-centricmarketing more effectively. On the basisof anewsegmentation model, customers of the bank have been segmented into variousmeaningful groups. Accordingly, a set ofrecommendations was provided to thebank on customer-centric marketing (D. Chen et al., 2012).

II. LITERATURE SURVEY

Banks operate in a competitive environment facing challenges in customer acquisition and service costs. In such an environment, the understanding and prediction of customer behavior in usage of services is becoming an important subject. The banks' intention is to shift customers to technology enabled self-service channels like ATMs, internet banking and more recently onto mobile banking services. Customers, these days are more and more pressed for time and they seek a channel that offers them convenience of anytime, anywhere banking and mobile banking services fits the bill very well. In Iran,mobile banking services seem to be high on priority for banks (Thakur, 2014).

Particularlyin Iran, banking services on mobile banking were launched few years ago yet the usage of such services has not reached thedesired level.Therefore, it becomes more important to look for the customer segments. The studies conducted on bank information technology adoption render insufficient information about customer segmentation(Sangle & Awasthi, 2011). In this regard the current study tends to emphasize customer data mining framework and identify the mobile user segments.

2.1. Mobile Banking

While the use of branch-based banking is still very popular, banks have other ways of providing customers with financial management services and one of them is mobile banking (Govender & Sihlali, 2014). The mobile phone as a channel for service consumption offers enormous potential since today, a mobile phone is an integral part of customers' life and a growing number of these devices are also equipped with internet connection. Currently mobile banking services enable consumers, for example, to request their account balance and the latest transactions of their accounts, to transfer funds between accounts, to make buy and sell orders for the stock exchange and to receive portfolio and price information(Laukkanen, 2007).Hence it is necessary to investigate mobile banking customer segments.

2.2. Cross-sellingAnalysis

The rationale for cross-selling, defined in the introduction as "the strategy of selling other products to a customer who has already purchased a product from the vendor" isnot only to "increase the customer's reliance on the company and decrease thelikelihood of switching to another provider" but also to exert a generally positiveinfluence on the relationship with the customer, strengthening the link betweenprovider and user (Kamakura, Wedel, De Rosa, & Mazzon, 2003). Increasing product holding leads to anincreased number of connection points with customers, as well as increasing theswitching costs they would face if they decided to take their custom elsewhere.Increased product holding also creates a situation in which the company can get toknow it customers better through a greater understanding of buying patterns andpreferences. This, in turn, puts it in a better position to develop offerings that meetcustomer needs. Consequently, it is argued that cross-sellingincreases the total value of a customer over the lifetime of the

relationship(Ansell, Harrison, & Archibald, 2007; Kamakura et al., 2003).
Cross-selling, and consequently cross-buying, is receiving considerable attention inboth research and management in the financial services industry. Denoting to termssuch as "bancassurance" and "allfinanz", i.e. the sales of insurance products by banks, and on the other hand "assurfinance", i.e. the salesof financial products by insurance companies, changes in the market such as deregulation and increasingcompetition have driven the once traditional financial service providers towardsincreasing provision of integrated financial services, that is, offering their customers aseamless service of banking, investment and insurance products(Mäenpää, 2012; Van den Berghe & Verweire, 2001).

2.3. Bank customer segmentation

Market segmentation has become one of the most dominant concepts in both marketing theory and practice. In banking industry, like any other service industries, segmentation is considered as a major way of operationalizingthe marketing concept, and providing guidelines for a bank's marketing(Edris, 1997). As theory, market segmentation is the process of dividing a market into distinct groups of individuals, or organizations, who share one or more similar responses to some elements of the marketing mix. The segmentation process calls for dividing the total market into homogeneous segments, selecting the target segments, and creating separate marketing programs to meet the needs and wants of these selected segments(Edris, 1997).
The identification of segments allows the evaluation and refinement of a bank's marketing strategy. The effectiveness of the segmentation process and strategy depends on identifying segments that are measurable, accessible, stable, substantial, and actionable(Edris, 1997).

2.4. CLV and RFM Analysis

Customer segmentation is used in differentsettings, for instance, using customer segmentationfor estimating customer future valueas a part of customer lifetime value (CLV) in banking scope (Khobzi, Akhondzadeh-Noughabi, & Minaei-Bidgoli, 2014). Generally, customersegmentation is often used to obtain moredetails about different customers in bankingscope. Actually, according to these studiesdiverse groups of banks' customers are identified by segmenting based on customers' financial transactions(Khobzi et al., 2014).
RFM analysis is a widely used method thatidentifies customer behavior and representscustomer behavior characteristics, and it standsfor the words: Recency, Frequency, and Monetary.Generally, these parameters are defined asfollows(Khobzi et al., 2014):

- Recency: The interval between the purchase and the time of analysis.
- Frequency: The number of purchases within a certain period.
- Monetary: The amount of money spent during a certain period.

These definitions are adaptable and can varyin different cases. In recent years, several researcherstried to extend the concept of RFManalysis, but there is lack of studies that analyze the customer segments and RFM analysis focusing banks over the mobile banking platform. Thus, although the increasing competitiveness in mobile banking is motivating an exponential growth in the number of studies, there is a call for studies that will help us to understand how customer behavior are formed in the mobile banking business in greater detail.

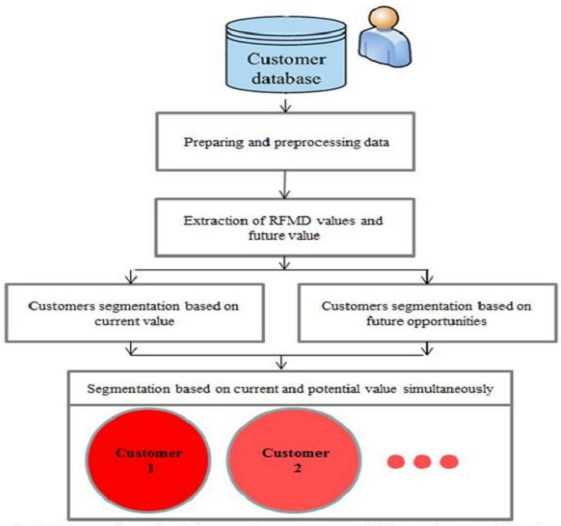

Fig. 1. Research methodology using RFMD variables and potential value.

Moreover, the rapid development of data mining methodsenables using large data bases of customer data toextract the knowledge, supporting marketing decisionprocess. Asthe ability to acquire new customers and retain existing iscrucial, especially in the finance marketplace, thepossibility of customer segmentation by obtaining theinformation on unknown hidden patterns has a majorsignificance. Until now only few papers present usingof data mining techniques in banks. In ourwork, we consider application of a new RFM segmentation algorithmin this area(Zakrzewska & Murlewski, 2005).

III. METHODOLOGY

In this study, numbers of mobile banking users of a major bank in Iran were studied. These user demographics were shown in table I. Additionally, bank customer table was shown in table II.The proposed methodology utilizeda new segmentation methodology, as shown in Fig. 1. In this work, customer priority number (CPN) or RFMD as a new model of RFM, was introduced for first time. It is the

product of the recency (R), frequency (F), average transaction amount or monetary (M) and customer deposit (D) ratings: RFMD = R × F × M×D

The rationale ofthe proposed approach is that if customers have hadsimilar purchasing behavior, then theyare very likely also to have similar RFMD values. RFMD values were used tocluster customers into groups with similar RFMD values. The scaling of R–F–M-D attributes was shown in table III.

TABLE I. Demographics of mobile banking users

Education	Percent (%)	Occupation	Percent (%)	Gender	Percent (%)	Age	Percent (%)
High school	0.56	Employee	0.364	Male	0.804	Young	0.36
College	0.34	Business	0.397	Female	0.196	Middle	0.578
Master and above	0.1	Engineer	0.054			Old	0.062
		Manager	0.016				
		Student	0.07				
		Physician	0.07				
		Faculty	0.01				
		Others	0.019				

TABLE II. Customer table.

Field Name	Data Type	Description	Value set
ID	Text	Customer ID code	-
Acct-NO	Text	Customer account number	-
Birth-Date	Text	Below 30; 30–40; 40–60; 60 and above	{Y, M, O}
Sex-code	Text	Gender	{F, M}
Marital_Status	Yes/No	-	{Y, N}
Education	Text	High school and below; college; master and above	-
Occupation	Text	Manager; employee of company; student; others	-
Operator-Network	Text	IR-TCI; MTN-Irancell; Talya	{I, M, T}
Service Type	Text	e.g. Payments, Transfers, Payments & Transfers	-
Open-Date	Date/Time	Account opening date	-
Amount	Number	-	-
Transaction-Date	Date/Time	-	-
Balance	Number	Account status	-

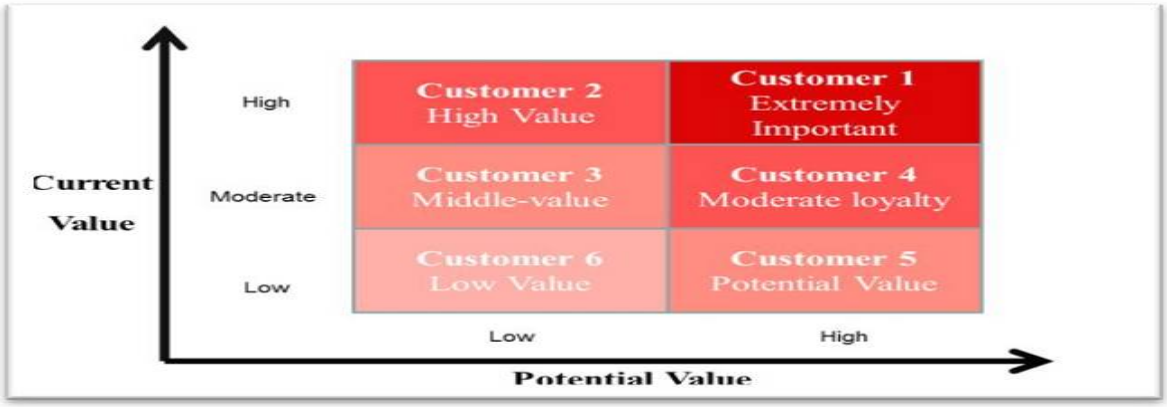

Fig. 2. Customer segmentation result based on CLV

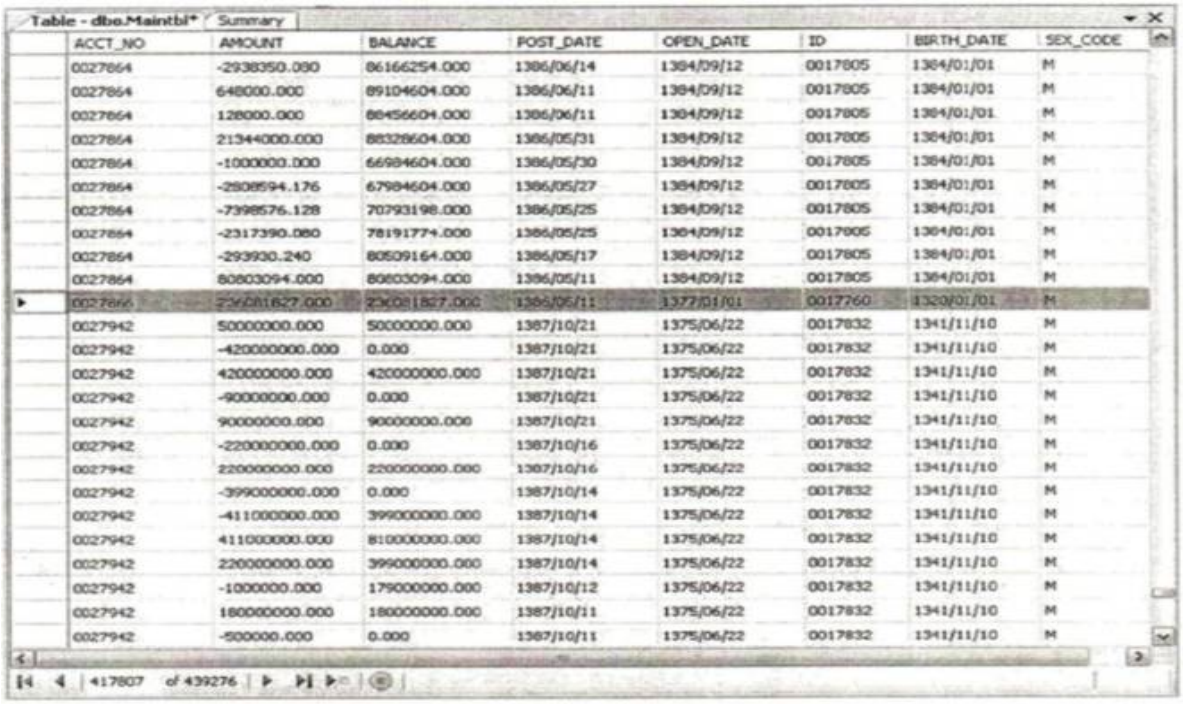

Table - dbo.Maintbl* | Summary

ACCT_NO	AMOUNT	BALANCE	POST_DATE	OPEN_DATE	ID	BIRTH_DATE	SEX_CODE
0027864	-2938350.080	86166254.000	1386/06/14	1384/09/12	0017805	1384/01/01	M
0027864	648000.000	89104604.000	1386/06/11	1384/09/12	0017805	1384/01/01	M
0027864	128000.000	88456604.000	1386/06/11	1384/09/12	0017805	1384/01/01	M
0027864	21344000.000	88328604.000	1386/05/31	1384/09/12	0017805	1384/01/01	M
0027864	-1000000.000	66984604.000	1386/05/30	1384/09/12	0017805	1384/01/01	M
0027864	-2808594.176	67984604.000	1386/05/27	1384/09/12	0017805	1384/01/01	M
0027864	-7398576.128	70793198.000	1386/05/25	1384/09/12	0017805	1384/01/01	M
0027864	-2317390.080	78191774.000	1386/05/25	1384/09/12	0017805	1384/01/01	M
0027864	-293930.240	80509164.000	1386/05/17	1384/09/12	0017805	1384/01/01	M
0027864	80803094.000	80803094.000	1386/05/11	1384/09/12	0017805	1384/01/01	M
0027866	23608\1827.000	23608\1827.000	1386/05/11	1377/01/01	0017760	1320/01/01	M
0027942	50000000.000	50000000.000	1387/10/21	1375/06/22	0017832	1341/11/10	M
0027942	-420000000.000	0.000	1387/10/21	1375/06/22	0017832	1341/11/10	M
0027942	420000000.000	420000000.000	1387/10/21	1375/06/22	0017832	1341/11/10	M
0027942	-90000000.000	0.000	1387/10/21	1375/06/22	0017832	1341/11/10	M
0027942	90000000.000	90000000.000	1387/10/21	1375/06/22	0017832	1341/11/10	M
0027942	-220000000.000	0.000	1387/10/16	1375/06/22	0017832	1341/11/10	M
0027942	220000000.000	220000000.000	1387/10/16	1375/06/22	0017832	1341/11/10	M
0027942	-399000000.000	0.000	1387/10/14	1375/06/22	0017832	1341/11/10	M
0027942	-411000000.000	399000000.000	1387/10/14	1375/06/22	0017832	1341/11/10	M
0027942	411000000.000	810000000.000	1387/10/14	1375/06/22	0017832	1341/11/10	M
0027942	220000000.000	399000000.000	1387/10/14	1375/06/22	0017832	1341/11/10	M
0027942	-1000000.000	179000000.000	1387/10/12	1375/06/22	0017832	1341/11/10	M
0027942	180000000.000	180000000.000	1387/10/11	1375/06/22	0017832	1341/11/10	M
0027942	-500000.000	0.000	1387/10/11	1375/06/22	0017832	1341/11/10	M

417807 of 439276

Fig. 3. The partial data of C-Bank dataset

TABLE VI. Segmentation results

ID	RFMD	Current Value	Potential Value	Customer Type or Segment	Segment	Marketing Strategy
0017805	108	High	High	Customer 1	Extremely important	Relationship management
0017760	12	Low	High	Customer 5	Potential value	Retention
0017832	24	Low	Low	Customer 6	Low value	Growing

TABLE III. The scaling of R–F–M-D attributes

Field Name	Description	Value set
ID	-	-
Recency	Below 15; 16~30; 31 and above (day)	{3, 2, 1}
Transaction Frequency	Below 5; 5~20; 21 and above (in a fiscal year)	{1, 2, 3}
Transaction amount average	NT$100 and below; 100~1,000; 1,001~3,000; 3,001 and above	{1, 2, 3, 4}
Deposit Average	NT$1,000 and below; 1,001~7,000; 7,001~20,000; 20,001 and above	{1, 2, 3, 4}

TABLE V. RFMD values for each customer

ID	Acct-NO	Recency	Transaction Frequency	Transaction amount average	Deposit Average	R	F	M	D
.	.	.	.	.	.	.	.	.	.
.	.	.	.	.	.	.	.	.	.
0017805	0027864	10	30	1200	41000	3	3	3	4
0017760	0027866	8	4	450	5120	3	1	2	2
0017832	0027942	25	12	150	15000	2	2	2	3
.	.	.	.	.	.	.	.	.	.
.	.	.	.	.	.	.	.	.	.

RFMD refers to the customer current value. It calculated for each stored customer data (Table II). RFMD or CPN ranking was illustrated in table IV.The rankings given are normally scored on a scale of 1-4. Therefore, CPN would be between 1 and 144. After the case priority number (CPN)was computed, customer current value could be determined.After RFMD computation, potential value of customer

based on future opportunitiesshould be estimated. The CPN and potential value of customer are main elements for customer segmentation (Fig. 2).

TABLE IV. Suggested CPN table for customer current value

Segment	Value
High value	81~144
Moderate	36~80
Low	1~35

IV. CASE STUDY

This workconsidered a bankcustomer records to conduct empirical research (Fig. 3). Three customers were selected to show methodology effectiveness. The real data of selected customers and related R, F, M, and Ds were shown in table V. RFMDs were computed and customer potential values were illustrated in table V. Meanwhile customer type and its marketing strategy were derived (Table VI).

V. MANAGERIAL IMPLICATIONS

The bank's marketing and business manager, bank branch manager, or analysts can employ the segments to:

- Better understand customers. The bank can track changes to customers' life styles. Better customer knowledge and understanding are the cornerstones of effective and profitable customer management(Zuccaro & Savard, 2010).
- Enhance the value of segmentation systems. Proactive segmentation systems are enhanced when they are updated regularly. This means that both demographic and transaction data are integrated into an ongoing process of customer segment management. Customer segments possess the built-in capacity to integrate demographic and transaction data. Up-to-date and relevant segmentation system provide the bank with invaluable data to plan new service offerings, predict customer reaction and determine profit levels on a segment-by-segment basis. Segmentation system enhances the bank's capacity to employ customer knowledge in a more strategically effective manner(Zuccaro & Savard, 2010).
- Improve marketing effectiveness. Without a sound segmentationsystem a bank would not be able to perform valid and reliable customerprospecting which in turn would seriously undermine the effectiveness andprofitability of customer targeting. The starting point for serious customerprospecting and targeting is the bank's customer data and transaction database.It provides the analyst with invaluable behavioral information (use of mobile banking by each customer). In addition, the database will contain rudimentarysocio-demographic data such as the customer's age, sex, maritalstatus and some employment information. Customer prospecting and targetingcould be undertaken employing such data. Customers would be placed in groups. Many organizations have realized that byenhancing their customer database they can significantly improve their customer prospecting and increase the lift ofcustomer targeting strategies. Thus, segmentation is designed to exploit thepotential of the bank's customer database. Once a specific customer segmentgenerated by RFMDsegmentation has been identified, it becomes relativelysimple to identify the customer prospects and target them with the appropriatestrategy and promotional tools(Zuccaro & Savard, 2010).
- Develop effective communications. In the age of segmentation, developingan effective communication strategy is not a simple task. The nature and varietyof potential communication messages and media to transmit the messages hasgrown exponentially during the last two decades. In addition, mostorganizations, including banks, are abandoning traditional communicationmedia such as television and radio and opting for more specialized vehicles suchas the web. Segmentation provides the bank with a richer set of segments that can be described with animpressive level of detail. The refined segments along with detailed financial life style of its membersallow the bank to design tailor-made communication strategies(Zuccaro & Savard, 2010).

CONCLUSION

Mobile phone handsets, which were initially used almost exclusively for voice calls are now often used to transmit data and undertake commercial transactions. In recent years, mobile phones have become very popular with a penetration rate in many of states of Iran. The term m-commerce has been widely used to describe a subset of e-commerce and refers to transactions with monetary value that are conducted via mobile devices(Koenig-Lewis et al., 2010).

Iranian banks today face intense competition inside and outside Iran. This in turn has forced these banks to be more oriented towards their customers. The main focus of this study was on the customer segmentation. Banks which are marketing-oriented are notonly required to be aware of the needs of theircustomers, but they should be able to satisfyeffectively the needs of each identified customersegment. This study provides evidencethat segmentation of the customers is of great importance to banks inorder to identify the behavior of each segmentand provide certain marketing actions that best suitthese behaviors.The results of this study provide a practicalapproach to Iranian banks that

wouldhelp in determining the true segments of mobile banking customers(Edris, 1997).

Furtheremore, one of the important factors for the success of a bank industry is to monitor their customers' behavior. The bank needs to know its customers' behavior to find interesting ones to attract more transactions which results in the growth of its income and assets.

The RFM analysis is an approach for extracting behavior of customers and is a basis for marketing and CRM, but it is not aligned enough for banking context(Bizhani & Tarokh, 2011). So, this study introducednew RFM model toimprove understanding of bank customers.

Furthermore, this paper presented a framework of segmentation by applying it to the customers of one of Iran's major banks. Also, this paper presented a synthesized example of segmentation in the banking sector.The proposed model improved current understanding of mobile banking customers. Meanwhile, from a practical perspective, insights provided by the study can help mobile banking managersto managemobile users' behavior.

REFERENCES

[1]. Ansell, J., Harrison, T., & Archibald, T. (2007). Identifying cross-selling opportunities, using lifestyle segmentation and survival analysis. Marketing Intelligence & Planning, 25(4), 394-410.

[2]. Bizhani, M., & Tarokh, M. (2011). Behavioral rules of bank's point-of-sale for segments description and scoring prediction. International Journal of Industrial Engineering Computations, 2(2), 337-350.

[3]. Chen, C.S. (2013). Perceived risk, usage frequency of mobile banking services. Managing Service Quality, 23(5), 410-436.

[4]. Chen, D., Sain, S.L., & Guo, K. (2012). Data mining for the online retail industry: A case study of RFM model-based customer segmentation using data mining. Journal of Database Marketing & Customer Strategy Management, 19(3), 197-208.

[5]. Edris, T. (1997). Services considered important to business customers and determinants of bank selection in Kuwait: a segmentation analysis. International Journal of Bank Marketing, 15(4), 126-133.

[6]. FRB. (2012). Current use of mobile banking and payments. www.federalreserve.gov/econresdata/mobile-devices/2012-current-use-mobile-banking-payments.htm.

[7]. Govender, I., & Sihlali, W. (2014). A Study of Mobile Banking Adoption among University Students Using an Extended TAM. Mediterranean Journal of Social Sciences, 5(7), 451.

[8]. IPSOS. (2012). Mobile internet and smartphone adoption statistics. available at: www. digitimes.com.tw/tw/dt/n/shwnws.asp?CnlID¼10andCat¼35 andCat1¼andid¼310528.

[9]. Kamakura, W.A., Wedel, M., De Rosa, F., & Mazzon, J.A. (2003). Cross-selling through database marketing: a mixed data factor analyzer for data augmentation and prediction. International Journal of Research in marketing, 20(1), 45-65.

[10]. Khobzi, H., Akhondzadeh-Noughabi, E., & Minaei-Bidgoli, B. (2014). A New Application of RFM Clustering for Guild Segmentation to Mine the Pattern of Using Banks'e-Payment Services. Journal of Global Marketing, 27(3), 178-190.

[11]. Koenig-Lewis, N., Palmer, A., & Moll, A. (2010). Predicting young consumers' take up of mobile banking services. International Journal of Bank Marketing, 28(5), 410-432.

[12]. Laukkanen, T. (2007). Internet vs mobile banking: comparing customer value perceptions. Business Process Management Journal, 13(6), 788-797.

[13]. Lee, K., & Chung, N. (2009). Understanding factors affecting trust in and satisfaction with mobile banking in Korea: A modified DeLone and McLean's model perspective. Interacting with computers, 21(5), 385-392.

[14]. Mäenpää, I. (2012). Drivers of cross-sectoral cross-buying behaviour among business customers. International Journal of Bank Marketing, 30(3), 193-217.

[15]. Robinson, T. (2000). Internet banking: still not a perfect marriage. Informationweek. com, 4(17), 104-106.

[16]. Sangle, P.S., & Awasthi, P. (2011). Consumer's expectations from mobile CRM services: a banking context. Business Process Management Journal, 17(6), 898-918.

[17]. Thakur, R. (2014). What keeps mobile banking customers loyal? International Journal of Bank Marketing, 32(7).

[18]. Van den Berghe, L., & Verweire, K. (2001). Convergence in the financial services industry. Geneva Papers on Risk and Insurance. Issues and Practice, 173-183.

[19]. Wilcox, H. (2009). Banking on the mobile. white paper, Juniper Research, Basingstoke, available at www. juniperresearch. com (accessed 23 October 2009).

[20]. Wong, Y.K., & Hsu, C.J. (2008). A confidence-based framework for business to consumer (B2C) mobile commerce adoption. Personal and Ubiquitous Computing, 12(1), 77-84.

[21]. Zakrzewska, D., & Murlewski, J. (2005). Clustering algorithms for bank customer segmentation. Paper presented at the Intelligent Systems Design and Applications, 2005. ISDA'05. Proceedings. 5th International Conference on.

[22]. Zuccaro, C., & Savard, M. (2010). Hybrid segmentation of internet banking users. International Journal of Bank Marketing, 28(6), 448-464.

★★★

ADVANTAGE OF MAKE-TO-STOCK STRATEGY BASED ON LINEAR MIXED-EFFECT MODEL

[1]YU-PIN LIAO, [2]SHIN-KUAN CHIU

[1]Chairman's Office, Winstar Display Corp., Taichung, Taiwan
[2]Ph.D. Program of Business, Feng Chia University, Taichung, Taiwan ,
[3]Department of International Trade, Feng Chia University, Taichung, Taiwan
E-mail: [1]panjc@winstar.com.tw, [2]skchiu@fcu.edu.tw

Abstract- In the past few decades, demand forecasting becomes relatively difficult because of the rapid changes of world economic environment. In this research, the make-to-stock (MTS) production strategy is applied as an illustration to explain that forecasting plays an essential role in business management. We also suggest that linear mixed-effect (LME) model could be used as a tool for prediction and against environment complexity. Data analysis is based on a real data of order quantity demand from an international display company operating in the industry field, and the company needs accurate demand forecasting before adopting MTS strategy. The forecasting result from LME model is compared to the common used approaches, times series model, exponential smoothing and linear model. The LME model has the smallest average prediction errors. Furthermore, multiple items in the data are regarded as a random effect in the LME model, so that the demands of items can be predicted simultaneously by using one LME model. However, the other approaches need to split the data into different item categories, and predict the item demand by establishing model for each item. This feature also demonstrates the practicability of the LME model in real business operation.

Index Terms- forecasting, linear mixed-effect model, make-to-stock, order demand, production strategy

I. INTRODUCTION

Demand forecasting is crucial for supply chain management. Production planning, inventory management, and manufacturing scheduling are typically formulated according to short- and long-term expected demand [1]. To reduce the occurrence of delivery delays caused by the "crowding out" effect of manufacturing processes, contemporary enterprises have gradually changed their production patterns from make-to-order (MTO) to make-to-stock (MTS), and increasingly fewer enterprises are using the MTO production strategy [2 , 3]. The MTO production involves commencing product production only after the customer places the order. The MTS production pattern entails a stocking-up production, in which a company manufactures products and stores them in inventory before customer orders are received. Subsequently, the company sells its stock as customer places orders. If a company receives orders requesting a high mix of products but in low volumes, it must be capable of forecasting their order demand accurately before attempting an MTS production strategy. Accordingly, the advantages of the MTS production strategy—including quick delivery, arranging a long-term manufacturing schedule, reducing the stock levels, and stabilizing product prices—can be realized. Worldwide, variation in customer demand has forced many manufacturers to adopt a high-mix low-volume production model. However, this type of enterprise is not as efficient as a low-mix high-volume enterprise. Therefore, determining how high-mix low-volume enterprises can enhance their business operation performance urgently requires a solution. Hence, accurately forecasting order demand is a fundamental to successfully applying the MTS production strategy to a high-mix low-volume business operation model. Because inaccurate demand forecast is a concern for high-mix low-volume enterprises, the MTO production strategy is typically adopted. However, this production pattern increases financial risks and requires a long delivery time, making centralized production difficult, which subjects production lines to frequent changes, resulting in high operating costs and low product quality. Complex operations are the primary cause of human error and low job satisfaction. Therefore, if the inefficiency of the high-mix low-volume business operation model cannot be solved, then, despite a high business revenue, business operation costs would increase rapidly, product quality would reduce, and employee job satisfaction and customer satisfaction would decrease, which result in that business development would stagnate. Therefore, the forecasting method proposed in this study can provide a crucial basis for transitioning from using the MTO to the MTS production, and may offer a viable solution for improving the business operation performance of high-mix low-volume enterprises. The application and improvement of the proposed forecasting method can assist researchers with understanding the characteristics of business operations and construct related business operation models. Forecasting ability depends on crucial information and reliable forecasting methods. In recent years, demand forecasting has become increasingly complex, primarily because the global economic environment has gradually changed. The underlying reasons for this change can be explained in terms of the following four dimensions: volatility, uncertainty, complexity, and ambiguity (VUCA) [4 , 5 , 6], all of which have been shown to influence

demand forecasting [7]. Volatility means that new products are rapidly developed, product lifecycles are shortened, customer preferences change suddenly, and organizations are frequently restructured; consequently, historical data diminishes in value. Uncertainty refers to unknown factors that cause sudden shifts in demand, and these factors are generally regarded as outliers or interferences. Complexity means that the interaction of these influential factors cannot be modelled easily, and ambiguity refers to fuzzy events and situations that cannot be quantifiably defined, leading to the loss of key influential factors. In summary, according to the influence of economics on demand forecasting, developing a reliable forecasting method requires analyzing whether historical data can contribute to demand forecasting, and whether the effects of influential factors can be identified. To meet the requirements of modern forecasting methodologies, this study proposed using linear mixed-effect models to perform forecasting. Linear mixed-effect models have been extensively developed and widely applied in various fields. However, no study has used this model to forecasting in business operation. Linear mixed-effect models are characterized by the inclusion of temporal factors and explanatory variables and the analysis of their significance. Accordingly, crucial influential factors can be identified to forecast demand. These characteristics fulfill the requirements of modern forecasting methodologies and can be used as the basis for companies to improve their operation efficiency and to develop competitive advantages. The following sections explore the influences of the MTO and MTS production strategies on business operation as well as the role of forecasting in the MTS strategy, provides a review of the literature on forecasting methodologies, and summarizes the strengths and weaknesses of commonly used forecasting methods. In addition, the proposed linear mixed-effect model as well as a method for model parameter estimation are introduced. Subsequently, the order demand of a manufacturer in central Taiwan is forecasted using product type as a crucial explanatory variable. Specifically, the linear mixed-effect model is applied to forecast the order demand for 20 individual product types. A 1-year forecast of monthly demand is reported, and three types of forecast errors are used to assess the forecasting ability of the model. The results show that the forecasting ability of the linear mixed-effect model in an empirical analysis is superior to those of a linear forecasting model, exponential smoothing method, and time-series forecasting method.

II. LITERATURE REVIEW

A. Influences of the MTO and MTS on Business Operations

Modern production strategies primarily involve two main production patterns: the MTO (based on customer orders), and the MTS (based on production capacity) [8]. From the perspective of customers, one competitive advantage of the MTS production is short delivery time and quick response [9]. Therefore, identifying the types of products that are specifically suitable for the MTS production pattern or both MTS and MTO patterns is a favored research topic in management science [8].

Regarding the influences of the MTO and MTS production strategies on business operations, Hendry and Kingsman [10] showed that the MTS and MTO production strategies are mostly used for manufacturing standard and customized products, respectively. Regarding the attributes of orders, order demand for MTS products is generally predictable, whereas that for MTO products is irregular and unpredictable. Concerning production planning, MTS production lines operate according to forecast results, and the production line schedule can be adjusted easily. However, the schedule of MTO production lines is determined based on recent order demand, and long-term manufacturing schedules are difficult to determine. In terms of product delivery, enterprises that adopt the MTS production strategy can ensure rapid product delivery, thus maintaining high customer satisfaction. The MTO production pattern requires long delivery times, and enterprises adopting this strategy must communicate with customers to achieve consensus regarding product delivery time. Concerning product price, compared with prices of products produced adopting the MTO strategy, the prices of MTS-produced products are relatively more stable. Soman, van Donk, and Gaalman [8] indicated that the MTO production pattern is effective for handling orders requesting high-mix customized products; the production planning for the MTO strategy must prioritize meeting order demands, while production effectiveness is determined according to crucial elements in the orders (e.g., the expected delivery volume and number of delayed delivery days). The goal of a company that manufactures MTO products is to shorten product delivery times; production efficiency emphasizes the importance of capability planning, orders that are lost due to problems with manufacturing processes, and on-time product delivery. By contrast, the MTS production pattern is effective for handling uniform product specifications and less customized products, where production planning is determined based on product demand forecasting and production effectiveness is production-oriented. Therefore, the goal of a company manufacturing MTS products is to enhance product availability, and its production efficiency emphasizes the importance of inventory policy, finished goods inventory, one-off or batch production, and accurate demand forecast. Rajagopalan [11] indicated that inventory costs are slightly higher for the MTS strategy than for the MTO strategy, particularly for one-off and batch production.

In summary, the MTS strategy relies heavily on the accuracy of product demand forecasting. Because of accurate forecasting, the advantages of the MTS production strategy, including short delivery time, manageable long-term manufacturing schedule, and stable product prices, can be realized. In addition, accurate forecasting can optimize inventory levels; therefore, companies applying the MTS strategy can effectively control inventory costs. Some researchers have explored the inventory policies and material control mechanisms in MTO production [12]. The forecasting method proposed in this study provides a relatively accurate basis for forecasting random customer orders (demand) for MTS production.

B. Forecasting Methodology

Two main types of forecasting methodology exist: (1) statistical methods; and (2) data mining and machine learning [13]. Both types of forecasting methodology are aimed at identifying the relationship between influential factors (independent variables) and research variables (dependent variables), and identifying the effects of the influential factors on research variables [7]. These two methodologies involve distinct approaches to interpreting analysis models. The statistical methodology is based on the data derived from a specific mathematical model as well as unobservable errors. The machine-learning methodology avoids fitting data to a specific model and develops algorithms that are suitable for various types of data. These two methodologies differ in their strengths and characteristics [13]. The statistical methodology uses the probability distribution of errors to infer the significance of the influential factors in a model. The reliability of inferences correlates positively with the mathematical model. The machine learning methodology uses the size of forecast errors as a basis for selecting the optimal forecasting model.

Several typical forecasting methods are introduced as follows, the characteristics of which are shown in Table 1. The exponential smoothing method was proposed by Holt [14] and the statistical theoretical foundation for this method was established by Muth [15]. This method involves using a demand observation and predictive value in the current period to determine the predictive value for the subsequent period by using weighted mean. To date, the exponential smoothing method has been widely applied to forecast demand under the bullwhip effect [16] and to plan inventory control strategies [17]. Moreover, the methodology for exponential smoothing has been developed in recent years into one that incorporates the effect of influential factors on the accuracy of demand forecasts [7, 18, 19]. Wang [19] used a model selection method where crucial influential factors were included in the selected model, and nonsignificant factors were removed to avoid over-fitting the model.

Time-series model was first developed in the nineteenth century, and past studies related to such model were then systematically compiled by Box and Jenkins [20] into a book. A time-series autoregressive integrated moving average (ARIMA) model integrates an autoregressive process and moving average process after obtaining a finite difference from time-series data. The ARIMA model is used to estimate the correlations parameter between the time points of observed values, and the estimated parameter

Table 1. CHARACTERISTICS OF F ORECASTING M ETHODS . (○: YES ; △: YES FOLLOWING MODIFICATION BY OTHER STUDIES

Forecasting method	Can handle temporal data	Can include influential factors	Analyzing the importance of influential factors (e.g., *p* value)
Linear mixed-effect model	○	○	○
Exponential smoothing method	○	△	△
ARMA	○	△	△
Linear model	△	○	○

values can then be used for forecasting. Subsequently, Box and Tiao [21] added other time-series influential factor to the ARIMA model. Pankratz [22] called this model the dynamic regression model.

Linear regression models are a type of linear model that are most frequently mentioned in statistical analyses. Linear models assume that research variables and influential factors are linearly related, and thus can be used to explore the effect of influential factors on research variables. Furthermore, linear models assume that observation values are mutually independent; thus, this model is applicable for analyzing data containing mutually independent observation values. If linear models are used to analyze time-correlated data, i.e., the observation values being correlated over time, then unbiased but invalid model coefficient estimators can be obtained. Consequently, the standard errors of the model coefficient estimators would be incorrect, and problems regarding statistical testing within the models arise, such as whether the model coefficients are significantly greater than 0, whether the models exhibit explanatory power, and whether the predictive intervals are reliable in forecast analysis [23, 24].

Linear mixed-effect models can be considered as an extension of linear models. The linear mixed-effect models add random effects to linear models with fixed effects. Hence, a model that has both fixed and random effects is called a linear mixed-effect model. Linear mixed-effect models are typically used to describe the relationship between research variables and categorical factors with correlated observation values. A characteristic of the mixed-effect models is that observation values at the same categorical level

have identical random effect values for dependent variables; observation values at different levels have distinct values of random effect. This characteristic explains the correlation between observation values at an identical level. Therefore, linear mixed-effect models differ considerably from linear models. The mixed-effect model can be applied to data where observation values are correlated (e.g., longitudinal data, repeated measures data, and multilevel data). However, linear models can be applied only to data where the observation values are mutually independent. In industrial operations, the pattern of data observations is often time-correlated. For example, when forecasting monthly product demand or monthly inventory levels, the observation values are correlated over time. Under such circumstances, the linear mixed-effect model is more accurate than linear models for identifying statistically significant factors.

In the past 2 years, the linear mixed-effect model has been broadly applied in various fields, such as the timber industry [25], medicine [26, 27], and ecology [28], to identify crucial influential factors. In addition, numerous studies have established models for forecasting [29, 30]. However, in industrial engineering and management science [24, 31, 32, 33], no study has used the linear mixed-effect model to make predictions by using time-correlated data or to identify key influential factors. Therefore, in this study, a linear mixed-effect model was applied to business operations to analyze the importance of influential factors, and to forecast product demand; in addition, the performance of the linear mixed-effect model was compared with that of other methods, which are the research contributions of this study.

III. LINEAR MIXED-EFFECT MODEL

According to parameter attributes, two types of effect exist in a linear mixed-effect model: fixed and random effects [34, 35]. In a linear model, the parameters are all fixed values and therefore its corresponding covariates are referred to as fixed-effect parameters. The fixed effect describes the true value of the coefficient for an entire population, or the true value of the coefficient for a factor that can be repeatedly tested under identical conditions. If a factor in a model exhibits a random effect, then the factor is sampled from an entire population. The random effect is a coefficient of the factor; moreover, the coefficient is a random variable and not a fixed value. The following section introduces the linear mixed-effect model developed by Laird and Ware [36] and the estimation of model parameters, and describes how the research variables are forecasted.

A. Linear Mixed-Effect Model

In contrast to a multilevel model, a single-level linear mixed-effect model [36] was employed in this study. The multilevel model differs from the single-level model in terms of the covariance matrix of the observation values. The single-level model involves only one level, whereas the multilevel model involves at least two levels. The covariance matrix of the multilevel model is more complex than that of the single-level model. In practice, whether using a single-level or multilevel model is more appropriate depends on the data structure of the observation values. Although the covariance matrices of the two models differ, the observation values of the various groups at a fixed level are independent of each other, and the within-group observation values are intercorrelated. In the multilevel model, a group at one hierarchy level becomes the next level of the hierarchy.

The single-level linear mixed-effect model developed by Laird and Ware [36] is expressed as follows:

$$\mathbf{y}_i = \mathbf{X}_i\boldsymbol{\beta} + \mathbf{Z}_i\mathbf{b}_i + \boldsymbol{\varepsilon}_i, \quad i = 1, \ldots, M \qquad (1)$$

$$\mathbf{b}_i \square N(\mathbf{0}, \boldsymbol{\Psi}), \boldsymbol{\varepsilon}_i \square N(\mathbf{0}, \boldsymbol{\Lambda}_i), \qquad (2)$$

where $\mathbf{b}_i$ is a matrix that is independent of $\boldsymbol{\varepsilon}_i$ (index i denotes the ith group at a single level), $\mathbf{y}_i$ contains n_i observation values for the ith group, M denotes the number of groups, $\boldsymbol{\beta}$ denotes a p-dimensional vector for the fixed effect, $\mathbf{b}_i$ denotes a q-dimensional vector for the random effect, $\mathbf{X}_i$ denotes an $n_i \times p$ covariance matrix for the fixed effect, $\mathbf{Z}_i$ is an $n_i \times q$ covariance matrix for the random effect, and $\boldsymbol{\varepsilon}_i$ denotes an n_i-dimensional within-group random error term. The variable $\boldsymbol{\varepsilon}_i$ obeys a multivariate normal distribution with an expected value of 0 and a covariance matrix of $\boldsymbol{\Lambda}_i$, and $\mathbf{b}_i$ obeys a multivariate normal distribution with an expected value of 0 and a covariance matrix of $\boldsymbol{\Psi}$. The model assumes that $\boldsymbol{\varepsilon}_i$ and $\boldsymbol{\varepsilon}_j$ are mutually independent ($i \neq j$); in addition, $\boldsymbol{\varepsilon}_i$ and $\mathbf{b}_i$ are mutually independent. Therefore, considering Models (1) and (2), the covariance matrix of the within-group observation values $\mathbf{y}_i$ is expressed as follows:

$$\mathbf{V}_i \equiv \mathrm{Var}(\mathbf{y}_i) = \mathrm{Var}(\mathbf{Z}_i\mathbf{b}_i) + \mathrm{Var}(\boldsymbol{\varepsilon}_i) = \mathbf{Z}_i\boldsymbol{\Psi}\mathbf{Z}_i^T + \boldsymbol{\Lambda}_i \qquad (1)$$

where the nondiagonal elements of $\mathbf{V}_i$ are not required to be 0. Therefore, according to (3), Models (1) and (2) allow the existence of the correlation between observation values within a group. This is a major difference that the two models have with the linear model.

B. Estimation of the Model Parameters

This section introduces estimation methods that adopt the linear mixed-effect model: the maximum likelihood (ML) and restricted ML (REML) estimation methods. Regarding the ML method, the

estimates of ML estimators are those that reach the maximum value of ML functions. By comparison, the REML method is aimed at identifying the estimators that exhibit unbiased characteristics. Therefore, estimators obtained using the REML method are unbiased, whereas those derived using the ML method could feature either biased or unbiased property. Therefore, most researchers prefer the REML method [34, 35]. We introduce the estimation procedures for both of these estimation methods, although only the REML method was used in this study.

First, the model $\boldsymbol{\beta}$ coefficient and covariance matrix of observation values $\mathbf{V}_i$ are estimated as follows. In Models (1) and (2), the expected values of $\mathbf{b}_i$ and $\boldsymbol{\varepsilon}_i$ are assumed to be 0; thus, the expected value of y_i is $X_i\beta$ (i.e., $E(\mathbf{y}_i)=\mathbf{X}_i\boldsymbol{\beta}$). Because the covariance matrix of y_i is V_i (i.e., $Var(\mathbf{y}_i)=\mathbf{V}_i$) and because $\mathbf{b}_i$ and $\boldsymbol{\varepsilon}_i$ obey an independent multivariate normal distribution, the marginal distribution of y_i is a multivariate normal distribution expressed as follows:

$$\mathbf{y}_i \square N(\mathbf{X}_i\boldsymbol{\beta},\ \mathbf{V}_i)$$

The ML function is expressed as follows:

$$L(\boldsymbol{\beta},\boldsymbol{\theta})=\prod_{i=1}^{M}(2\pi)^{\frac{-n_i}{2}}\det(\mathbf{V}_i)^{\frac{-1}{2}} \times\exp\left\{-\frac{1}{2}(\mathbf{y}_i-\mathbf{X}_i\boldsymbol{\beta})^T\mathbf{V}_i^{-1}(\mathbf{y}_i-\mathbf{X}_i\boldsymbol{\beta})\right\}$$

where $\boldsymbol{\theta}$ denotes the set of $\mathbf{V}_1,...,\mathbf{V}_M$. To facilitate differentiation, the natural logarithm of the ML function is used instead of the ML function to evaluate the ML and REML estimators, and define $l(\boldsymbol{\beta},\boldsymbol{\theta})=\ln L(\boldsymbol{\beta},\boldsymbol{\theta})$.

ML estimation method The ML estimates of β and θ are the values that maximize $l(\boldsymbol{\beta},\boldsymbol{\theta})$ and thus are also the values that maximize L(β,θ). Calculating the maximum value of $l(\boldsymbol{\beta},\boldsymbol{\theta})$ is challenging. Typically, let $\boldsymbol{\theta}=\hat{\boldsymbol{\theta}}$, and evaluate the value of β such that it maximizes $l_{\boldsymbol{\theta}=\hat{\boldsymbol{\theta}}}(\boldsymbol{\beta},\boldsymbol{\theta})$. Subsequently, let $\boldsymbol{\beta}=\hat{\boldsymbol{\beta}}$, and calculate the value of θ such that it maximizes the value of $l_{\boldsymbol{\beta}=\hat{\boldsymbol{\beta}}}(\boldsymbol{\beta},\boldsymbol{\theta})$. This process is iterated until the change in $\hat{\boldsymbol{\beta}}$ and $\hat{\boldsymbol{\theta}}$ is within a tolerance error (i.e., the $\hat{\boldsymbol{\beta}}$ and $\hat{\boldsymbol{\theta}}$ values converge).

Specifically, we first let $\boldsymbol{\theta}$ be $\hat{\boldsymbol{\theta}}$ (equivalent to letting $\mathbf{V}_i$ be $\hat{\mathbf{V}}_i$, $i=1,...,M$). Under these conditions, $\mathbf{y}_i$ obeys $N(\mathbf{X}_i\boldsymbol{\beta},\hat{\mathbf{V}}_i)$. An analytical solution for $\boldsymbol{\beta}$ can be obtained by using the generalized least squares method.

$$\hat{\boldsymbol{\beta}}=(\sum_i\mathbf{X}_i^T\hat{\mathbf{V}}_i^{-1}\mathbf{X}_i)^{-1}\sum_i\mathbf{X}_i^T\hat{\mathbf{V}}_i^{-1}\mathbf{y}_i \qquad (4)$$

Accordingly, $l_{\boldsymbol{\theta}=\hat{\boldsymbol{\theta}}}(\hat{\boldsymbol{\beta}},\boldsymbol{\theta})$ is the maximum value. Next, fix $\boldsymbol{\beta}$ in $l(\boldsymbol{\beta},\boldsymbol{\theta})$ as $\hat{\boldsymbol{\beta}}$, denoted by $l_{\boldsymbol{\beta}=\hat{\boldsymbol{\beta}}}(\boldsymbol{\beta},\boldsymbol{\theta})$, to obtain a $\boldsymbol{\theta}$ that maximizes the value of $l_{\boldsymbol{\beta}=\hat{\boldsymbol{\beta}}}(\boldsymbol{\beta},\boldsymbol{\theta})$, where

$$l_{\boldsymbol{\beta}=\hat{\boldsymbol{\beta}}}(\boldsymbol{\beta},\boldsymbol{\theta})=-\frac{1}{2}\left(\sum_i n_i\times\ln(2\pi)+\sum_i\ln(\det(\mathbf{V}_i)) +\sum_i(\mathbf{y}_i-\mathbf{X}_i\hat{\boldsymbol{\beta}})^T\mathbf{V}_i(\mathbf{y}_i-\mathbf{X}_i\hat{\boldsymbol{\beta}})\right) \qquad (5)$$

where $\mathbf{V}_1,...,\mathbf{V}_M$ are functions of $\boldsymbol{\theta}$. Typically, $l_{\boldsymbol{\beta}=\hat{\boldsymbol{\beta}}}(\boldsymbol{\beta},\boldsymbol{\theta})$ is not a linear function for $\boldsymbol{\theta}$. Consequently, no analytical solution for $\boldsymbol{\theta}$ exists, and an algorithm must therefore be used to obtain a numerical solution for $\boldsymbol{\theta}$. Commonly used algorithms include the expectation-maximization (EM) algorithm, Newton's method, and Fisher's scoring algorithm. Previous studies have described these algorithms in detail [36, 37, 38], including a comparison of their strengths and weaknesses [35]. An algorithm can be used to obtain a numerical solution for $\boldsymbol{\theta}$ (i.e., $\hat{\boldsymbol{\theta}}$), the result of which can be converted to $\hat{\mathbf{V}}_i$. Subsequently, the calculation is performed iteratively by using Equations (4) and (5) until the values of $\hat{\boldsymbol{\beta}}$ and $\hat{\boldsymbol{\theta}}$ converge.

REML estimation method The REML method is another approach for estimating $\boldsymbol{\theta}$. The REML estimate of $\boldsymbol{\theta}$ is obtained by applying an iterative method to a restricted natural-logarithm ML function.

$$l_{REML}(\boldsymbol{\theta})=-\frac{1}{2}\left((\sum_i n_i-p)\times\ln(2\pi)+\sum_i\ln(\det(\mathbf{V}_i)) +\sum_i(\mathbf{y}_i-\mathbf{X}_i\hat{\boldsymbol{\beta}})^T\mathbf{V}_i(\mathbf{y}_i-\mathbf{X}_i\hat{\boldsymbol{\beta}}) +\sum_i\ln(\det(\mathbf{X}_i^T\mathbf{V}_i\mathbf{X}_i))\right) \qquad (6)$$

Regarding the difference between the restricted natural-logarithm ML function (6) and Equation (5), Equation (6) accounts for the loss in degrees of freedom. Therefore, the estimator of $\boldsymbol{\theta}$ obtained using the REML is an unbiased estimator. The REML method involves applying Equation (4) to obtain the estimator of $\boldsymbol{\beta}$. For the REML, Equations (4) and (6) are iteratively used until the values of $\hat{\boldsymbol{\beta}}$ and $\hat{\boldsymbol{\theta}}$ converge. Equation (4) is used in both the ML and REML estimation methods to estimate $\boldsymbol{\beta}$. However, the functions employed to estimate θ (i.e., the ML and REML methods use Functions (4) and (6) to estimate $\boldsymbol{\theta}$, respectively) differ between these methods, and they thus yield different values for $\hat{\boldsymbol{\theta}}$. In addition, because $\hat{\mathbf{V}}_i$ is a function of $\hat{\boldsymbol{\theta}}$, different values are

obtained for $\hat{\mathbf{V}}_i$; consequently, different $\hat{\boldsymbol{\beta}}$ values are obtained through using these two methods.

Estimating random effect parameters Given $\mathbf{b}_i$, the following equation can be derived from (1):

$$\mathbf{y}_i \mid \mathbf{b}_i \overset{d}{=} N(\mathbf{X}_i\boldsymbol{\beta} + \mathbf{Z}_i\mathbf{b}_i, \boldsymbol{\Lambda}_i)$$

where "$\overset{d}{=}$" represents "distribution equals" and $\boldsymbol{\Lambda}_i$ is given by (2). Therefore, the generalized least squares method can be applied to estimate $\mathbf{b}_i$, which is equal to $(\sum_i \mathbf{Z}_i^T\boldsymbol{\Lambda}_i^{-1}\mathbf{Z}_i)^{-1}\sum_i \mathbf{Z}_i^T\boldsymbol{\Lambda}_i^{-1}(\mathbf{y}_i - \mathbf{X}_i\boldsymbol{\beta})$. In the equation, $\boldsymbol{\Lambda}_i$ (a function of $\boldsymbol{\theta}$) and $\boldsymbol{\beta}$ are true values. Therefore, by substituting the ML or REML estimates (i.e., $\hat{\boldsymbol{\beta}}$ or $\hat{\boldsymbol{\Lambda}}_i$), we can obtain the estimator of $\mathbf{b}_i$ as follows:

$$\hat{\mathbf{b}}_i = (\sum_i \mathbf{Z}_i^T\hat{\boldsymbol{\Lambda}}_i^{-1}\mathbf{Z}_i)^{-1}\sum_i \mathbf{Z}_i^T\hat{\boldsymbol{\Lambda}}_i^{-1}(\mathbf{y}_i - \mathbf{X}_i\hat{\boldsymbol{\beta}}).$$

C. Forecasting Research Variables

After the explanatory variables $\mathbf{X}_i^{new}$ and $\mathbf{Z}_i^{new}$ have been obtained, the estimates of $\boldsymbol{\beta}$ and $\mathbf{b}_i$ (i.e., $\hat{\boldsymbol{\beta}}$ and $\hat{\mathbf{b}}_i$) described in the previous section can be used to forecast the research variable $\mathbf{y}_i$. The predictive value is as follows:

$$\hat{\mathbf{y}}_i = \mathbf{X}_i^{pred}\hat{\boldsymbol{\beta}} + \mathbf{Z}_i^{pred}\hat{\mathbf{b}}_i. \quad (7)$$

IV. A CASE STUDY

This study adopted a single-level linear mixed-effect model to forecast product demand. In the case study, the sample was a leading professional industrial LCD/OLED display manufacturer. This manufacturer produces products that are critical components of various devices used in daily life and are applied in various industries. Moreover, the company has an international customer base. Table 2 shows the number of orders, total product demand, average product demand per order, and quantity of finished goods from 2009 to 2013. Before 2013, the manufacturer produced more than 5,000 product types, and the average quantity of products required in an order was approximately 400. Thus, the manufacturer is considered to be a suitable example of a business that produces a diverse combination of high-mix products.

A characteristic of high-mix low-volume manufacturers is that they typically commence production only after receiving a customer order. This production pattern is typical of the MTO production pattern, which is mainly adopted to serve customers in niche markets. In recent years, the manufacturer's profits have decreased despite an increasing revenue and market share. Therefore, the manufacturer aimed at changing its production strategy by adopting the MTS production strategy for some product types in order to increase its batch production capacity, reduce its production costs, and improve its production efficiency. In addition, the manufacturer believed that adopting the MTS production strategy would enhance customer satisfaction by ensuring the rapid delivery of customer orders, thereby providing a competitive advantage. Thus, being able to accurately forecast product demand was crucial. Following evaluation, to test the implementation of the MTS production strategy, this study selected the top 20 standard finished products that were most frequently ordered between 2011 and 2013 by customers of the sample manufacturer. As shown in Figure 1, these 20 standard products accounted for 20% of the manufacturer turnover for standard products in 2013, with 86 orders placed in the same year. After implementing the MTS production strategy, the manufacturer planned to run production of each product type once per month per year. Accordingly, the production frequency, cost of handling orders, and frequency of changing production lines was reduced. Thus, its long-term production capacity plans can be implemented to maximize the benefits of producing a high volume of products with fewer runs.

Table 2. NUMBER OF ORDERS AND PRODUCT DEMAND

Year	Number of orders	Total product demand	Average product demand for an order	Finished goods quantity
2009	12,929	3,603,141	278.69	2,727
2010	17,968	8,343,884	464.37	3,518
2011	20,169	6,721,194	333.24	4,546
2012	22,589	8,062,890	356.94	5,822
2013	22,361	9,045,056	404.50	5,468

A. Data Structure

The data structure comprised 20 types of standard finished products. The monthly product demand data were collected from January 2007 to December 2013 for each product type (see S1 Table). The historical data before 2012 were used to estimate model parameters, and the model was used to forecast the product demand for 2013 (January–December). Not all 20 products were manufactured from 2007. The historical data used to estimate model parameters comprised 1295 observation values (64 observation values on average for each product type). The product lifecycle varied by year, and the product demand varied by month. Therefore, year and month were crucial predictors. For each type of product, the monthly product demands in each month were related. In this study, the explanatory variables (year and month) were added to the linear mixed-effect model to analyze the monthly product demand data. Regarding product sales, the product demand varied

by product type. Accordingly, product type was regarded as a crucial categorical variable because of its influence in forecasting the product demand. In this study, according to the characteristics of the mixed-effect model, we used product type as a random-effect term and included the demand for each product type in a universal model to

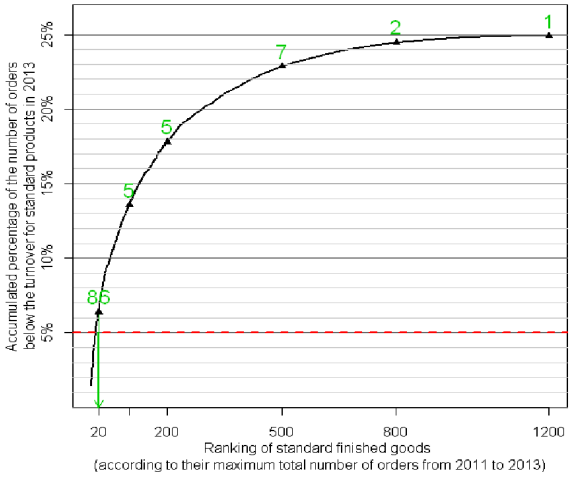

Figure 1. Maximum total number of orders (2011–2013). The plot shows that the accumulated percentage of the maximum total number of orders from 2011 to 2013 is less than the turnover of standard products in 2013. The first 20 products accounted for approximately 20% of the turnover for of standard products. The numbers in green denote the number of orders for standard products in 2013 corresponding to the horizontal axis. forecast the demand for type separately. Subsequently, we compared other commonly used forecasting methods. Unlike the mixed-effect model, other methods did not have a universal model to account for 20 unique product types. Therefore, for the other forecasting methods, the data are required to be divided into multiple data sets according to product type, and the partitioned data are then applied to the forecasting methods depending on the product type for analysis and forecasting. This approach substantially reduces the sample size, reducing the accuracy of the forecast.

B. Model Development

Product demand differed by product type, and thus we assumed the demand for each type of product to be mutually independent. In Model (1), which is the single-level model, random effect was set to be product type, thus yielding various random-effect coefficient for each product type. The model is expressed as follows:

$$\begin{aligned}\mathbf{y}_i &= \beta_0 + \beta_1 \times (\text{year-2007}) \\ &+ \beta_2 \times (\text{year-2007})^2 + \text{month} \times \boldsymbol{\beta}_3 \\ &+ b_{i0} + b_{i1} \times (\text{year-2007})^2 + \boldsymbol{\varepsilon}_i\end{aligned} \quad (8)$$

where $\mathbf{y}_i$ is a vector that denotes the monthly product demand (the vector length is equal to the data quantity for product i); β_0, β_1, β_2, and β_3 denote the intercept, year, year-squared, and month for the fixed-effect term; and b_{i0} and b_{i1} denote the intercept and year-squared for the random-effect term. In Model (8), year was considered as a continuous variable with 2007 used as the baseline. Month was a categorical variable; therefore, the month term in Model (8) was a dummy variable. The dummy variable for month had 11 indicator variables with a value of 0 or 1, and the total product demand in January was used as the baseline. Expressing Equation (1) as Model (8), the fixed-effect explanatory variable $\mathbf{X}_i$ is a matrix comprising a column of 1's vector for the intercept, year, year-squared, and month covariates. Thus, the expression $\boldsymbol{\beta}=[\beta_0\ \beta_1\ \beta_2\ \boldsymbol{\beta}_3^T]^T$ is a 14 × 1 vector, where $\boldsymbol{\beta}_3$ is the coefficient of the dummy variable for the month covariate and has 11 elements. To account for the various product types, we chose the intercept and year-squared covariate as the random-effect explanatory variable, where the intercept was used to account for the average difference of demands between product types, and the year-squared covariate was used to consider the difference between product demands decreased or increased over time. The explanatory variable $\mathbf{Z}_i$ in the random-effect explanatory variable comprised the intercept and year-squared covariate, of which the coefficients are a 2 × 1 vector expressed as $\mathbf{b}_i=[b_{i0}\ b_{i1}]^T$. In Model (8), the year-squared covariate in the random-effect explanatory variable was also a part of the fixed-effect explanatory variable, and was used to account for the fact that the expectation of $\mathbf{b}_i$ was probably unequal to 0; thus, the assumption that $\mathbf{b}_i$ in (2) was equal to 0 was reasonable. The year-squared covariate was included to prevent the annual growth trend from being linear, which enabled the model to more accurately reflect the current situation. The year-squared covariate is crucial to practical operations. The year and year-squared covariates added into the fixed-effect explanatory variable facilitated establishing a grand model for the 20 product types. The year and year-squared covariates for the fixed effect indicated the average growth trend for the 20 product types, whereas the random effect reflected the specific annual growth trends for each product type. To forecast the monthly product demand for 2013, 2013 was used as the value for the year and year-squared covariates. Both covariates and the target month were input into the explanatory variable to form $\mathbf{X}_i^{new}$ and $\mathbf{Z}_i^{new}$. Subsequently, $\hat{\boldsymbol{\beta}}$ and $\hat{\mathbf{b}}_i$ in (7) were used to obtain the forecasted value $\hat{\mathbf{y}}_i$.

C. Other Forecasting Methods

Comparing forecasting methods is crucial in methodological studies [39 , 40 , 41 , 42 , 43]. The model proposed in this study was compared with commonly used statistical forecasting methods, beginning with the following linear model:

$$Y_j = \alpha_0 + \alpha_1 \times (\text{year}_j\text{-}2007) + \alpha_2 \times (\text{year}_j\text{-}2007)^2 + \alpha_3 \times \text{month}_j + \delta_j \quad (9)$$

Table 3. Linear Mixed-Effect Model Versus the Linear Model.

Explanatory variable	Linear mixed-effect model			Linear model		
	Coefficient	Standard error	P value	Coefficient	Standard error	P value
The intercept term	39.46	320.14	.9019	174.54	294.07	.5529
(Year-2007)	800.55	133.52	.0000 ***	746.35	153.69	.0000 ***
(Year-2007)^2	-99.97	25.82	.0001 ***	-93.23	27.62	.0008 ***
February	206.41	283.03	.4660	171.14	327.19	.6010
March	736.88	281.57	.0090 **	716.23	325.51	.0280 *
April	753.30	281.56	.0076 **	762.56	325.50	.0193 *
May	536.51	280.89	.0564 -	504.53	324.70	.1205
June	253.56	281.62	.3681	218.06	325.53	.5031
July	591.73	271.46	.0295 *	556.53	313.77	.0764 -
August	91.35	271.48	.7366	56.21	313.77	.8579
September	711.75	271.46	.0088 **	664.40	313.77	.0344 *
October	297.69	271.05	.2723	255.00	313.28	.4158
November	473.91	272.52	.0823 -	432.47	314.94	.1699
December	360.30	270.62	.1833	308.34	312.71	.3243

" - ": p < .1; " * ": p < .05; " ** ": p < .01; " * ": p < .001.**

where α_0, α_1, α_2, and α_3 are regression coefficients and α_3 denotes the coefficient of the dummy variable for the month covariate, and δ_j is the error term. Model (9) (i.e., the linear model) includes only the fixed-effect term in Model (8) (i.e., the mixed-effect model); therefore, Model (9) was compared with Model (8) to examine the differences when the random-effect term is present or absent in the model. A total of 1295 observations of monthly product demand (Y_j, $j = 1,...,1295$) were used to estimate the coefficients in Model (9) and the significance of the coefficients with P values. In the Results section, Models (8) and (9) are compared regarding forecast accuracy and the P values.

Next, the model proposed in this study was compared with the exponential smoothing method, in which the product demand observation values Y_t's and its predictive values F_t's were used to obtain the predictive values for the subsequent period by calculating a weighted mean. The forecast formula is as follows:

$$F_{t+1} = \alpha Y_t + (1 - \alpha) F_t$$

where α is the weighted coefficient. To accurately forecast the monthly product demand in this case, we adjusted the exponential smoothing method to account for two influential factors (i.e., month and product type). The data were divided into 20 data sets according to each product type, and each data set was divided into 12 subsets (one for each month). For each product type, no more than six observations from each month in the historical data were used. The pre-2012 monthly product demand data were used to forecast the product demand for the corresponding months in 2013. The weighed coefficient was $\alpha = \frac{1}{2(N+1)}$, where N is the number of observations for a month ($N \leq 6$).

Finally, the model proposed in this study was compared with a seasonal time-series model; specifically, the autoregressive moving average model ($ARMA(2,2)_{12}$), which was considered to be a suitable model because the data were not nonstationary time-series data. The mathematical model for ARMA $(p,q)_s$ is expressed as follows:

$$(1 - \sum_{i=1}^{p} \phi_i B^{s \times i}) Y_t = (1 + \sum_{i=1}^{q} \theta_i B^{s \times i}) \xi_t$$

where ϕ_i is the ith order autoregressive process coefficient, B is a backward shift operator, θ_i is the ith order moving-average process coefficient, ξ_t is a normally distributed confounding term, and s is a seasonal parameter. Longitudinal data were collected for each of the 20 product types. A time-series model was established for each of the 20 product types. In this case, the month was regarded as a crucial influential factor for forecasting and thus the seasonal parameter s was set to 12, which indicates the existence of correlations in the data for every 12 month. The samples were categorized by product type, yielding an average of 64 samples for each type of product. The parameters p and q were determined based on the characteristics of an autocorrelation function, a partial autocorrelation function, and an extended autocorrelation function (p = 2 and q = 2). Finally, the $ARMA(2,2)_{12}$ model was used to forecast the product demand for each product type.

Table 4. Error Indicators for the Four Forecasting Methods.

	MAE		MAPE		RMSE	
	M	*SD*	*M*	*SD*	*M*	*SD*
Linear mixed-effect model	1,412.71	1,500.04	1.52%	1.50%	1,849.42	1,919.86
Linear model	1,828.96	2,091.93	3.77%	6.00%	2,259.99	2,712.69
$ARMA(2,2)_{12}$	1,509.22	1,938.23	1.92%	2.04%	1,942.48	2,533.25
Exponential smoothing method	1,565.54	1,547.88	2.01%	1.77%	2,003.87	2,193.16

D. Results

In this study, mean of absolute error (MAE), mean of absolute percent error (MAPE), and root-mean-square error (RMSE) were used as error indicators. The definitions for these error indicators are provided as follows:

$$MAE = n^{-1} \sum_{t=1}^{n} |F_t - Y_t|$$

$$MAPE = 100 n^{-1} \sum_{t=1}^{n} \left| \frac{F_t - Y_t}{Y_t} \right|$$

$$RMSE = \left(n^{-1} \sum_{t=1}^{n} (F_t - Y_t)^2 \right)^{0.5}$$

where n denotes the number of months to be forecasted (n = 12 in this case), Y_t represents the true product demand for month t of 2013, and F_t is the forecasted product demand for month t. The fixed-effect term in the linear model was compared with that in the linear mixed-effect model. As shown in Table 3, the absolute values of the coefficients for the explanatory variables in the linear mixed-effect model containing the random-effect term are greater (i.e., further from 0) than all of those in the linear model except for April. In addition, the standard errors and P values for all of the explanatory variables in the linear mixed-effect model are smaller than those in the linear model. Regarding the linear fixed-effect model, compared with January in a given year, the product demand was significantly greater in May and November (P value < 0.1), in July (P value < 0.05), and in March, April, and September (P value < 0.01). Compared with the linear fixed-effect model, the linear model yielded less significant results. The linear model is suitable for data containing mutually independent observation values. In this case, the observation values for product demand were correlated over time, thereby violating the assumption of the linear model. Therefore, the standard errors and P values for the linear model (Table 3) are not valid estimates, whereas those for the linear mixed-effect model are more reliable. Table 4 shows the error indicators for the four forecasting methods. Because this case involved three error indicators for each of the 20 product types, Table 4 presents the mean and standard deviation of the three error indicators. As shown in Table 4, the means and standard deviations of MAE, MAPE, and RMSE for the linear mixed-effect model are lower than those for the linear, ARMA, and exponential smoothing models, indicating that, in this case, the linear mixed-effect model is superior to the other three models. Regarding the model comparison (Table 5), the predictive values obtained through using the linear model to process the correlated data are unbiased [23]. However, the linear mixed-effect model (8) contains the random-effect term, whereas the linear model (9) does not. Therefore, in Model (8), the intercept and year-squared terms differ according to the product type, and thus the corresponding intercept values and coefficients differ based on the product type. In Model (9), the covariate of product type is not included in the explanatory variables, which generates identical predictive values for various product types in the same years and months. Thus, this model cannot predict the product demand for the individual product types, rendering its forecasting effectiveness inferior to that of Model (8). Regarding the exponential smoothing method, we considered product type and month as crucial influential factors, which were used as the basis for dividing the data into 240 data sets. For each product type, the pre-2012 monthly data were used to forecast the monthly product demand for 2013. In this manner, the exponential smoothing method was applied 12 times for each of the 20 product types. In addition, less than six observations from the historical data were used in the exponential smoothing method (for a given month, there were at most 6 sets of data from 2007 to 2012); consequently, the risk of inferential error was high because only a few observations were involved in the prediction. Regarding the seasonal time-series model $ARMA(2,2)_{12}$, we considered product type as a crucial influential factor and divided the data into 20 data sets according to product type. For each product type, 64 observations were used on average. The $ARMA(2,2)_{12}$ model was used to forecast the product demand for each product type by considering the correlation between the data for every 12 month. For both the exponential smoothing method and the $ARMA(2,2)_{12}$ model, the data were divided into subsets according to the product type and then used to estimate the monthly effect of each product type. Accordingly, although such procedure could consider the various monthly effects for various product types and the interaction between product type and month, it reduces the number of data observations involved in the prediction. In the linear mixed-effect model, 1295 data observations were used to estimate the random effect for each product type. The number of data observations used in the linear mixed-effect model was considerably more than that used in the exponential smoothing and time-series models, which could explain why the linear mixed-effect model produced lower forecast errors. In addition, in Model (8), the random effect of the interaction term for month and year-squared term was considered and the likelihood ratio test was employed to examine whether this term is significant to this model. The results showed that only the random effects of the intercept and year-squared terms were significant, and the random effect of the month term did not significantly enhances its explanatory power for the data. Therefore, the random effect of the interaction term was not included in Model (8).

Table 5. Comparison of the Four Models.

	Number of models	Number of samples	Consideration for the effect of product type	Consideration for the effect of month	Consideration for the interaction effect of product type and month
Linear mixed-effect model	1	1,295	○	○	※1
Linear model	1	1,295		○	
ARIMA(2,2)	20	≤72	○	○	○
Exponential smoothing method	240	≤6	○	○	○

※1 This effect is nonsignificant

V. DISCUSSION

In summary, when applying the linear mixed-effect model, all of the historical data were used in one model to predict the monthly product demand for each product type, and to avoid problems resulting from dividing the data into smaller data sets. In this case study, using the linear mixed-effect model enables manufacturers who adopt the MTS production strategy to predict the amount of inventory they should stock. Furthermore, the model is more effective in forecasting product demand than is the time-series, exponential smoothing, and linear models.

Similar to the linear model, the linear mixed-effect model is typically used to examine the relationship between explanatory and research variables. Unlike the linear model, which assumes the observation values to be mutually independent, the linear mixed-effect model is suitable for examining correlated data. Because the data pertaining to business operations are generally correlated over time, the linear model is limited in applicability. By contrast, the linear mixed-effect model was initially developed to handle correlated data. Other methods such as the time-series and exponential smoothing methods formulate the correlation between observation values as parameters, and then estimate the parameters by data and forecast the observations by the estimates. When the time-series and exponential smoothing models were first developed, these methods were not aimed at analyzing the relationship between explanatory and dependent variables. Wang [19] proposed an exponential smoothing method that included explanatory variables and can be used to explore the association of research variable. Because this method is a relatively new development, most of statistical software packages have not yet incorporated related functions, and thus this method has not been widely used. By contrast, the linear mixed-effect model was developed more than 30 years ago, and related functions have been included in various statistical software packages.

Using linear mixed-effect, time-series, and linear models to forecast product demand can yield negative predictive values. This phenomenon occurs when the linear mixed-effect model is used because $\boldsymbol{\varepsilon}_i$ in (2) is assumed to be normally distributed and the link function is an identity function. Negative values are usually obtained from historical data where product demand is zero or very low. To prevent this, predictive value was truncated at 0 (i.e., $F_t = \max(\hat{Y}_t, 0)$, where $\hat{Y}_t$ denotes a predictive value derived from any method, and F_t denotes an actual predictive value obtained from any prediction method). In other words, if $\hat{Y}_t > 0$, then $F_t = \hat{Y}_t$; if $\hat{Y}_t \le 0$, then $F_t = 0$. Some link functions in generalized linear mixed-effect model can deal with the case where dependent variable is restricted to $\hat{Y}_t \ge 0$ [44]. However, the prediction intervals for the random-effects in linear mixed-effect model are well developed [45, 46, 47, 48, 49]. It is useful to apply the prediction intervals in business operations for knowing whether the random-effect exists.

Implementing an MTS production strategy can enhance the competitive advantages of a manufacturer, enabling the manufacturer to rapidly satisfy product demand, thereby reducing internal and external transaction costs for handling orders. Employing this strategy also enables high batch centralized production and thus can reduce production costs and assist manufacturers in negotiating with material suppliers about the cost of materials. Because this approach enables short delivery times, customer satisfaction can be improved, thus attracting potential customers who need products immediately. Consequently, market share can be increased. MTS production also enhances the usage rate of production equipment. Companies that adopt an MTS strategy require an accurate forecasting method to realize these advantages. This study proposed an accurate forecasting method for determining the stock levels a company should determine for adopting the MTS production strategy, a topic that has seldom been discussed in studies on MTS production.

Using an MTS production strategy involves the potential risk of increasing inventory costs. Therefore, future studies should adequately apply the strengths of the linear mixed-effect model (e.g., accurately forecasting demand for multiple product types in one go) when forecasting. Future studies should consider investigating whether the forecasting intervals of the linear mixed-effect model can be coupled with various inventory strategies to assist manufacturers with adopting the MTS production strategy in order to develop an optimal business operation model in terms of optimal inventory time points and minimal inventory costs. In addition, to remain competitive, companies should enhance their organizational capability for elevating the threshold that enables competitors to develop similar operating models. Future studies are also recommended to explore the benefits that the MTS production strategy involving a linear mixed-effect model brings to the various departments of an enterprise and the effects of such strategy on customer satisfaction and loyalty.

REFERENCES

[1] P. Danese and M. Kalchschmidt, "The role of the forecasting process in improving forecast accuracy and operational performance," International Journal of Production Economics, vol. 131, no. 1, pp. 204-214, 2011.

[2] I. J. Adan and J. Van der Wal, "Combining make to order and make to stock," Operations-Research-Spektrum, vol. 20, no. 2, pp. 73-81, 1998.
[3] T. Williams, "Special products and uncertainty in production/inventory systems," European Journal of Operational Research, vol. 15, no. 1, pp. 46-54, 1984.
[4] W. M. Guillot, "Strategic leadership: Defining the challenge," Air and Space Power Journal, vol. 4, 2003.
[5] R. R. Magee, "Strategic leadership primer," DTIC Document, Tech. Rep., 1998.
[6] S. A. Shambach, "Strategic leadership primer," DTIC Document, Tech. Rep., 2004.
[7] R. Blackburn, K. Lurz, B. Priese, R. Gob, and I.-L. Darkow, "A predictive analytics approach for demand forecasting in the process industry," International Transactions in Operational Research, 2014.
[8] C. A. Soman, D. P. Van Donk, and G. Gaalman, "Combined make-to-order and make-to-stock in a food production system," International Journal of Production Economics, vol. 90, no. 2, pp. 223–235, 2004.
[9] W. Popp, "Simple and combined inventory policies, production to stock or to order?" Management Science, vol. 11, no. 9, pp. 868–873, 1965.
[10] L. C. Hendry and B. Kingsman, "Production planning systems and their applicability to make-to-order companies," European Journal of Operational Research, vol. 40, no. 1, pp. 1–15, 1989.
[11] S. Rajagopalan, "Make to order or make to stock: model and application," Management Science, vol. 48, no. 2, pp. 241–256, 2002.
[12] M.-K. Chen and A. Cheng, "The study of supply chain inventory strategy under bto production environment," Journal of the Chinese Institute of Industrial Engineers, vol. 20, no. 4, pp. 398–410, 2003.
[13] L. Breiman., "Statistical modeling: The two cultures (with comments and a rejoinder by the author)," Statistical Science, vol. 16, no. 3, pp. 199–231, 2001.
[14] C. C. Holt, "Forecasting seasonals and trends by exponentially weighted moving averages," International Journal of Forecasting, vol. 20, no. 1, pp. 5–10, 2004.
[15] J. F. Muth, "Optimal properties of exponentially weighted forecasts," Journal of the american statistical association, vol. 55, no. 290, pp. 299–306, 1960.
[16] F. Chen, J. K. Ryan, and D. Simchi-Levi, "The impact of exponential smoothing forecasts on the bullwhip effect," Naval Research Logistics, vol. 47, no. 4, pp. 269–286, 2000.
[17] S. C. Graves, "A single-item inventory model for a nonstationary demand process," Manufacturing & Service Operations Management, vol. 1, no. 1, pp. 50–61, 1999.
[18] R. Gob, K. Lurz, and A. Pievatolo, "Electrical load forecasting by exponential smoothing with covariates," Applied Stochastic Models in Business and Industry, vol. 29, no. 6, pp. 629–645, 2013.
[19] S. Wang, "Exponential smoothing for forecasting and Bayesian validation of computer models," Ph.D. dissertation, Georgia Institute of Technology, 2006.
[20] G. E. Box, "Time series analysis: Forecasting and control,," Time Series and Digital Processing, 1976.
[21] G. E. Box and G. C. Tiao, "Intervention analysis with applications to economic and environmental problems," Journal of the American Statistical association, vol. 70, no. 349, pp. 70–79, 1975.
[22] A. Pankratz, "Forecasting with dynamic regression models," Wiley Series in Probability and Mathematical Statistics. Applied Probability and Statistics, New York: Wiley, 1991, vol. 1, 1991.
[23] L. C. Hamilton and D. Press, Regression with graphics: A second course in applied statistics. Duxbury Press Belmont, CA, 1992, vol. 1, no. 1.
[24] J. G. De Gooijer and R. J. Hyndman, "25 years of time series forecasting," International journal of forecasting, vol. 22, no. 3, pp. 443–473, 2006.
[25] P. Hiesl and J. G. Benjamin, "Estimating processing times of harvesters in thinning operations in maine," Forest Products Journal, 2014.
[26] M. L. Bourbonnais, T. A. Nelson, M. R. Cattet, C. T. Darimont, G. B. Stenhouse, and D. M. Janz, "Environmental factors and habitat use influence body condition of individuals in a species at risk, the grizzly bear," Conservation Physiology, vol. 2, no. 1, p. cou043, 2014.
[27] Y.-C. Tsai, Y.-W. Chiu, J.-C. Tsai, H.-T. Kuo, S.-C. Lee, C.-C. Hung, M.-Y. Lin, S.-J. Hwang, M.-C. Kuo, and H.-C. Chen, "Association of angiopoietin-2 with renal outcome in chronic kidney disease," PloS one, vol. 9, no. 10, p. e108862, 2014.
[28] T. G. Holmes, W. M. Tonn, C. A. Paszkowski, and G. J. Scrimgeour, "Effects of winter surface aeration on pelagic zooplankton communities in a small boreal foothills lake of alberta, canada," Journal of Freshwater Ecology, no. ahead-of-print, pp. 1–14, 2014.
[29] N. Mohsin, G. Mourad, M. Faure, I. Szawarc, and J. Bringer, "Metabolic syndrome performs better than the individual factors in predicting renal graft outcome," in Transplantation proceedings, vol. 45, no. 10. Elsevier, 2013, pp. 3517–3519.
[30] A. Schwalm, Y.-S. Feng, J. Moock, and T. Kohlmann, "Differences in eq-5d-3l health state valuations among patients with musculoskeletal diseases, health care professionals and healthy volunteers," The European Journal of Health Economics, pp. 1–13, 2014.
[31] Y. Acar and E. S. Gardner, "Forecasting method selection in a global supply chain," International Journal of Forecasting, vol. 28, no. 4, pp. 842–848, 2012.
[32] P. G. Allen and B. J. Morzuch, "Twenty-five years of progress, problems, and conflicting evidence in econometric forecasting. what about the next 25 years?" International Journal of Forecasting, vol. 22, no. 3, pp. 475–492, 2006.
[33] R. Fildes, "The forecasting journals and their contribution to forecasting research: Citation analysis and expert opinion," International Journal of forecasting, vol. 22, no. 3, pp. 415–432, 2006.
[34] J. C. Pinheiro and D. M. Bates, Mixed-effects models in S and S-PLUS. Springer Science & Business Media, 2000.
[35] B. T. West, K. B. Welch, and A. T. Galecki, Linear mixed models: a practical guide using statistical software. CRC Press, 2014.
[36] N. M. Laird and J. H. Ware, "Random-effects models for longitudinal data," Biometrics, pp. 963–974, 1982.
[37] N. Laird, N. Lange, and D. Stram, "Maximum likelihood computations with repeated measures: application of the EM algorithm," Journal of the American Statistical Association, vol. 82, no. 397, pp. 97–105, 1987.
[38] M. J. Lindstrom and D. M. Bates, "Newton Raphson and EM algorithms for linear mixed-effects models for repeated-measures data," Journal of the American Statistical Association, vol. 83, no. 404, pp. 1014–1022, 1988.
[39] P.-F. Pai, K.-P. Lin, and J.-S. Wang, "Stock price forecasting in Taiwan using ellipsoidal fuzzy system," Journal of the Chinese Institute of Industrial Engineers, vol. 21, no. 2, pp. 146–155, 2004.
[40] W.-Y. Hwang and J.-S. Lee, "A new forecasting scheme for evaluating long-term prediction performances in supply chain management," International Transactions in Operational Research, vol. 21, no. 6, pp. 1045–1060, 2014.
[41] Y. Cao, G. Wan, and F. Wang, "Predicting financial distress of Chinese listed companies using rough set theory and support vector machine," Asia-Pacific Journal of Operational Research, vol. 28, no. 01, pp. 95–109, 2011.
[42] F. B. e Silva, E. Koomen, V. Diogo, and C. Lavalle, "Estimating demand for industrial and commercial land use given economic forecasts," PloS one, vol. 9, no. 3, p. e91991, 2014.
[43] X. Zhang, T. Zhang, A. A. Young, and X. Li, "Applications and comparisons of four time series models in epidemiological surveillance data," PloS one, vol. 9, no. 2, p. e88075, 2014.
[44] J. Jiang, Linear and generalized linear mixed models and their applications. Springer Science & Business Media, 2007.
[45] D. R. Cox, "Prediction intervals and empirical Bayes confidence intervals," Perspectives in Probability and Statistics, pp. 47–55, 1975.

[46] C. Morris, "Parametric empirical Bayes inference: theory and applications," Journal of the American Statistical Association, vol. 78, no. 381, pp. 47–55, 1983.
[47] R. Basu, J. K. Ghosh, and R. Mukerjee, "Empirical Bayes prediction intervals in a normal regression model: higher order asymptotics," Statistics & probability letters, vol. 63, no. 2, pp. 197–203, 2003.
[48] S. Chatterjee, P. Lahiri, and H. Li, "On small area prediction interval problems," The Annals of Statistics, vol. 36, pp. 1221–1245, 2008.
[49] M. Yoshimori, and P. Lahiri, "A second-order efficient empirical Bayes confidence interval," The Annals of Statistics, vol. 42, no. 4, pp. 1–29, 2014.

★★★

WATER QUALITY STUDY OF KARAJAE RIVER ESTUARY AT TIDAL CONDITION

[1]RAHMAWATI, [2]MUH.SALEH PALLU, [3]MARY SELINTUNG, [4]FAROUK MARICAR

[1]Doctoral Student, Department of Civil Engineering, Hasanuddin University, Indonesia
[2]Professor, Department of Civil Engineering, Hasanuddin University, Indonesia
[3]Professor, Department of Civil Engineering, Hasanuddin University, Indonesia
[4]Associate Professor, Department of Civil Engineering, Hasanuddin University, Indonesia
E-mail: [1]rahmawatiramli09@gmail.com, [2]salehpallu@hotmail.com,[3]mary.selintung@yahoo.com,[4]fkmaricar@yahoo.com

Abstract- A river is one of the surface water that can be used as a raw water source that is commonly used by the Regional Water Company (PDAM) in Indonesia. One of the alternative sources planned river of raw water in the city of Parepare is Karajae River where interaction between freshwater and seawater occurs. These interactions will affect the spread of salinity. The research used was survey method. There were 10 sampling point with a distance between of 100 meters each point. The location is about 3.6 KM from the beach. The water samples taken directly to the laboratori and immediate tested in less than 24 hours. Sampling was done 1 time and carried out during the rainy season in a state of high tide and low tide. The results showed that the water quality in the Karajae river during the rainy season is still meet the water quality standards in accordance with Regulation No. 82 of 2001.The maximum turbidity standard is 3.64 NTU, the maximum salinity is 26.96 mg/L, the temperature is 28-32 ^{o}C, and pH of 6.5-7.8 mg/L. So the raw water quality of Karajae River is in accordance with the regulation. There are no significant differences in each point of observation at high tide and at low tide.

Keywords- Karajae River, Water Quality, Salinity, Tidal.

I. INTRODUCTION

River is a surface water that can be used as a raw water source that is commonly used by the Regional Water Company (PDAM) in Indonesia. One of the planned river into alternative sources of raw water in Parepare city is Karajae River where interaction between freshwater and seawater occurs.

These interactions will affect the spread of salinity. In addition, the driving factors such as tidal influence, can lead to sea water intrusion. Karajae river is located in the city of Parepare within 155 km north of Makassar, South Sulawesi Province.

Salinity usually relates directly to the sea or estuary is strongly influenced by the water flow from the sea. Therefore, seawater intrusion occurs . The greater the height tidal wave, the further seawater intrusion. Sea water intrusion in the river can incrase the salinity so that the water tasted salty. This study try to evaluate the water quality in the Karajae river estuary.

II. METHODS

2.1. Time and Research Location

Research was held on June 5th, 2017 at 06.00 AM to 8:10 AM on high tide condition and at 11:00 AM to 14:05 PM on low tide it was in the rainy season.

The data used in this study consists of river water temperature, turbidity, pH and salinity (salt content). The research location is about 1400 KM from Jakarta the state capital of Indonesian,can be seen on Fig.1.

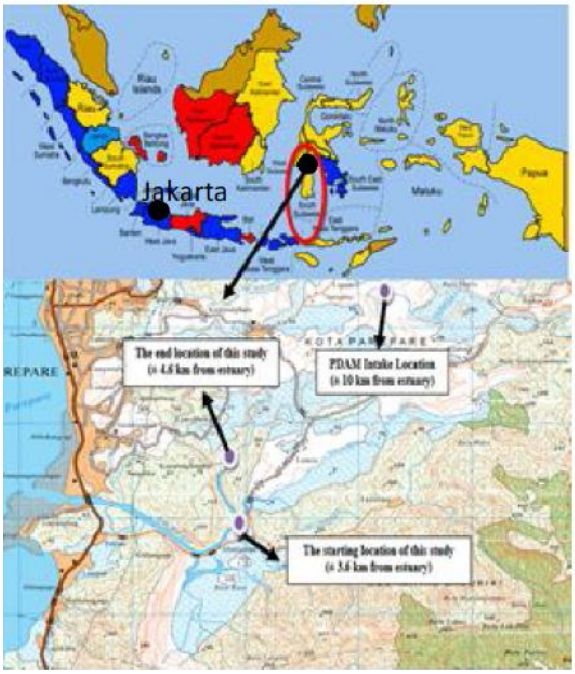

Fig.1. Research location

2.2 Sample Analysis Method

Water samples were taken from 10 point of observation which has been labeled for each point. Samples taken directly to the laboratori and immediate tested in less than 24 hours. Sampling was done by one time sampling and carried out during the rainy season in a state of high tide and low tide.

Karajae River water sampling referring to SNI 6989.57: 2008 in Section 7 and 8. Figure 2 showed the sample point taken from the river discharge.

The water discharge are between 5 m^3/sec to 150 m^3/sec, the sampling was done from two points at a

distance of 1/3 and 2/3 of the surface river width and of 0.5 the depth from the surface. But for the improvement in the pattern of spread of salinity then we also added the sampling point which is located at the midpoint.

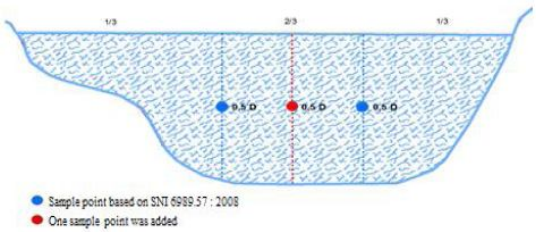

Fig.2. Sampling technique based on SNI 6989.57 : 2008.

III. RESULTS AND DISCUSSION

3.1. Physical-Chemical Quality Condition of the Estuary of the River Karajae

Karajae river physical chemical quality measured in this study were turbidity, salinity, pH, and temperature showed in Table 1.

Station	Turbidity (NTU)		Salinity (mg/L)		pH (mg/L)		Temperature (°C)	
	High Tide	Low Tide	High Tide	Low Tide	High Tide	Low Tide	High Tide	Low Tide
1	3.64	2.45	26.96	15.19	6.5	7.8	28.9	28.9
2	2.35	2.35	14.21	11.76	6.5	7.4	28.9	28.8
3	1.81	1.81	12.74	13.23	7.4	7.4	28.8	28.8
4	1.43	3.64	12.25	19.11	7.2	7.2	28.8	28.9
5	2.49	2.49	13.71	13.71	7.8	7.8	28.9	28.9
6	1.72	1.72	9.31	9.8	7.2	7.2	28.9	28.9
7	2.05	2.05	9.31	14.7	7.6	7.6	28.6	28.6
8	1.17	1.17	6.86	9.8	7.6	7.6	28.7	28.7
9	0.87	0.87	8.33	10.29	7.2	7.2	28.9	28.8
10	2.35	2.35	6.37	9.31	7.2	7.2	28.9	28.8

Table 1: Physical-Chemical Quality Condition on the Karajae River Estuary

Turbidity measurement results for each observation point shows the average value of the maximum are at point 1 of 3.64 at the time of high tide and 3.64 at point 4 at low tide (Fig.3). At high tide minimum average value is 0.87 at point 9 at the time of low tide. The average value of turbidity at high tide is greater than the turbidity at low tide. Based on the results showed that each point of observation at high tide and low tide has met the water quality standards.

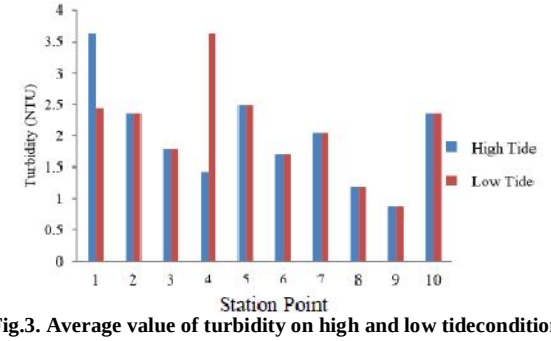

Fig.3. Average value of turbidity on high and low tidecondition.

pH Resultof each point observation at the high tide and the low tide were 6.5-7.8. There are no significant differences in each point of observation (Fig.4). This shows that the pH in the estuary of the River Karajae still meet water quality standards quality Indonesia.

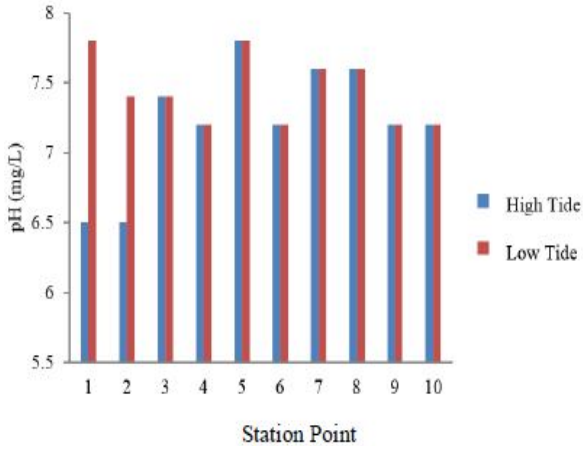

Fig.4. Average value of pH on high and low tide condition.

Temperature measurement results for each point of observation showed that the average temperature measurement at high tide and low tide ranging between 28.6 - 28.9°C (Fig.5). There is no differences between point 1 to point 10 at high tide and at low tide. Water temperature range based on quality standards of water quality that is equal to 28-32°C so that the water temperature conditions during the observation is still in a good condition.

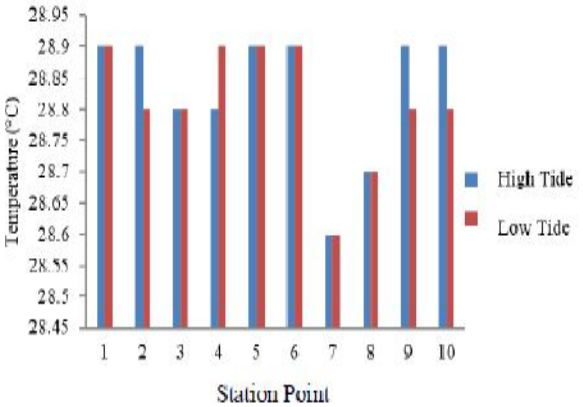

Fig.5. Average value of the current temperature on high and low tide condition.

Salinity measurement results for each observation point shows the maximum average value is on point 1 is 26.96 at high tide and 19.11 on point 4 at low tide(Fig.6.). At high tide minimum average value 6.37 and at low tide minimum average value 9.31 at point 10. The average value of salinity at high tide is greater than the salinity at low tide. Based on the results showed that the value of the salinity in the rainy season on each point of observation at high tide and low tide is in compliance with water quality standards.

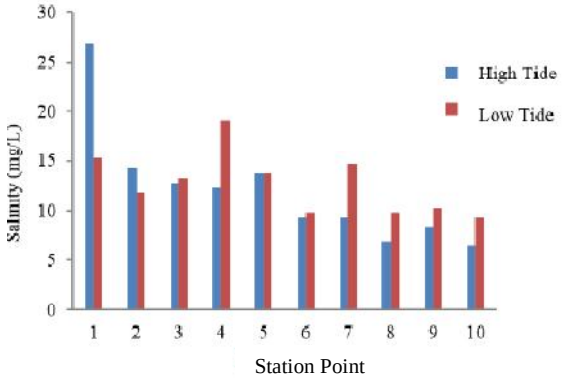

Fig.6. Average salinityon nign and low tide condition.

CONCLUSIONS

Based on the results of the discussion the results of water quality during the rainy season in KarajaeRiver still meet the water quality standards in accordance with Regulation PP No. 82 of 2001.The maximum turbidity standard is 3.64 NTU, the maximum salinityis 26.96 mg/L, the temperatureis 28-32 ^{o}C, and pH of 6.5-7.8 mg/L. So the raw water quality of Karajae River is in accordance with the regulation. There are no significant differences in each point of observation at high tide and at low tide.

ACKNOWLEDGMENTS

Acknowledgments author goes to infinity entire laboran laboratory taps Parepare for their help and support in the completion of this study.

REFERENCES

[1] Alade AO, Jameel AT, Muyubi SA, Karim MIA, and Alam MZ, "Removal of oil and grease as emerging pollutants of concern (EPC) in wastewater stream", IIUM Engineering Journl. 12(4): 161-169, 2011.

[2] Agustiningsih D, Sasongko SB, and Sudarmo, "*Analisiskualitas air danstrategipengendalianpencemaran air sungaiBelukarKabupaten Kendal*", JurnalPresipitasi. 9(2): 64-71, 2012.

[3] Akbar MA, Pallu MS , and Johannes, "*StudiKuantitasdanKualitas Air Sungai TallosebagaiSumber Air Baku*", JurnalPenelitianJurusanSipilFakultasTeknik, UniversitasHasanuddin, Makassar, 2012.

[4] BadanStandarNasional 2008, *StandarNasional Indonesia (SNI) 6989.57:2008 Air dan Air Limbah-Bagian57 :MetodePengambilanContoh Air Permukaan*, Jakarta, DewanStandardisasiNasional.

[5] Effendi, H, "*TelaahKualitas Air BagiPengelolaanSumberDayadanLingkunganPerairan*", Yogyakarta: Kanisisus, 2012.

[6] PeraturanPemerintahNomor 82 Tahun 2001 tentangPengelolaanKualitas Air danPengendalianPencemaran Air.

[7] Mary S,"*PengenalanSistemPenyediaan Air Minum*", Makassar: ASPublishing, 2011.

[8] Surbakti H, "*Karakteristikpasangdansurutdanpolaarus di muara Sungai Musi Sumatera Selatan, JurnalPenelitianSains*", vol.15(1D):35-39, 2012.

[9] Yisa J and Jimoh T, "Analytical Studies on Water Quality Index of River Landzu", American Journal of Applied Sciences, vol.7(4): 453-458, 2010.

★★★

THE EFFECT OF STRUCTURE SUBMERGED UN SYMMETRIC TO THE SEMI CIRCLE MODEL AGAINST REFLECTION OF WAVES

[1]ERNI RANTE BUNGIN, [2]SALEH PALLU, [3]ARSYAD THAHA, [4]RITA LOPA

[1]Doctoral Student Hasanuddin University, [2,3,4] Civil Engineering Department Hasanuddin University
E-mail: [1]erni_bungin@yahoo.co.id,[2]salehpallu@hotmail.com,[3]athaha_99@yahoo.com,
[4]ritalopa04@yahoo.com

Abstract- A reflection of a wave is a reflection of a wave that occurs when a wave is coming against a wall or a barrier. The problem of wave reflection is very important in coastal building planning especially port. The water in the harbor pool should be calm so the ship can dock. To get the calm in the harbor pool, then must be made buildings that can absorb energy or destroy wave energy. Breakwaters are buildings that serve to absorb or destroy wave energy. One form of the breakwater is a sinking wave breaker. The wave breaker is a wave breaker in which the muted wave is permitted to crush over the construction. The purpose of this research is to understand wave reflection with unsymmetrical sink structure. This research is done with a wave breaker model that is semicircle model. The model will be arranged asymmetrically to see the effect of wave reflection changes across the model. The results of this study indicate that the reflection coefficient value with a density of 4 x 6 cm, 6 x 9 cm and 8 x 12 cm is inversely proportional to the wave steepness value (Hi / L). The larger the density of the model, the greater the reflection coefficient.

Keywords- Submerged Breakwater, The Arrangement Is Not Symmetrical, The Reflection Coefficient

I. INTRODUCTION

Various activities in coastal areas such as settlement, industry, port, agriculture / fishery, tourism and so on can cause problems in coastal areas such as coastline changes. The coastline changes caused by human factor that can be port development activities. Port Development activities conducted continuously is expected by negative effect against nature conservation. Negative impacts can be a situation on the harbor pond due to sedimentation. To overcome the negative impact of erosion or coastal abrasion or sedimentation problem, it can be made a breakwater construction to reduce wave energy. The reduction of wave energy depends on the magnitude of the reflection coefficient. The reflection coefficient of the sink tends to increase as the slope gradient of the steeper sink. Another investigation is conducted by ArkalVittal et al (2013) on the influence of a quarter-circle submersed wave with several variations of a radius results in the addition of a reflection coefficient proportional to the steepness of the waves and also to the radius of the increasingly enlarged model. From the previous research, it was developed again in terms of arrangement of models that are made

II. LITERATURE REVIEW

A. Reflection Wave

A reflection of wave is a reflection of a wave that occurs when a wave is coming to hit wall or barrier. The phenomenon of reflection can be found in the harbor pool. The reflection of waves is determined by different coefficients for different types of building. The great ability of a building reflects that the wave given by the reflection coefficient, i.e. the comparison between the wave height of Hr reflection and the high of coming wave Hi:

Hi:

$$X = Hr/Hi \quad (1)$$

Where

X = reflection coefficient
Hr = reflection wave height (m)
Hi = wave height coming (m)

The building reflection coefficient is estimated based on the model tested. The reflection coefficients for various building types are presented in Table 1 below

Building Type	Reflection Coefficient (X)
Vertical walls with tops above water	0.7 - 1.0
Vertical walls with submerged peaks	0.5 - 0.7
Pile of oblique side stones	0.3 0.6
Pile of concrete blocks	0.3 - 0.5
Vertical building with energy damper (given aperture)	0.05 - 0.2

(Source :Triatmojo, 1996)

Table1. Reflection Coeficient

The vertical and non-permeable walls reflect most of the wave energy. In such buildings the reflection coefficient is X = 1 and the reflected wave height is equal to the coming wave height

B. Breakwater

The breakwater is a building that serves to break the waves of sea water so as to reduce energy in the waves of sea water. The structure of breakwaters can be made of massive or rigid structures and flexible structures of life, rubblemount and floating plants. During this time the breakwaters can be used as a tool in maintaining coastal damage. The form of the breakwater is divided into 4 parts, namely:

1. The tilted sidewall
2. Up right side wave breaker

3. Mixed breakwaters
4. Submerged breakwater

The breakwater as an energy damper is essentially composed of four kinds:

a. Submerged breakwaters are breakwaters where muted waves are permitted to crush over construction.
b. Non-submerged breakwaters are breakwaters that are frontally hit by waves in construction so that the waves break directly during construction
c. Floating breakwaters are breakwaters that are floated above the water surface so that kinetic and dynamic energies are muted together by construction (Harms, 1979).
d. Submerged (submerged horizontal plate) is a built float breakwater in the form of a plate-shaped construction (Xiping, 2004).

The submerged breakwater can serve to direct the movement of wave propagation as desired (Herbich, 2000). If the shape of the contours of the sea floor is convex in the direction of the coming wave, then the wave will be centered (converging) and cause the wave will rise. Similarly, when the seabed is concave in the direction of the coming wave, then the wave will be widened (divergent) and the wave height becomes lower. This theory shows that when the shape of the sinking construction is concave curved with the direction of the coming wave, then the wave will widen (divergent) and the wave height becomes lower. This theory shows if the form of sunken concave-shaped construction concave with the direction of the arrival of the wave will cause a refraction effect (widening of the wave behind the construction)

C. Wave Theory

Waves can occur due to wind, ups and downs, artificial disturbances such as ship movement and earthquakes. The effect of the wave on port planning is:

1. The size of the waves determines the dimensions and the depth of the building breakwater.
2. Waves create additional forces that must be accepted by ships and dock buildings.

Waves are a major factor in the determination of port layouts, shipping lanes and coastal building planning (Triatmojo, 1996).

waves can be classified into three parts based on the water depth of shallow water waves, transitional water waves and deep water waves (Triatmojo, 2011). Based on the water depth, the three types of waves can be differentiated according to the following limits:

wave category	d/L	2πd/L	Tanh 2πd/L
shallow water waves	> 0.5	> π	1
transitional water waves,	0.05 – 0.5	0.25 - π	Tanh 2πd/L
deep water waves	< 0.05	< 0.25	2πd/L

(Source :Triatmojo, 2011)

Table 2. Types of Waves Based on the Water Depth

D. Wave characteristics

Waves arising on the surface are one form of energy transfer caused by the wind that blows on the surface of the ocean. The characteristics of the waves leading to the coast are strongly influenced by the water depth, the shape of the beach profile and the wave character itself. Parameters to consider in explaining waves are wavelength, wave height, and water depth. These parameters can be explained as follows:

a. Wavelength (L) is the horizontal distance between two peaks or the highest point of successive waves
b. The wave period (T) is the time required by two successive wave peaks / passes through a given point
c. The wave propagation velocity (C) is the ratio between the wavelength (L / T) when the water waves propagate at speed, the water particle does not move toward the wave propagation
d. Amplitude (a) is the vertical distance between the peak / highest point of the wave or valley / lowest point of a wave with calm water level (H / 2)

III. RESEARCH METHODOLOGY

Material collection of modeling, model will be adjusted to channel size, calibration of laboratory apparatus, determine wavelength according to wave period, no model test to determine the wavelength, model test with three unsymmetrical arrangement to determine wave height and transmission height.

A. Type Model

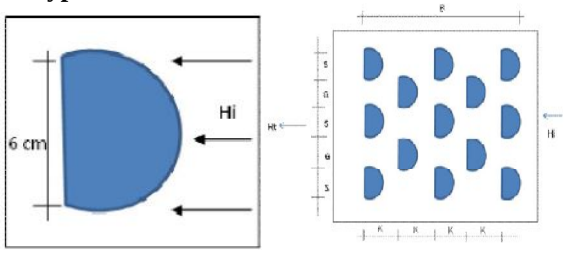

Figure 1.examples of unsymmetrical arrangement

The place of research was conducted at Hasanuddin University Hydrolical and Engineering Laboratory.

B. Research Implementation

Standard testing is done by calibrating the probe. The probe calibration aims to get the actual wave height by using Eagle software for readability. The readings obtained are wave amplitude. By entering the wave amplitude value of the probe calibration equation, it will be obtained by the coming wave height and the transmission height

C. Testing without model

The Model testing was performed at the Laboratory to determine the wavelengths with two different depths of 12 cm depth and 16 cm depth, then with three periods and three strokes. The wavelength to be obtained is then used as a standard for subsequent tests

D. Testing with a model for three unsymmetrical arrangements

The semicircle-test was performed with three density variations for each depth of 12 cm and 16 cm. Three variations of density are 4 cm x 6 cm, 6 cm x 9 cm and 8 cm x 12 cm. The density in question is the horizontal and vertical distance between the asymmetrically arranged models. This test is done to see the effect of reflection coefficient on the model which is arranged asymmetrically.

E. Implementation Walk

After obtaining the wave amplitude value for each density variation through the aid of the Eagle program, the subsequent wave amplitude values are substituted into the probe calibration equation to obtain readings of wave height and transmission wave height. After that the wave height data comes and the transmission wave height data are processed by using the reference to get the reflection coefficient value

IV. RESULT AND DISCUSSION

A. Semi circle model for density 4 cm x 6 cm

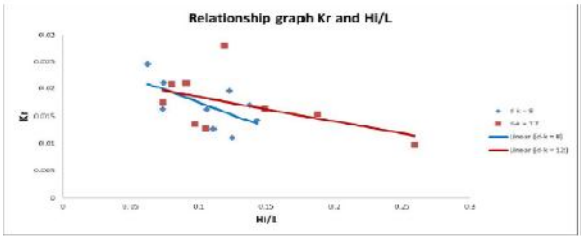

Figure 2.Relationships Kr and Hi / L for Density 4 cm x 6 cm

Figure 2 shows the reflection coefficient value to the steepness of the wave (Hi / L) decreased significantly. The greater the value of Hi / L, the reflection coefficient is smaller. The reflection coefficient value in Figure 2 at 16 cm depth for a density of 4 cm x 6 cm decreased from 1.8% to 1.2%, while for depth 12 cm decreased from 2.2% to 1.4%.

B. Semi circle model for density 6 cm x 9 cm

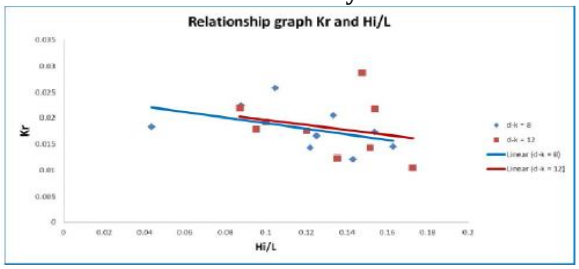

Figure 3.Relationships Kr and Hi / L for Density 6 cm x 9 cm

Figure 3 shows the reflection coefficient value to the steepness of wave (Hi / L) decreased significantly. The greater the value of Hi / L, the reflection coefficient is smaller. The reflection coefficient value of Figure 3 at a depth of 16 cm for a density of 6 cm x 9 cm decreased from 2.0% to 1.6% while for depth 12 cm decreased from 2.4% to 1.5%.

C. Semi circle model for density 8 cm x 12 cm

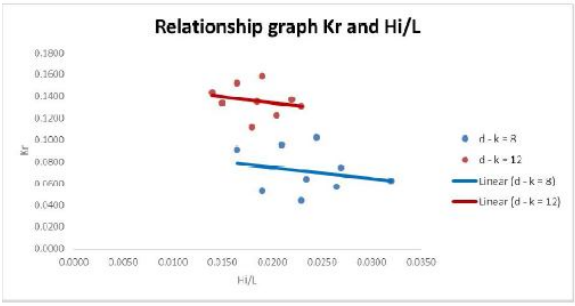

Figure 4.Relationships Kr and Hi / L for Density 8 cm x 12 cm

Figure 4 shows the reflection coefficient value to the steepness of wave (Hi / L) decreased significantly. The greater the value of Hi / L, the reflection coefficient is smaller. The reflection coefficient value of Figure 4 at a depth of 16 cm for a density of 8 cm x 12 cm decreased from 14 % to 13 % while for depth 16 cm decreased from 8 % to 6 %.

D. Percentage Reflection Coefficient

Density Semi Circle Model					
4 cm x 6 cm		6 cm x 9 cm		8 cm x 12 cm	
Depth		Depth		Depth	
12 cm	16 cm	12 cm	16 cm	12 cm	16 cm
2.2 % - 1.4 %	1.8 % - 1.2 %	2.4 % - 1.5 %	2.0 % - 1.6 %	14 % - 13 %	8 % - 6 %

Table 2.Percentage Reflection Coefficient

From the percentage value of the reflection coefficient, it found that for the density of 4 cm x 6 cm, 6 cm x 9 cm and 8 cm x 12 cm, the reflection coefficient is inversely proportional to the steepness of the wave (Hi / L). the greater the density of the model, the smaller the reflection coefficient value

CONCLUSION

From the results of research and analysis can be drawn conclusions as follows;

1. The density of the model affects the value of the reflection coefficient
2. The greater the density of the model, the smaller the reflection coefficient value

REFERENCE

[1] ArkalVittal H., L. Ravikiran., 2013, *Wave Structure Interaction For Submerged Quarter Circle Breakwaters Of Different Radii – Reflection Characteristics*, World Academy Of Science Engineering and Technology, Volume 7

[2] Armono, H.D., Hall, K. R., 2002, Wave Transmission On Submerged Breakwaters Made Of Hollow

Hemispherical Shape Artificial Reefs, Canadian Coastal Conference.

[3] Azhar M. Rian, Wurjanto A., Yuanita N, 2011, Coastal Protection Study Type Breaking Waves Sink at TanjungKait Beach, Thesis

[4] Biria A. H., Neshaei L.A.M., Ghabraei A., Mehrdad A.M., 2015, *Investigation of Sedimen Transport Pattern and Beach Morphology In The Vicinity Of Submerged Groyne*, Springer Journal, Volume 9: PP 82-90

[5] Chang K.H., Liao C.J., 2007. *Long Wave Reflection From Submerged Trapezoidal Breakwaters*. Elsevier Journal. 34 : 185-191.

[6] Dong L., Akira W., Masahiko I., 1996, *Nonlinear Wave Transformation Over a Submerged Triangular Breakwater*, Research Engineer, River Engineering.

[7] Dauhan Kristie S., 2013, Wave Break Characteristic Analysis of Coastal Lines Change at Oki Atep, Journal of Static Civil Engineering, Volume 1 no.12: 784-796

[8] Fatnanta F., 2011, Transmission Behavior and Stability Study of Sandwave Sand Types of Sink Type, Dissertation

[9] Fatnanta F., Pratikto W. A., Armono H. D., Citrosiswoyo W., 2011. Behavior Deformation Wave Sand Bag Type Drowning.Journal of Theoretical and Applied Field of Civil Engineering. 18: 171-179.

[10] Fatnanta F., Jaji A., 2011, Stability Behavior Breaking Wave Sandbox Type Sink, Journal of Civil Engineering Volume 11: 1-8

[11] Gangadhar K., 2013, *Wave Transmission Of Submerged Inclined Serrated Plate Breakwater*, International Journal Of Chemical, Volume 1

[12] NurYuwono. 1994. Hydraulic Model Planning. Hydraulic and Hydrology Laboratory of UGM.Yogyakarta.

★★★

THE COMBINATION OF HOLLOW PRECAST BLOCK AND VEGETATION TO REDUCE RUNOFF ON SLOPES

[1]ARSYUNI ALI MUSTARY, [2]MUH. SALEH PALLU, [3] RITA TAHIR LOPA, [4] DAN ARSYAD THAHA

[1]Doctoral Student of Civil Engineering, [2,3,4] Lecturer of Civil Engineering
Department Hasanuddin University, Jalan Poros Malino Km. 6 Gowa
E-mail - [1]arsyuni.jinne02@gmail.com, [2]salehpallu@hotmail.com, [3]ritalopa04@yahoo.com, [4]athaha_99@yahoo.com

Abstract - Rain fall is an important factor in runoff rate especially if the land is not covered by vegetation, all this time various methods to reduce runoff have been used but the existing method has not been able to answer all problems and tend not to pay attention to the effect on the environment, along the development of the concept of river- and slope restoration, becomes a demand for slope protection for the characteristic of ecological to be maintained. Various types of cliff protective have advantages and disadvantages both pure vegetation or pure structures, hence we evaluate and design the model of cliff protective of both methods, i.e by designing hollow precast block and varying with grass vegetation to obtain the benefits of both methods.The research aimed to determine the amount of runoff discharge that occurs on land cover variation with Hollow Precast Block and Grass Vegetation on the slope of ground level 15°, 25° and 40°.Sampling is started with rainfall calibration so that it can get 3 (three) types of rainfall, then make scale model with soil slope 15°, 25° and 40° on rain fall simulator tub, then variation of land cover model including also a model of Hollow Precast Block is arranged on slope model and performed running with 3 (three) variant of rainfall, 4 (four) variants of land cover model, and 3 (three) variants of slope, the three variants of rainfall, total average runoff indicates land cover using Hollow Precast Block with a combination of grass vegetation can significantly reduces runoff by 41.06%, 45.41% and 41.77% of 15°, 25° and 40°, respectively of land without cover, also steeper the slope of land then amount of runoff is also getting higher.

Keywords - Runoff, slope, Hollow Precast Blocks, vegetation, rain fall simulator

I. INTRODUCTION

Rain falling to the ground forms runoff that flows back into the sea,some of them into the soil (infiltration) and move downwards (percolation) into the saturated zone under the surface of the groundwater. The water in the soil moves slowly passing the aquifer into the river or sometimes directly into the sea. Infiltration is defined as the movement of water down through the soil surface into the soil profile. Runoff occurs when the amount of rainfall exceeds the rate of infiltration and evaporation. After the infiltration rate is met, the water begins to fill the basin or depression on the soil surface. After the filling is complete the water will flow freely on the soil surface. Factors affecting runoff are divided into 2 (two) groups, namely meteorological and physical properties or characteristics of the drainage region. The effect of rainfall intensity on runoff depends on the infiltration rate;hence runoff will occur in line with the increase of rainfall intensity. The relation between percolation and density variation is inversely proportional; percolation will increase if the level of density decreases. The result of runoff hydrograph represents a consideration in overcoming hydrological problems such as plan water sources and flood approximation. This is because the hydrograph describes a time distribution of the surface flow at a measurement site, which results in graphical form can indicate when a peak discharge occurs. Through rainfall simulatordevice, the rain becomes an alternative modeling to displaying the rain-runoff process. Rainfall simulator is a device that can remove water from nozzle as artificial rain, where for rainfall intensity and slope of land can be arranged as needed. The problem attracted us to evaluate these two methods, so we raised this issue to investigate, that is how the combination of structure and eco-hydraulic in managing the erosion of slope that caused by Hexagonal Precast Block rain with vegetation. The method of research is to examine the model of river cliff protective with Hollow Precast Block with a combination of vegetation to run off.

II. THEORETICAL REVIEW

2.1. Previous Research

The concept of eco-protection by using vegetation or a combination of vegetation with civil structures needs to be developed because the combined models tend to be cheaper and environmentally friendly (ArsyadThaha, 2003). The resulting runoff hydrograph will have an ascending branch (during rain) and a descending branch (after rain). The amount of difference between the intensity of rain and runoff each time between 0 and t, indicates loss and equal to the amount of infiltration (HalidinArfan, 2010). Long-term soil erosion rates for Vetiver treatment independently and a combination of Vetiverwith bahia both showed a decrease in erosion rate over 96% or almost no erosion (Nanny Kusumaningrum, 2011). River restoration is the compatibility of art and techniques to explore the sights and river function (Rita Lopa, 2012). The increase of soil erosion due to cliff slope is greater than 4.89 times from its original condition compared to the increase of rain intensity which only 1.75 times

from its original condition (AlvianSaragih, 2014). A structure of river cliff intensifier with eco-hydraulic positively impacts the decreasing speed of water flow on river banks during the increase of water discharge, also increases the stability of river banks that experiences erosion and enlarge littoral zone during high water discharge, thus creating new habitat for the growth of various types of river water biota (DayuSetyoRini, 2015).

2.2. Runoff

Rain falls on the sea terminates this cycle and will start with a new cycle. It falls on the mainland will go through a longer path to reach the sea. Every drop of rain falling to the ground is a small blow to the ground. This water blow breaks soft ground to hard rock. These fractional particles then flow into mud, and the mud covers the pores of soil, so it blocking the rain that will seep into the soil. Thus, more water that flows in the soil surface. This surface flow then carries rocks and other boulders, which will further strengthen scouring on the ground. Scratches due to scouring water and other particles to the ground will become larger. These scratches then become small grooves, then form a small trench, and eventually gathered into a tributary. These tributary then gathered together to form a river. Runoff is part of the rainfall that flows on the soil surface. The amount of water to be runoff depends on the amount of rainfall in the time unit (intensity), the condition of soil cover, topography (especially cliff slope), the type of soil, and the presence of previous rainfall or not (water level before the rain). While the amount and speed of runoff depends on the catchment area, runoff coefficient and maximum rain intensity.

Runoff is a part of the rainfall (rainfall minus evapotranspiration and other water losses) flowing in river water due to gravity; the water comes from the surface as well as from the sub-surface. It can be expressed as runoff thickness, river discharge and runoff volume. At the beginning, the water/river flow occurs because the water flows following the cracks/joints that exist on the surface of the earth. So that initially the area is not a watershed, but the accumulation of water, then there are further processes such as weathering, erosion, dissolution and so on. The process continues, thereby evolving into a small trench that longer is eroded either laterally or vertically. Eventually, small rivers created as a river system.

2.3. Factors Affecting Runoff

Regardless of rainfall characteristics, such as rainfall intensity, period and distribution, there are several specific factors (catchment areas) that are directly related to the occurrence and runoff volume.

a. Soil type. Such condition is only apply if the soil surface conditions remain intact and not experience disruption. It is known that the size average of raindrop increases with increasing rain intensity.
b. Vegetation. The large of interception deposits in the vegetation canopy depends on the type of vegetation and its growth phase. Common interception values are 1-4 mm. Also, vegetation inhibits the flow of surface water, especially on cliff slopes, so that water has more chance to soak in the soil or evaporate.
c. Slope and size of the catchment area. Observations on runoff plots indicate that plots on cliff produce more runoff than with plots on sloping slopes. In addition, the amount of runoffs decreases with increasing slope length.

2.4. Sounding of runoff

The sounding of runoff depends on 3 (three) factors:

a. The maximum amount of rainfall per time unit (maximum intensity)
b. Rainfall that becomes runoff (factor value of runoff). The large of this factor depends on topography, cliff slope, soil texture, and also the type of land cover and its management.
c. Catchment area

The result of runoff hydrograph represents a consideration in overcoming hydrological problems such as plan water sources and flood approximation. This is because the hydrograph describes a time distribution of the surface flow at a measurement site, which results in graphical form can indicate when a peak discharge occurs. Through rainfall simulator device, the rain becomes an alternative modeling to displaying the rain-runoff process. The rain simulator is Measurements at rainfallsimulator laboratory use the formula:

$Q = Vl / t$ ……..(1)

Where:
Q = Runoff discharge (litre/sec)
Vl = Measurable runoff volume (litre)
t = Time (sec)

2.5. Rainfall Intensity

Rainfall intensity is the amount of rain per time unit (mm/h, mm/min, mm/s). Rain period is the duration of rain, duration of rain is the duration of rainfall in minutes or hours. In this case can representing the total rainfall or rain period that abbreviated with relatively uniform rainfall (Asdak, 2010).

It is critical in the calculation of runoff, the magnitude can be obtained from field observations. The amount of rain intensity will depend on the width and duration and frequency of rain by comparing the rainfall with the height of rain in mm/hour or by the equation:

$$I = \frac{d}{t} \quad \text{…….. (2)}$$

$$d = \frac{V}{A} \quad \text{.....(3)}$$

Where:
I = rain intensity (mm/h)
d = rainfall height (mm)
t = time (hour)
V = rainfall volume in an area (mm^3)
A = width of rain area (mm^2)
Short-term rainfall is expressed in intensity per hour called rainfall intensity (mm/hr). The mean rainfall intensity in t hours (I_t) is expressed by the following formula:

$$I_t = \frac{R_t}{t} \quad \text{.....(4)}$$

Where:
It = average rainfall intensity
Rt = rainfall for t hours
t = time

The intensity of rain is critical in the calculation of runoff, the magnitude can be obtained from field observations. The amount of rain intensity will depend on the thickness and duration and frequency of rain by comparing the height of rainfall and the duration of rain in mm/hour. The magnitude of rainfall intensity varies depending on the duration and frequency of rainfall. High intensity of rainfall generally takes place with a short duration and covers limited area. Rain that covers a large area is rarely with high intensity, but can take a long duration. The effect of rainfall intensity on surface flow depends on infiltration capacity. If the rainfall exceeds the infiltration capacity, then the magnitude of surface flow will increase immediately as rainfall intensity increases (Triatmodjo, Bambang, 2013). The intensity of artificial rain is calculated by using the following equation:

$$I = \frac{V}{AT} \times 600 \quad \text{.....(5)}$$

Where:
I = rain intensity (mm/h)
V = water volume in container (ml)
A = container surface area (cm^2)
T = time (min)

III. METHOD OF RESEARCH

The research was conducted by making Hollow Precast Block as well as Grass Vegetation models, it further simulated with the aid of Rainfall Simulator instrument. The research was conducted at Hydraulics Laboratory, Department of Civil Engineering, Faculty of Engineering, Hasanuddin University. Duration of research is planned for 6 months. As picture we make specimen of Hollow Precast Block. Hollow Precast Blockwithout vegetation attachment in each sloping variation (15°, 25°, and 40°), before making the specimens, the firstly the cast is made according to the predetermined size (model size), after that the material is casted with concrete precast K125, after the Precast model is finished and then dried, after it is finished and then neatly arranged and closing each other with the formation of 7 rows of 12 columns, as in Figures 1 and 2.

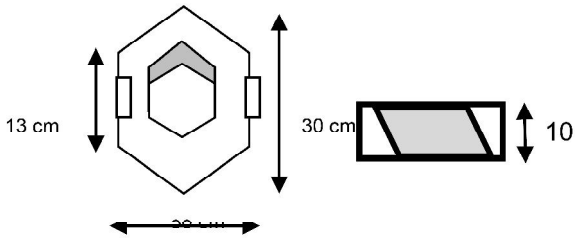

Figure 1. Dimension of Hollow Precast Block

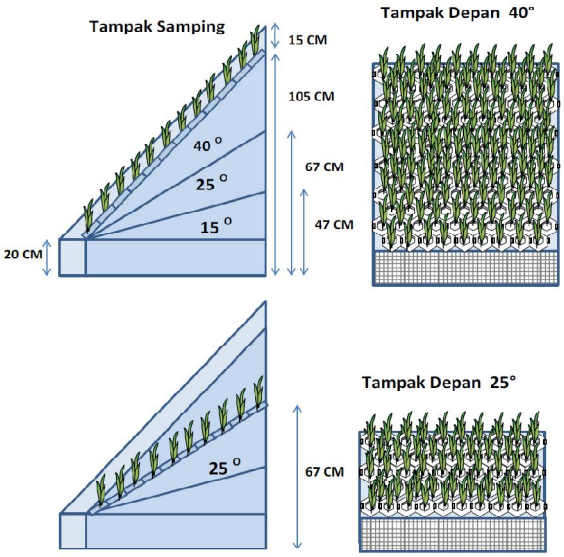

Figure 2.Formation of Hollow Precast Block and grass vegetation on the variation of soil slope on Rain fall simulator tub

IV. RESULTS

4.1. Rainfall analysis

Rain intensity is the amount of rain per time unit (mm/h, mm/min, mm/s). Rain period is the duration of rain, the duration of rain is the duration of rainfall in minutes or hours. Rain intensity is defined as the measurement of rainfall is done to determine the amount and duration of rainfall.

Types of Rainfall	Types of Rainfall	Rain Mean Average observation (ml)	Observation Time (minutes)	Rainfall Intensity (mm / Hr)
Rainfall I	Low	68	15	61.6
Rainfall II	Medium	107	15	96.93
Rainfall III	High	122	15	110.5

Table 1. Result of rainfall intensity calibration on Rainfall Simulatordevice

Calculated by the formula:

$$I = \frac{Q}{A.t} \times 600$$

$$I = \frac{68}{441.56 \times 15} \times 600 = 61.6 \text{ mm/hr}$$

4.2. Runoff Analysis

Amount of runoff illustrates how large the effect of land cover variation with soil slope against runoff by using vegetation, precast and without using land cover (empty running).CX. The calculation result of how large the effect of land cover variation against runoff and the treatment used in the research, for the slope of 15° and CH = 61.6 mm/hr, it obtained by equation:

Q = Vl/ t

Q = 9,1 / 600

= 0,0151667 L/det

Table description:

S: experiment model I with soil without cover

SG: experiment model II using the grass vegetation model

SB: experiment model III using Hollow Precast Block

SGB: experimental model IV using a combination of grass vegetation andHollow Precast Block.

Rainfall 1 , I = 61.1 mm/ hour									
Time / Soil Closure		Slope of 15°							
		Soil (S)		Soil + Grass Vegetasion (SG)		Soil + Block Precast (SB)		Soil + Grass Vegetasion +Block Precast (SGB)	
Time (Minutes)	Time (Hours)	Run off (L)	Discharge (L/Sec)	Run off (L)	Discharge (L/Sec)	Run off (L)	Discharge (L/Sec)	Run off (L)	Discharge (L/Sec)
0	0	0	0	0	0	0	0	0	0
10	0.1667	9.1	0.015166667	2.77	0.0046167	4.2	0.007	2.92	0.0048667
20	0.3333	9.85	0.016416667	3.1	0.0051667	4.35	0.00725	3.15	0.00525
30	0.5	11.1	0.0185	3.55	0.0059167	5.15	0.0085833	3.98	0.0066333
40	0.6667	12.15	0.02025	4.20	0.007	5.66	0.0094333	4.21	0.0070167
50	0.8333	12.25	0.020416667	5.15	0.0085833	5.93	0.0098833	5.06	0.0084333
60	1	13.3	0.022166667	6.21	0.01035	6.72	0.0112	5.29	0.0088167
70	1.1670	13.3	0.022166667	6.21	0.01035	6.72	0.0112	5.29	0.0088167
80	1.3333	3.2	0.005333333	2.15	0.0035833	3.2	0.0053333	2.41	0.0040167
90	1.5	0	0	0	0	0	0	0	0

Table 2. The results of runoff discharge analysis at rainfall intensity of 61.1 mm/hr on a variation of land cover with a slope of 15°

The table above obtained the analysis with the graph as follows:

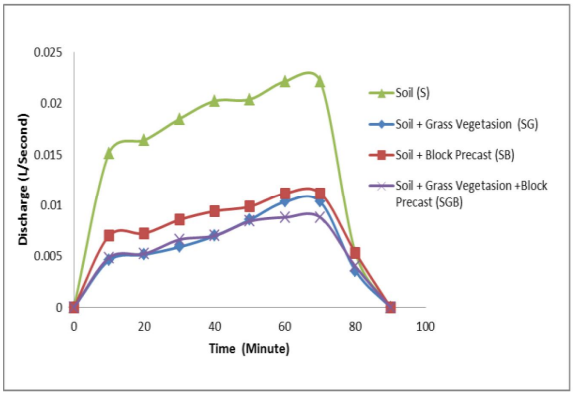

Figure 3. Relation of runoff discharge on a variation of land cover with a slope of 15° at rainfallintensity of 61.6 mm/hr

In figure 3,the graph of runoff discharge on the slope of 15° indicates that runoff discharge on the soil with a slope of 15° (ramp) on the soil without cover (S) has a large runoff discharge, while for land cover with (SB) Hollow Precast Blockand a combination of Hollow Precast Blockand grass vegetation tends to be low and almost equal to soil cover with full grass vegetation. This proves that the combination of Hollow Precast Blockand grass vegetation (SGB) on the slope of 15° is very effective in reducing runoff.

Rainfall 2 , I = 96.93 mm/ hour									
Time / Soil Closure		Slope of 25°							
		Soil (S)		Soil + Grass Vegetasion (SG)		Soil + Block Precast (SB)		Soil + Grass Vegetasion +Block Precast (SGB)	
Time (Minutes)	Time (Hours)	Run off (L)	Discharge (L/Sec)	Run off (L)	Discharge (L/Sec)	Run off (L)	Discharge (L/Sec)	Run off (L)	Discharge (L/Sec)
0	0	0	0	0	0	0	0	0	0
10	0.1667	12	0.02	3.22	0.005367	4.59	0.00765	3.42	0.0057
20	0.3333	13.1	0.021833	3.9	0.0065	5.86	0.009767	4.55	0.007583
30	0.5	13.5	0.0225	5.2	0.008667	6.33	0.01055	4.98	0.0083
40	0.6667	13.99	0.023317	5.46	0.0091	6.8	0.011333	5.9	0.009833
50	0.8333	14.8	0.024667	6.25	0.010417	7.2	0.012	6.57	0.01095
60	1	14.8	0.024667	6.25	0.010417	7.2	0.012	6.57	0.01095
70	1.16667	3.8	0.006333	2.56	0.004267	2.76	0.0046	2.3	0.003833
80	1.3333	1.31	0.002183	1.56	0.0026	1.36	0.002267	1.26	0.0021
90	1.5	0	0	0	0	0	0	0	0

Table 3. The results of runoff discharge analysis at rainfall intensity of 96.93 mm/hr on a variation of land cover with a slope of 25°

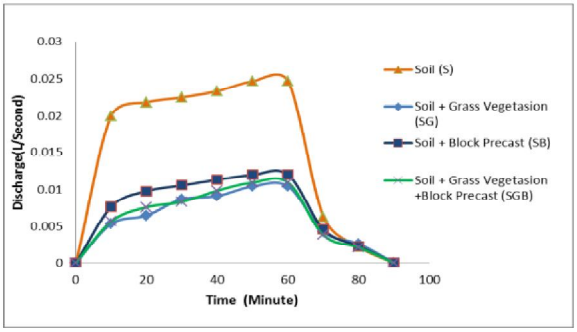

Figure 4. Relation of runoff discharge on a variation of land cover with a slope of 25° at rainfall intensity of 96.93 mm/hr

In figure 4, the graph of runoff discharge on the slope of 25° at the rainfall intensity I = 96.93 mm/hr (medium rain) indicates that runoff discharge on the soil with a slope of 25° (medium slope) on the soil without cover (T) has a large runoff discharge, while for land cover with (TB) Hollow Precast Block and a combination of Hollow Precast Block and grass vegetation tends to be low and almost equal to soil cover with full grass vegetation. This proves that the combination of Hollow Precast Block and grass vegetation (TRB) on the slope of 25° is very effective in reducing runoff.

Rainfall 3 , I = 110.5 mm/ hour									
Time / Soil Closure		Slope of 40°							
		Soil (S)		Soil + Grass Vegetasion (SG)		Soil + Block Precast (SB)		Soil + Grass Vegetasion +Block Precast (SGB)	
Time (Minutes)	Time (Hours)	Run off (L)	Discharge (L/Sec)	Run off (L)	Discharge (L/Sec)	Run off (L)	Discharge (L/Sec)	Run off (L)	Discharge (L/Sec)
0	0	0	0	0	0	0	0	0	0
10	0.1667	13.02	0.0217	3.43	0.005716667	7.35	0.01225	3.71	0.006183333
20	0.3333	14.18	0.023633333	4.82	0.008033333	8.24	0.013733333	5.23	0.008716667
30	0.5	16.23	0.02705	5.26	0.008766667	9.87	0.01645	5.90	0.009833333
40	0.6667	17.29	0.028816667	7.84	0.013066667	12.15	0.02025	8.78	0.014633333
50	0.8333	17.29	0.028816667	7.84	0.013066667	12.15	0.02025	8.78	0.014633333
60	1	5.71	0.009516667	5.64	0.0094	8.75	0.014583333	6.03	0.01005
70	1.167	4.01	0.006683333	2.45	0.004083333	4.56	0.0076	3.20	0.005333333
80	1.3333	1.01	0.001683333	1.05	0.00175	2.56	0.004266667	1.20	0.002
90	1.5	0	0	0	0	0	0	0	0

Table 4. The results of runoff discharge analysis at rainfall intensity of 110.5 mm/hr on a variation of land cover with a slope of 40°

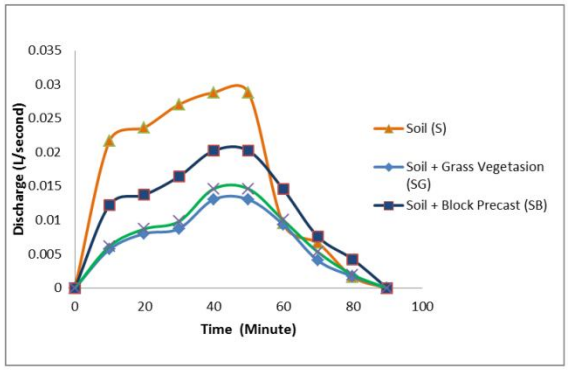

Figure 5. Relation of runoff discharge on a variation of land cover with a slope of 40° at rainfall intensity of 96.93 mm/hr

In figure 5, the graph of runoff discharge on the slope of 40^{o} indicates that runoff discharge on the soil with a slope of 40° (steep) on the soil without cover (T) has a large runoff discharge, while for land cover with (TB) Hollow Precast Blockhas high enough runoff, but for land cover with a combination of Hollow Precast Block and grass vegetation tends to be low and almost equal to soil cover with full grass vegetation. This proves that the combination of Hollow Precast Block and grass vegetation (TRB) on the slope of 40° is very effective in reducing runoff.

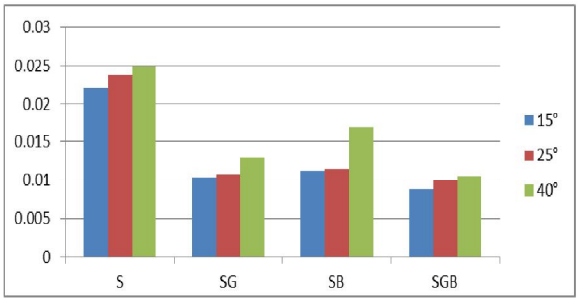

Figure 6.A graph of maximum runoff (Ql) with a rainfall of 61.1 mm/hr on soil slope variation

In figure 6, The relation of soil slope variation to runoff at low rain intensity (61.1 mm/hr) indicates that runoff discharge on soil with a slope of 15° (ramp) has a smaller runoff discharge compared to runoff on soil with a moderate or steep slope of 25°-40° (medium - steep), for soil cover with Hollow Precast Block (TB) has high enough runoff at a slope of 40°, but on soil cover with a combination of Hollow Precast Blockand grass vegetation tends to be low and almost equal to soil cover with full grass vegetation (TR) for all slopes (ramp – steep). This proves that the combination of Hollow Precast Block and grass vegetation (TRB) on the variation of slope is very effective in reducing runoff.This phenomenon is also seen in moderate rain intensity (96.93 mm/hr) and high (110.5 mm/hr). As calculation analysis shows the effect of runoff for 4 (four) experiments of variation of land cover, whether soil without cover, grass vegetation, Hollow Precast Block, or a combination of grass vegetation and hexagonal precast block showed a smaller tendency when passing land cover with a slope of 15°, 25° and 40°.

CONCLUSIONS

As results of laboratory analysis and research on the effect of variation of land cover with the slope of soil to runoff, the following conclusions are obtained:

1. The magnitude of runoff discharge that occur on the soil cover using the combination of grass vegetation and Hollow PrecastBlock (TRB) on the slope of α = 15° the maximum runoff discharge occurring at 60 minutes (1hr) is Q = 0.0088 L/s at low CH (61.1 mm/hr), at moderate CH (96.93 mm/hr) Q = 0.01002 L/s, at high CH (110.5 mm/hr) Q = 0.0105 L/s, on the slope of 25° the maximum runoff discharge occurring at 60 minutes (1hr) is Q = 0.0099 L/s at low CH (61.1 mm/hr), at moderate CH (96.93 mm/hr) Q = 0.01095 L/s, at high CH (110.5 mm/hr), while on a slope of 40° the maximum runoff discharge occurring at 60 minute (1hr) is Q = 0.0105L/s at low CH (61.1mm/hr), at moderate CH (96.93mm/hr) Q = 0.01103 L/s, at high CH (110.5 mm/h) Q = 0.011283 L/s.
2. Decreased average runoff occurring on a slope of 15° as large 41.06% of soil without cover, on a slope of 25° occurred at 45.41% of soil without cover, while on a slope of 40° occurred at 41.77% of soil without cover, so that obtained that soil cover with a combination of grass vegetation and Hollow Precast Blockis effectively reduce the rate of ground runoff at a slope of 15° to 40° in low rainfall to high CH so that it can be recommended is used as a cliff protection from erosion hazards as result of rain.

REFERENCES

[1] ArsyadThaha. M, A.B Muhiddin. The CombinationOfLow CrestedBreakwater WithMangroves ToReduce The Vulnerability Of The Coast Due ToClimate Change,Proceedings ofthe Sixth InternationalConferenceonAsianandPacific Coasts (APAC2011)December 14–16,2011,HongKong,China

[2] AlvianSaragih, Wiwik Y. Widiarti, Sri Wahyuni, 2014. Effect of Rain Intensity and Tilt of Slope Against Rate of Land Loss Using Rainfall Simulator Tool, Journal of Jember University.

[3] Arfan, H., and Pratama, A. 2010. Experimental Model of Effect of Density, Rainfall Intensity and Tilt on the Absorption on Organic Soil. Department of Civil Engineering Faculty of Engineering Hasanuddin University. Makassar.

[4] Arsyad. Sitanala, 2012. Soil & Water Conservation, Second Edition, PT.Penerbit IPB Press,ISBN:978-979-493-415-9.Bogor.Indonesia.

[5] Asdak.C,2010.Hydrology,Fifth Printing (Revision),GadjahMada University Press.ISBN 979-420-737-3.Jogyakarta.Indonesia.

[6] Bentroup, G. and J.C Hoang. 1998. The practical streambank bioengineering guide. USDA NRCS. Aberdeen, ID 55p, USA.

[7] DayuSetyoRini,. 2015. PenerapanRekayasaEkohidrolikauntukPenguatanTebing

Sungai danPemulihan Habitat KawasanSuakaIkan Kali Surabaya, JurnalEkoHidraulik, Malang.
[8] Fischenic, JC .1989. Channel Erosion Analysis and Control. In Woessmer, W .and DFology..Potts ,eds Proceeding Headwater Hydrology. American Water Resources Association. Bethesda, Md
[9] Garanaik, Amrapalli and Sholtes, Joel. 2013. River Bank Protection. New York.USA.
[10] Gerken, B., 1988: Auen, verborgeneLebensadern der Natur (River Plate represents the Lives of the Hidden Life), RombaRainfall, Freiburg.
[11] Kaharuddin, 2014. 1939. Study of Sediment Rate Control With Control Building In Upper Dice BatangGadisProvinsi Sumatera Utara
[12] Kodoatie, R.J and Sharif, Rustam, 2005. Integrated Water Resources Management. Andi, Yogyakarta
[13] Kusminingrum, Nanny.2011.Vetiver and Bahia Grass Underweight in Minimizing Slope Erosion, The Journal of Eko Hydraulics.
[14] Laoh OEH. 2002. Linkages of Physical Factors, Socioeconomic Factors and Land Use Efforts in water catRainfallment areas with erosion and sedimentation (Thesis). Bogor Postgraduate Program, IPB.
[15] Maryono, A. 2008: Eco-Hydraulic Eco-Friendly River Management. Yogyakarta: GadjahMada University Press.
[16] Maryono, A., 2005. Eko-Hydraulic River Development. Yogyakarta: Master of Engineering System of Graduate Program of GadjahMada University
[17] M. Galib Isaac, M. SalehPallu, M. ArsyadThaha, Dan Rita TahirLopa, 2014. The Rainfallanges Of SuperelevationCoefficient Of Flow With Pillar Installed Simultaneously At Interval Of 300 And 600 Along The Rainfallannel Of Bend 1800.Asian Academic ResearRainfall Journal Of Multidisciplinary, Japan
[18] Patt, H., Jurging, P., Kraus, W., 1999: NaturnaherGewasserausbau (River / Watermark renaturalization), Springer Verlag, Berlin.
[19] Rini, DaruSetyo. 2015. Application of Ecohydrolic Engineering for Reinforcing River Cliffs and Habitat Recovery of Asylum Area of Surabaya River, JurnalEkoHidraulik.
[20] Rita Lopa, Yukihiro Shimatani, 2013. Evaluating The River Healthof Pre- And Post-Restoration In The Kamisaigo River, Fukuoka, Japan River Restoration Center 13th Annual Network Conference
[21] Suprayogi.Slamet, Purnama.Setyawan, DarmantoDarmokusomo. 2015. Watershed Management, GadjahMada University Press. Yogyakarta.
[22] Triatmodjo, Bambang, Applied Hydrology. 3rd Print, Beta Offset, Yogyakarta, 2013.
[23] Truong, P., Tran Tan Van and Elise Pinners. 2008. Vetiver Grass - The Plant. The Vetiver System, Vietnam2000-2008

★★★